
Three degrees of freedom weakly coupled resonators used for mass measurement.

Auteur : Baijot, Mathieu

Promoteur(s) : Kraft, Michael

Faculté : Faculté des Sciences appliquées

Diplôme : Master en ingénieur civil électricien, à finalité approfondie

Année académique : 2015-2016

URI/URL : <http://hdl.handle.net/2268.2/1526>

Avertissement à l'attention des usagers :

Tous les documents placés en accès ouvert sur le site le site MatheO sont protégés par le droit d'auteur. Conformément aux principes énoncés par la "Budapest Open Access Initiative"(BOAI, 2002), l'utilisateur du site peut lire, télécharger, copier, transmettre, imprimer, chercher ou faire un lien vers le texte intégral de ces documents, les disséquer pour les indexer, s'en servir de données pour un logiciel, ou s'en servir à toute autre fin légale (ou prévue par la réglementation relative au droit d'auteur). Toute utilisation du document à des fins commerciales est strictement interdite.

Par ailleurs, l'utilisateur s'engage à respecter les droits moraux de l'auteur, principalement le droit à l'intégrité de l'oeuvre et le droit de paternité et ce dans toute utilisation que l'utilisateur entreprend. Ainsi, à titre d'exemple, lorsqu'il reproduira un document par extrait ou dans son intégralité, l'utilisateur citera de manière complète les sources telles que mentionnées ci-dessus. Toute utilisation non explicitement autorisée ci-avant (telle que par exemple, la modification du document ou son résumé) nécessite l'autorisation préalable et expresse des auteurs ou de leurs ayants droit.

University of Liège
Faculty of applied sciences



**Three degrees of freedom weakly coupled
resonators used for mass measurement**

By
Mathieu Baijot

Master thesis in Electrical and Electronics
Engineering

Academic year 2015 - 2016

I would like to thank Professor M. Kraft and his PhD team (Delphine Cerica, Vinayak Pachkawde, Chen Wang, Yuan Wang) for their support.

I would also like to thank Mr. Thierry Legros for his precious advice and all the reviewers of this master thesis.

Finally I would like to thank my family for their encouragements and especially my father for his advice and support during my studies and especially this master thesis.

Contents

1	Introduction	4
1.1	Organization	5
2	Motivation and objectives	6
2.1	Motivation	6
2.2	Objectives	6
3	State of the art	7
3.1	Mass measurement methods	7
3.2	MEMS fabrication	9
3.2.1	Bulk micromachining	9
3.2.2	Surface micromachining	10
3.2.3	Other types	11
3.3	Three degrees of freedom weakly coupled resonators for stiffness measurement.	12
3.4	Measurement tool	15
4	MEMS Modelization	18
4.1	Mechanical Modelization	18
4.1.1	Method of eigenvalues	19
4.2	Electrical modelization	25
4.2.1	Lump elements	25
4.2.2	Common value	29
4.3	Approximated model with high quality factor	31
5	Modelization results	33
5.1	Mechanical Modelization	33
5.1.1	Two degrees of freedom without damping	33
5.1.2	Two degrees of freedom with damping	34
5.1.3	Three degrees of freedom without damping	37
5.1.4	Three degrees of freedom with damping	40
5.2	Electrical Modelization	45
5.2.1	Three degrees of freedom with damping using LTspice	45
5.2.2	Effect of adaptation process	48
5.2.3	Experimental measurement	51
5.3	Approximated model with high quality factor	52

6	Measurement strategy for mass variation	56
6.1	Resonant frequency shift	56
6.1.1	Frequency tracking circuit	56
6.2	Relative amplitude variation at resonant frequency	57
6.2.1	Amplitude detection circuit	57
6.3	Amplitude ratio variation at resonant frequency	58
7	Results about measurement strategy	60
7.1	Resonant frequency shift	60
7.2	Relative amplitude variation at resonant frequency	61
7.3	Amplitude ratio variation at resonant frequency	62
7.4	Low sensitivity for small measurements	64
8	Conclusion	66
9	Further Improvements	67
	Appendices	71
A	MATLAB codes	72
A.1	TwoDofNoDamp.m	72
A.2	TwoDofWithDamp.m	73
A.3	ThreeDofNoDamp.m	75
A.4	ThreeDofWithDamp.m	76
A.5	Meca2Elec.m	78
A.6	amplitudeRatioShift_2Dof.m	79
A.7	amplitudeRatioShift_3Dof.m	81
A.8	amplitudeShift_2Dof.m	83
A.9	amplitudeShift_3Dof.m	85
A.10	freqShift_2Dof.m	87
A.11	freqShift_3Dof.m	88
B	Others	91

Chapter 1

Introduction

Measurement processes have interested the human being for a long time. Since the prehistoric period, men have tried to compare and share their resources[32]. Even if the first measurements are supposed to have been made with counting devices such as their own fingers[29], tally marks[33] and clay tokens[29]), the need for more precise measurement tools quickly emerged.

There is a wide variety of measurands that can be measured but quite few natural tools to measure them. Even if the human body was the origin of many length units[9] (one inch, one foot, one cubit, ...) and the nature cycle the origin of time units (moon calendars, seasons, days, ...), tools were needed to measure other measurands (temperature, force, mass, ...). Indeed, the human body is not very appropriate to make a quantitative measurement of a mass. That is why the first known weighing process was realized with seeds[30]. For example, the current name of gemstone and pearl mass unit, the carat(ct), comes from Italian ("carato") and Greek("kerátion") and means "carob seed"[27].

For millenia, mankind has developed a huge variety of techniques to measure mass. Obviously, since the mass palette currently known stretches from lower than 10^{-36} kg, which is for a simple neutrino, to higher than 10^{53} kg for the estimated mass of the universe[27], many different tools are required to cover the whole range. In this master thesis, we are interested in masses ranging from 10^{-20} kg (for tiny viruses) to 10^{-15} kg, for a common bacteria like the E. coli bacteria)[31].

Nowadays, fashionable systems used to take measurements are microelectromechanical systems (MEMS). They are very famous and still improve their reputation. It must be said they have plenty of advantages compared to usual systems. Due to the continuous reduction of their size and consumption and the continuous increase of their precision and reliability, they can be used for many different applications. The probably most famous one is the accelerometer in which a system with proof masses uses their position to determine the force applied on the chip. Another well known type of MEMS is the gyroscope family where rotation effects are used. Those small chips are really met everywhere : from common devices like smartphones, hard drives, game pads, etc. to more specialized systems like planes, rockets, satellites,

etc. MEMS could be used in different ways : they could act as a sensor (i.e. to measure acceleration, pressure, force, ...) or as an actuator (i.e. dispenser in inkjet printers, micro-mirror matrix in beamers, microphones in mobile phones, ...). Another significant advantage of those components comes from the production means which allow mass production at a relatively low cost.

The biomedical application market is thus more and more interested in using MEMS. They could replace strong intrusive techniques and measure very small signals from the body. Blood pressure sensors, micro-needles and implantable microelectrodes are a few examples of what is currently done with MEMS. They have a huge potential for developing countries where heavy and costly medical equipments are not available.

This master thesis will concentrate on a MEMS used to measure tiny masses in the context of a bio sensor.

1.1 Organization

After this introduction, this dissertation will be organized in the following way :

- Chapter 2 highlights the motivation for this research and its objectives.
- Chapter 3 gives a description of the current state of the art concerning the topic.
- Chapter 4 is devoted to a modelization of the MEMS. It will be divided in two sections : a mathematical modelization in four parts (2 degrees of freedom without damping, 2 degrees of freedom with damping, 3 degrees of freedom without damping, 3 degrees of freedom with damping), an electrical modelization (conversion process into an electrical model, scaling to common component values (R,L,C), the use of resonators to achieve high Q as MEMS).
- Chapter 5 exposes the results of the modelization in the same order as the chapter 4.
- Based on the obtained results, chapter 6 introduces several techniques to measure mass variation.
- Chapter 7 shows the results of the different techniques suggested.
- Chapter 8 is the conclusion of this work.
- Chapter 9 suggests further improvements.

Chapter 2

Motivation and objectives

2.1 Motivation

In the measurement field, many techniques already exist to measure with precision tiny masses (10^{-15}kg to 10^{-20}kg). However, those techniques often imply very complex systems like mass spectrometry or electron microscopy which have many drawbacks : they are very expensive, they take up a large space, it takes a long time to learn how to use them and become efficient with them. Finally the collection of data is time consuming. Based on this premises, MEMS were used to solve those problems. Microsystems usually use resonant devices to compute a mass variation. The easiest one is the one degree of freedom system often built by simply using a cantilever beam that oscillates on its own resonant frequency. However, this technique has shown its limits in terms of sensitivity. The system was then extended to a two degrees of freedom model which showed a better sensitivity to perturbation. In extension, three degrees of freedom systems were built to measure stiffness perturbation and showed very good results. It was then decided to investigate the effect of mass perturbation on a three degrees of freedom system.

2.2 Objectives

The research on three degrees of freedom weakly coupled systems is still in its early research phase. A lot of information could be interesting in that field and many people are already working on this subject. The task that was assigned to this master thesis was to study the existing chips and to create models in order to represent their response to mass perturbation. Models should be able to provide information such as the resonant frequency, the amplitude response at resonant frequency and at other frequencies, ... Another important task was to find techniques with a better sensitivity to quantify the mass perturbation based on model results.

Chapter 3

State of the art

3.1 Mass measurement methods

It was not necessary to await the emergence of very specific MEMS to be able to measure tiny masses. Many techniques already exist and they all have strengths and weaknesses. Hereunder, a brief overview of some techniques :

Electron microscopy[10, 21, 28] The electron microscope uses a beam of electrons to illuminate a sample. This type of microscope can reach a zooming factor of 10 millions due to the electron that can have a wavelength 100,000 times smaller than a photon. By assuming that the density of the sample is known or can be obtained, the electron microscope is used to measure the size of the sample. It is then easy to compute the mass of the sample by integrating the density over the size. For an odd shape particle (such as Au), this solution could achieve an error of 20%. However, the measurement process is very slow and the equipment is very expensive. Moreover, this technique requires the ability to isolate the sample of interest. An example of picture obtained by electron microscopy is shown in figure 3.1.

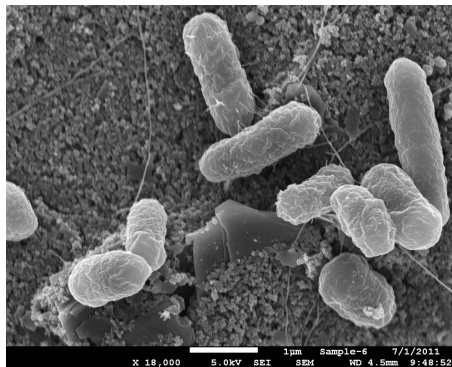


Figure 3.1: *E. coli O157:H7* bacteria seen by a electron microscope. Picture from [20]

Mass spectroscopy[10] This technique consists in cutting and ionizing a sample (molecule, protein, ...) to sort its components in function of the ratio mass over charge. There are many ways to ionize the sample (electrospray ionization (ESI)[4], matrix-assisted laser desorption/ionization (MALDI)[4], fast atom bombardment(FAB)[4], ...). This assumes the sample and its components can be cut and ionized. The main drawback of this technique is the destruction of the sample. Figure 3.2 shows an example of graphic obtained by mass spectrometry.

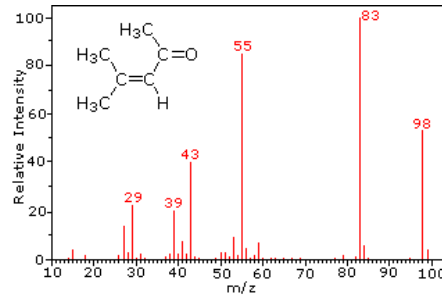


Figure 3.2: Example of a mass spectrum obtained by mass spectroscopy. Each peak represents a fragment of the molecule. The graph often contains a peak of unbroken sample on the right. Based on those peaks, it is possible to compute the mass of the sample. Picture from [22]

Nanometer-scale pore[18] For this third case, a membrane with a single nanometer-scale pore is used to separate two chambers. Particles of interest are put on one side and are driven into the membrane or possibly to the other side by an electric field. When particles go through the pore, it induces a change in the pore's ionic conductance. The rate of crossing particles can be measured. The mass density and the mass of the particles can be determined using the previous measurements with a sedimentation process. The membrane can be made in two ways : using a stretchable elastomeric membrane containing a pore which can be tuned, or using a solid-state membrane in which a pore is etched. This mass measurement system is small and relatively quick (data acquisition last less than 2 minutes)

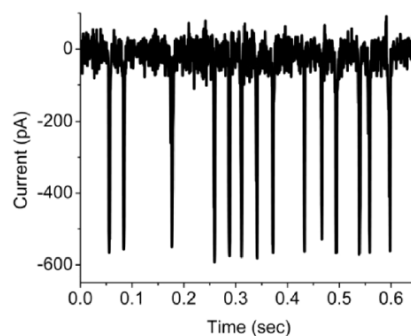


Figure 3.3: Example of current measurement resulting from particle crossing the membrane. Picture from [18].

Nanoscale cantilever[3, 13, 6] This technique uses nanoscale cantilever beams. Based on their design dimensions and material properties, the resonant frequency of these beams is known. When a bacteria, a virus or any other type of mass is added on the top of the beam, its resonant frequency is changed. By measuring this new frequency, the addition mass can be measured. This technique is cheap and easy to produce.

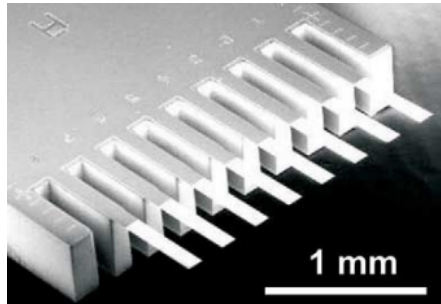


Figure 3.4: Example of an array of cantilever beams developed by IBM. Picture from [8]. By adding a mass on one beam, its resonant frequency is changed. The measurement of the new frequency allows to determine the mass variation. It is also possible to measure the beam deflection by using optical devices, strength gauges, ...

3.2 MEMS fabrication

MEMS can be made in two main ways : bulk micromachining where the MEMS is etched from a piece of material, and surface micromachining where the MEMS is grown on a substrate. Those two types of MEMS have their own creation processes which are listed and described hereunder.

3.2.1 Bulk micromachining

The most common technique to etch MEMS in bulk micromachining process is lithography[15]. The material to etch (let us assume it is made of polysilicon) is covered with a first photoresistive layer. A mask is placed on this protective layer and the MEMS is illuminated. The effect of the light is to chemically change the first layer which can be removed (resp. kept) when put in contact with an etchant. The result of this first operation is then etched by a second etchant that will attack the second layer (polysilicon one) everywhere except where the photoresistive layer is still present. Finally, the remaining photoresistive layer is removed to keep only the initial layer (polysilicon). All those steps are represented in figure 3.5. The mask can be positive (i.e. the mask is colored as the pattern we want to reproduced on the MEMS and the light make the photoresistive layer etcheable) or negative (i.e. the mask is colored as the patern we want to remove on the MEMS and the light make the photoresistive layer resistant to etchant). The etchant can be a liquid (we speak about wet etching) or a gaz (we speak about dry etching) and in both cases, the etching process can be isotropic (the etching is made equally in all directions, making round structures) or anisotropic (the etching is stronger in certain directions,

making sharp structures). In order to illuminate the MEMS light was used as an example. However, this could be done with electron beams, X-rays, etc.

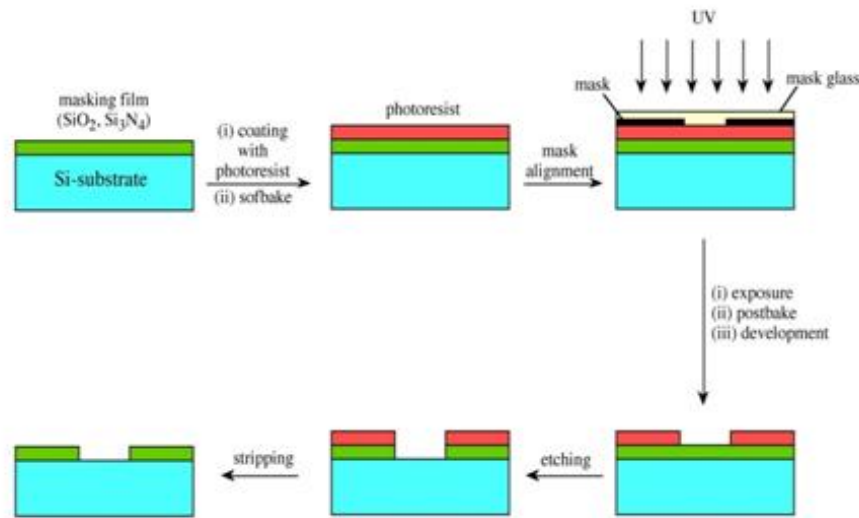


Figure 3.5: Representation of the many steps made to etch a MEMS. The first layer (SiO_2 , Si_3N_4) is protected by a photoresistive material. A mask is applied to activate the photoresistive layer. Activated (resp. non activated) zones of the photoresistive layer are etched in positive (resp. negative) masking. A silicon layer is then etched where the photoresistive layer is etched. Finally, the remaining photoresistive layer is removed. Picture from [2]

3.2.2 Surface micromachining

The surface micromachining[15] process uses sacrificial layers. An example of a cantilever beam (see figure 3.6) will be used to explain more easily the different processes of growing a MEMS. A first sacrificial layer (SiO_2) is deposited on the medium (step 1 in picture) with a second layer (photoresistive layer) which is added on the top (step 2). By using a mask, the photoresistive layer can be activated (step 2) and etched. A second etching process will remove the sacrificial layer which is not anymore covered by the photoresistive layer (step 3). The remaining part of the photoresistive layer is then removed to keep the remaining part of the sacrificial layer only (step 4). A new layer (made for example in polysilicon) is added. This layer will be a part of the final structure (step 5). A new photoresistive layer is added on the top, is activated by using a mask and is partially removed to keep the wanted shape (step 6). One more etching is realized to remove the unwanted part of the polysilicon layer (the one used for the final structure) (step 7). The leftovers of the photoresistive layer are removed (step 8), and the sacrificial layer (SiO_2) is also removed (step 9) to keep the final structure only which is a cantilever beam. This process was quite simple using only one sacrificial layer. In practice, MEMS could be produced by using several sacrificial layers.

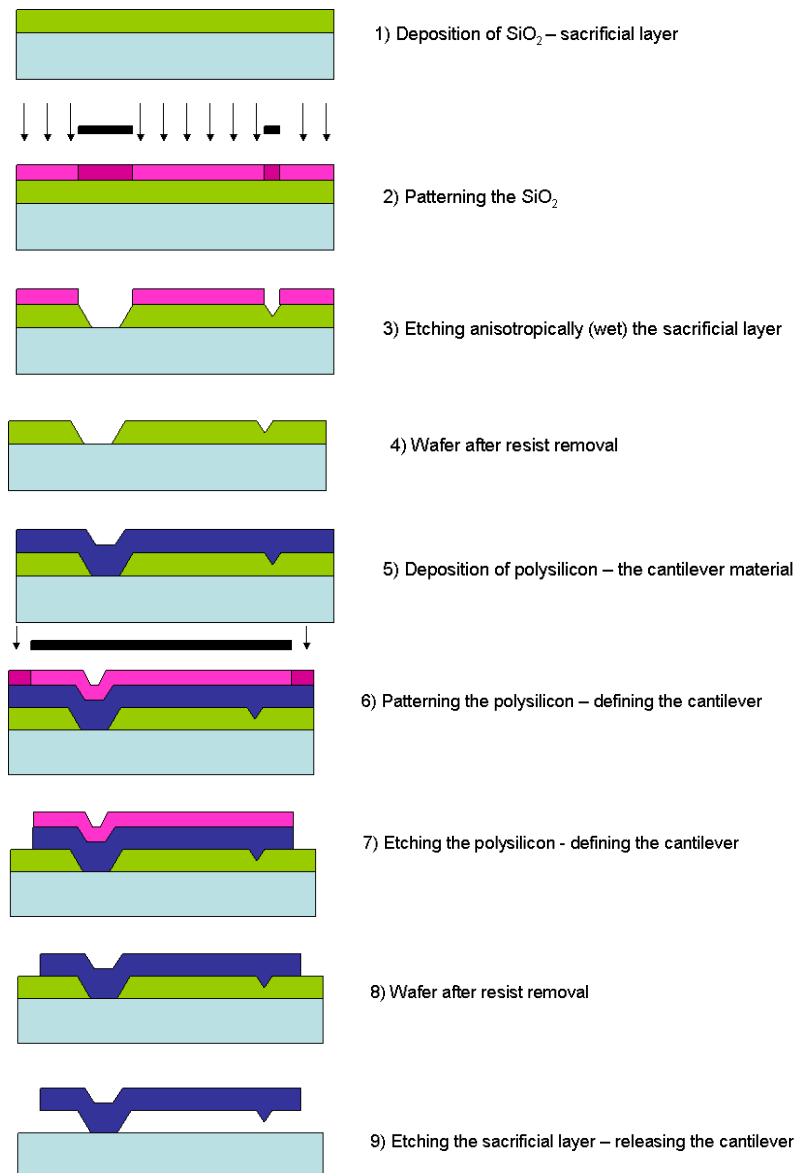


Figure 3.6: Different steps used to grow a MEMS by surface micromachining process. Some complex MEMS require the use of several sacrificial layers. Picture from [11]

3.2.3 Other types

Although the two previous techniques (Bulk and Surface micromachining) are the most famous ones, there are some other processes to create MEMS. They are briefly explained in the list hereunder :

Pop-Up structure[15, 23] MEMS are built like origami. A thin sheet (made for instance of polysilicon) is cut in a clever way. This sheet is then folded to obtain the structure. The folding process can be made by several techniques like fluid agitation, on-chip actuators, magnetic forces, surface tension, ...

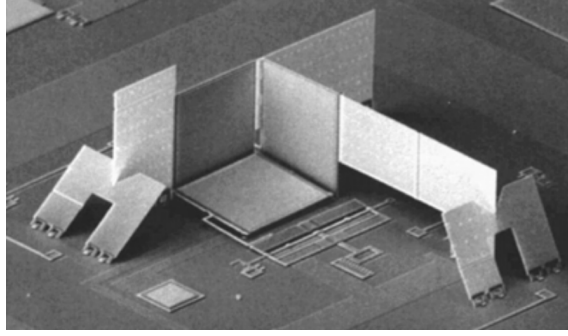


Figure 3.7: Corner cube reflector made by using pop-up structure. Picture from [23]

LIGA[15, 19] LIGA comes from the German words "Lithographie", "Galvanik" and "Abformung" which mean "Lithography", "electroplating" and "molding". In this process, a mask is applied on the substrate and a deep X-Ray lithography is made. The exposed substrate is then removed to get a mold of the MEMS. The mold is then filled for instance with nickel to get a pattern which will be used to emboss many MEMS.

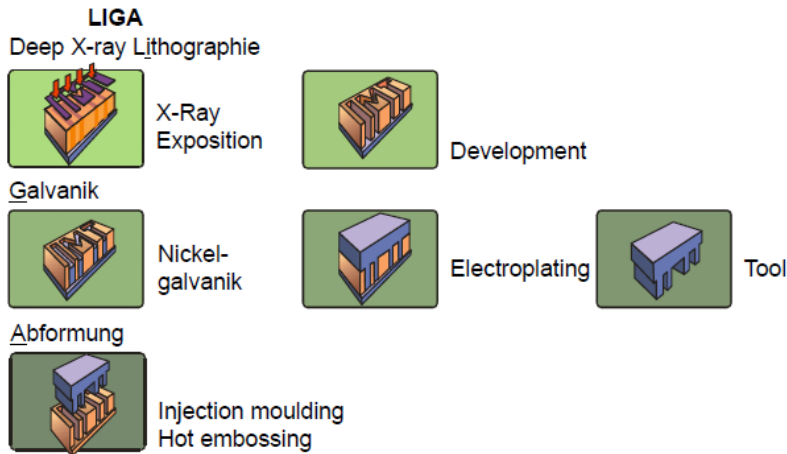


Figure 3.8: Illustration of the LIGA process. Picture from [15]

3.3 Three degrees of freedom weakly coupled resonators for stiffness measurement.

Chun Zhao[34] has developed a MEMS based on three proof masses coupled by electrostatic force between each other and linked to the medium by beams. A picture taken by a scanning electron microscope is shown in figure 3.9. There are many important parts in the figure that should be detailed :

- There are three proof masses which are used as resonators. They are supposed to be identical in the initial configuration.

- Each proof mass is connected to the medium by four beams. The beams of the middle mass are thicker to have a higher stiffness.
- Lower beams of resonator 1 and resonator 3 are not directly connected to the medium. There is a small gap that can be adapted by applying a coupling voltage to change its size and thus change the stiffness of the beam. This allows to introduce a perturbation easily.
- Mass 1 and 3 have comb fingers which can be used to measure their displacement. Since mass 2 does not have any comb fingers, it will not be possible to measure its position. Notice that masses possess two groups of comb fingers (upper and lower) which are not the same and which can be used for a differential measurement.
- Mass 1 (resp. Mass 3) can be excited by applying a voltage on the left (resp. right) electrode next to it.

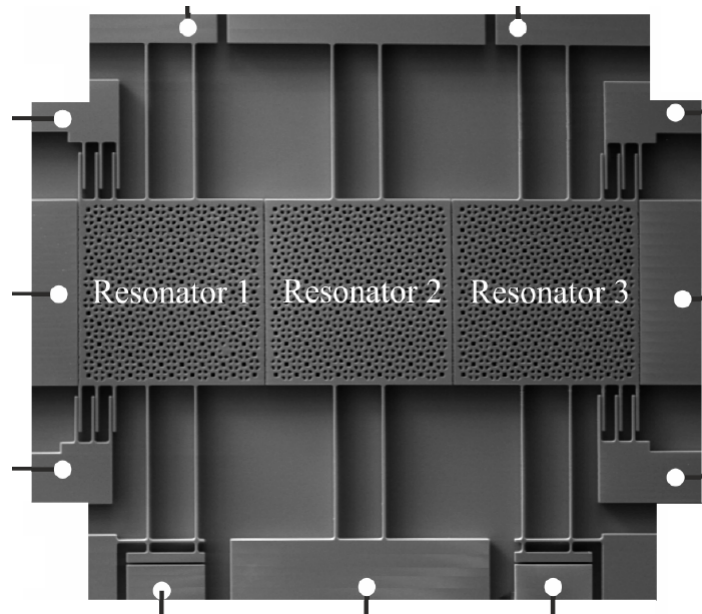


Figure 3.9: Scanning electron microscope picture of the three degrees of freedom weakly coupled resonators used by Chun Zhao and in this master thesis. White dots represent connection pads. Picture from [34].

Chun Zhao[34] has built models based on stiffness perturbation to compute the shifting of resonant frequencies, the variation of amplitude of movement of masses. Thoses models assumed the MEMS operated in vacuum. Based on those models he showed that the resonant frequency and the amplitude change linearly with the stiffness in certain zones and remain constant in other ones. Moreover, he showed that the amplitude ratio variation (between mass 1 and mass 3) is more sensitive to stiffness than frequency shifting. A summary of the results about stiffness perturbation is shown in figure 3.10

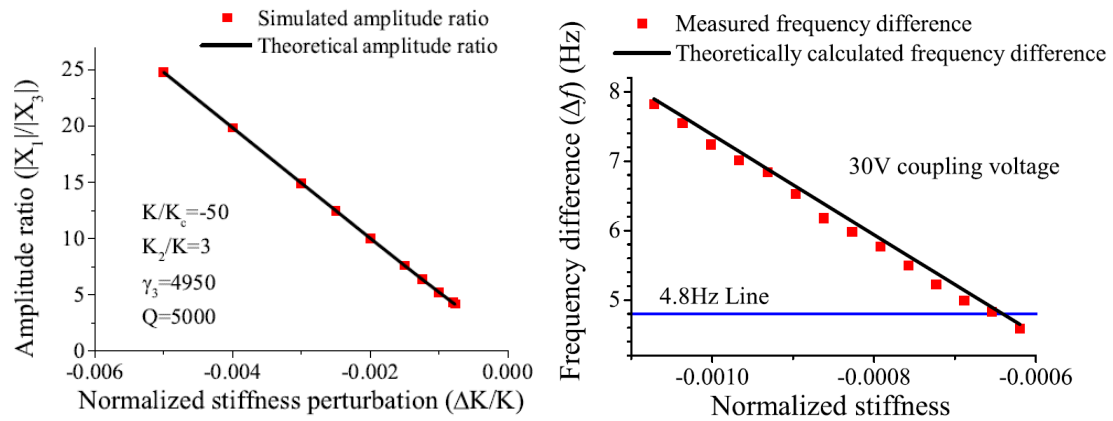


Figure 3.10: Summary of Chun Zhao's results about stiffness perturbation. It can be seen that except for around zero perturbation, the response of the absolute amplitude ratio and the frequency is linear to the stiffness. Picture from [34] and [5]

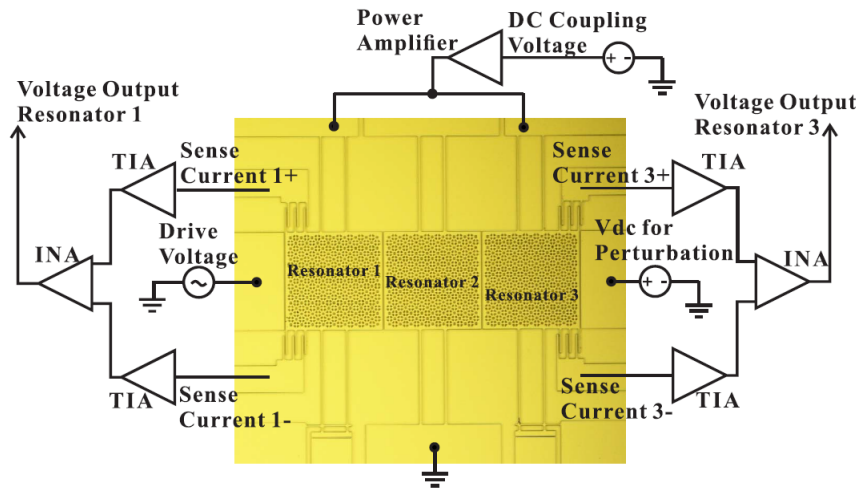


Figure 3.11: Schematics of the differential measurement circuit proposed by Chun Zhao. Picture from [5]

In order to be able to measure the tiny motional current created by masses displacement, Chun Zhao proposed an electrical measurement circuit based on the two differential circuits that output an amplified voltage in function of the current. The schematics of this circuit are shown in figure 3.11 and the built board used to make measurements is shown in figure 3.12

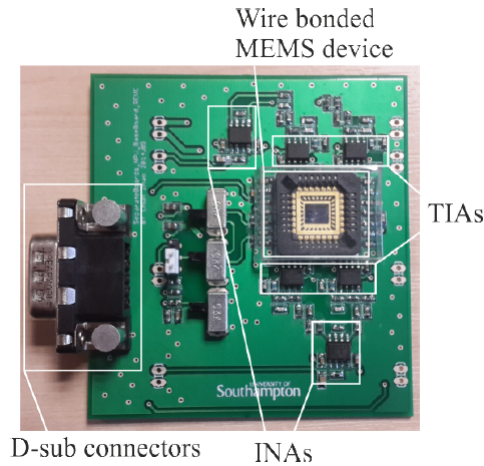


Figure 3.12: Board used by Chun Zhao to make measurements with the MEMS. This board is based on the schematics visible in picture 3.11. Picture from [5]

M.H. Montaseri[17] also tried to use the MEMS in air (i.e. with a much higher damping and then a lower Q factor). He noticed that the MEMS was still working and could achieve good results as shown in figure 3.13.

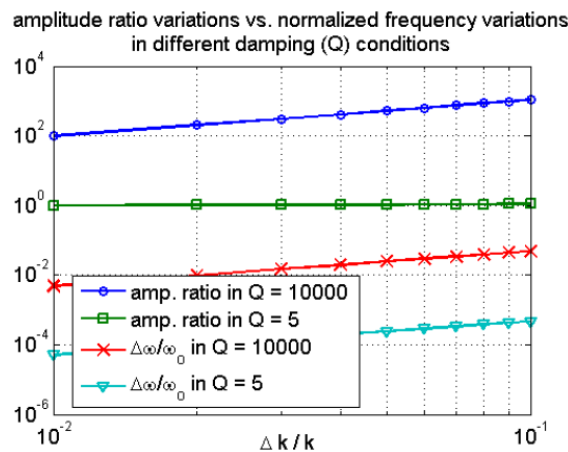


Figure 3.13: Comparison between sensitivity in vacuum and in air. Picture from [17]

3.4 Measurement tool

If there is a need for measuring the amplitude of a very noisy AC signal like in figure 3.14, neither a rectifier nor a typical sampler can be used to measure this amplitude.

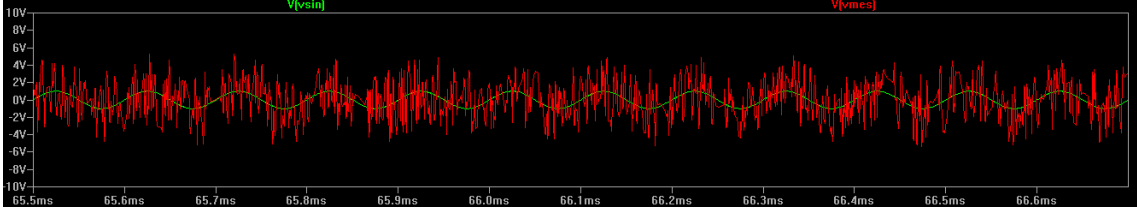


Figure 3.14: Example of a noisy sine wave simulated on LTspice. In green the pure sine wave, in red the sine wave with noise.

The lock-in amplifier is a powerful tool which can be used to extract the amplitude of a noisy sine wave, provided a reference signal of the same frequency as the noisy sine wave is available. This measurement tool is mainly composed of a "Phase Sensitive Detector" (PSD) which will multiply the reference signal with the measured signal and filter the result with a low pass filter. Figure 3.15 show a diagram of the working principle of a lock-in amplifier.

Phase Sensitive Detection (PSD)

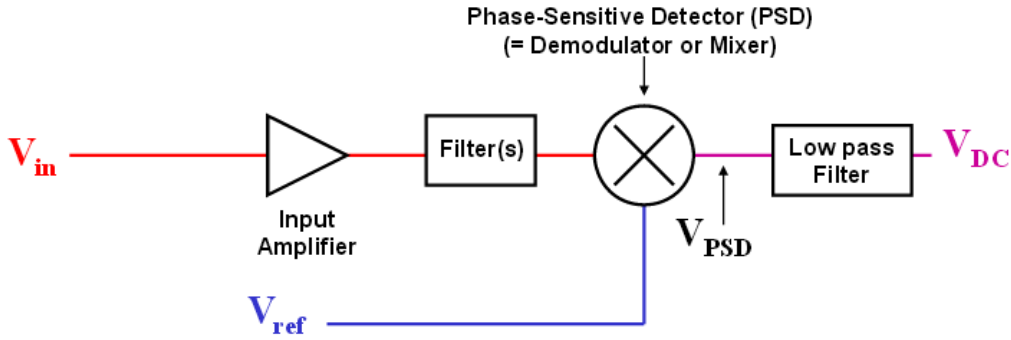


Figure 3.15: Working principle of a lock-in amplifier. The signal of interest is multiplied by a reference signal and filtered. Picture from [24]

By assuming the input signal is : $V_{in} = A\sin(\omega t) + N(t)$, with $N(t)$ an additive noise signal. And by supposing the reference signal is : $V_{ref} = B\sin(\omega t + \phi)$ a sine wave at the same frequency as the input signal with a phase shift of ϕ compared to V_{in} . Then, after the PSD block, the output is the product of the two signals, which is :

$$\begin{aligned}
 V_{product} &= V_{in} \cdot V_{ref} \\
 &= (A\sin(\omega t) + N(t)) \cdot (B\sin(\omega t + \phi)) \\
 &= A \cdot B \cdot \sin(\omega t) \cdot \sin(\omega t + \phi) + B \cdot N(t) \cdot \sin(\omega t + \phi)
 \end{aligned} \tag{3.1}$$

By using Simpson's formula :

$$\sin(\alpha) \cdot \sin(\beta) = \frac{1}{2}(\cos(\alpha - \beta) - \cos(\alpha + \beta)),$$

it comes :

$$V_{product} = \frac{1}{2}AB\cos(\phi) - AB\cos(2\omega t + \phi) + BN(t)\sin(\omega t + \phi)$$

When $V_{product}$ is filtered, only the low frequency components are kept. The output signal is thus :

$$V_{mes} \approx \frac{1}{2}AB\cos(\phi)$$

Typical evolution of the output signal is shown in figure 3.16

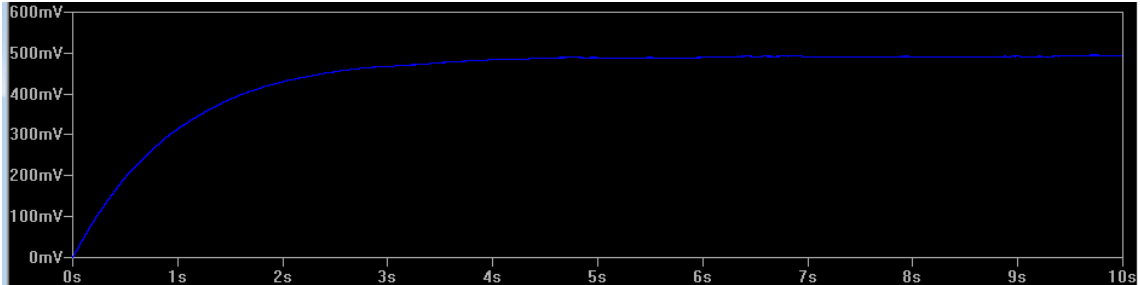


Figure 3.16: Typical output signal of a lock-in amplifier low pass filter.

Chapter 4

MEMS Modelization

As it was exposed in the previous section, the MEMS is supposed to be used for a new type of measurement. The first step to correctly use the chip is to characterize it. This key step starts with the modelization process. In this section, different approaches will be described. It will start with a mechanical modelization including a mathematical model. This first approach will be followed by the conversion of the system into an electrical model. This one will provide an easier way to make frequency analysis and time-domain simulation. Thanks to the equivalent circuit obtained, it will be possible to substitute the MEMS that is costly and fragile with an equivalent electrical circuit that is more robust and easy to build.

4.1 Mechanical Modelization

The MEMS, which was designed by Chun Zhao, is shown on figure 3.9. As it can be seen, it is composed of three masses all linked to the medium by four beams. On the two external masses, comb fingers were placed either to measure their position or to excite the system. To couple the three subsystems, a DC voltage is applied between masses. This leads to an electrostatic coupling. The MEMS can therefore be modeled by the mechanical system shown on figure 4.1.

This model can be perturbed in three main ways :

Changing the stiffness of a beam : The MEMS was designed to be able to change one beam stiffness by applying a DC voltage. This is the approach that was used by Chun Zhao in his thesis. This approach shows good results but is not easily useable. Indeed it is not easy to find a measurand whose effect is a change in the stiffness of a beam (temperature and humidity are a few examples).

Changing the damping of the system : The MEMS is supposed to operate in vacuum. Using it in air or in any other environment would lead to a variable damping coefficient. This way was already explored[17]. Again, this is not the way we are interested in.

Changing the value of one mass in the system : By adding a small additional mass to one of the three reference masses, the system will exhibit a change

in characteristics usable to determine this mass variation. Making the mass change is an easy process which could be done by biological ligands, surface tension forces, etc.

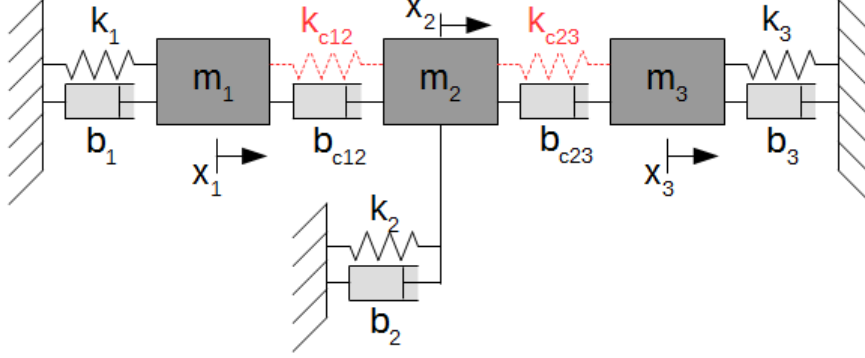


Figure 4.1: Mechanical modelization of the MEMS. Three masses (m_1 , m_2 and m_3) linked to the chip by beams which are represented here by springs (k_1 , k_2 and k_3) and damping pots (b_1 , b_2 and b_3). The three masses are coupled with their neighbors by an electrostatic coupling obtained by a DC voltage and represented with a spring in dashed lines (k_{c12} and k_{c23}). Depending on the medium (vacuum, air, water), a damping effect can appear. It is modelized by a damping pot (b_{c12} and b_{c23}).

4.1.1 Method of eigenvalues

Based on the model exposed above and the values obtained by Chun Zhao[34] the study of the MEMS could be done with usual mathematical tools, as for common mechanical systems. A first important information to determine is the single or multiple natural resonant frequencies of the chip. The first technique used to determine them is the eigenvalues method. Based on the variable stiffness model[34], the variable mass model was created and the equations are detailed hereunder. The following explanations will start with an easier model, simpler to understand, which is a two degrees of freedom system without any damping. A second one with added damping will then be obtained and finally the same principle will be applied to the three degrees of freedom MEMS.

Two degrees of freedom

The explanation of the computation is started with a two degrees of freedom (see figure 4.2).

The first Newton's law gives :

$$\sum_i \vec{f}_{i,j} = m_j \cdot \vec{a}_j = m_j \cdot \vec{\ddot{x}}_j \quad (4.1)$$

Where $f_{i,j}$ is the i -th force acting on mass j .

When 4.1 is applied to the first mass (m_1) and if we initially assume there is no external excitation, no damping ($b_1 = b_2 = b_{c12} = 0$), no coupling between the masses ($k_{c12} = 0$) and that x_j is the displacement of the j-th mass compared to its rest position, we simply obtain :

$$\begin{cases} f_1(t) = m_1\ddot{x}_1(t) + k_1x_1(t) = 0 \\ f_2(t) = m_2\ddot{x}_2(t) + k_2x_2(t) = 0 \end{cases} \quad (4.2)$$

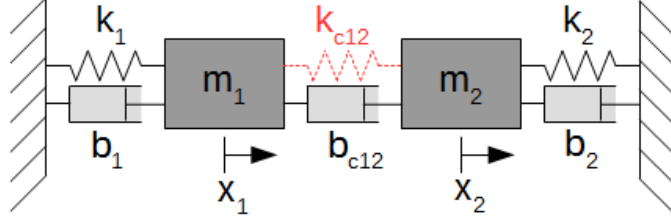


Figure 4.2: Simpler mechanical system used to study the model shown in the figure 4.1. Two masses (m_1 and m_2) linked to a reference medium by springs (k_1 and k_2) and damping pots (b_1 and b_2). The two masses are coupled with their neighbor by an electrostatic coupling represented with a spring in dashed line (k_{c12}). An hypothetical damping effect is modeled by a damping pot (b_{c12}).

If an electrostatic coupling is created between the two masses ($k_{c12} < 0$)¹, equations from system 4.2 become :

$$\begin{cases} f_1(t) = m_1\ddot{x}_1(t) + k_1x_1(t) + [x_1(t) - x_2(t)]k_{c12} = 0 \\ f_2(t) = m_2\ddot{x}_2(t) + k_2x_2(t) + [x_2(t) - x_1(t)]k_{c12} = 0 \end{cases} \quad (4.3)$$

System 4.3 could also be written in a matrix form :

$$\begin{aligned} \begin{bmatrix} f_1 \\ f_2 \end{bmatrix} &= \begin{bmatrix} m_1 & 0 \\ 0 & m_2 \end{bmatrix} \begin{bmatrix} \ddot{x}_1 \\ \ddot{x}_2 \end{bmatrix} + \begin{bmatrix} k_1 + k_{c12} & -k_{c12} \\ -k_{c12} & k_2 + k_{c12} \end{bmatrix} \begin{bmatrix} x_1 \\ x_2 \end{bmatrix} \\ &= \begin{bmatrix} 0 \\ 0 \end{bmatrix} \end{aligned} \quad (4.4)$$

By using the Laplace transform, equations from system 4.3 become :

$$\begin{cases} m_1x_1(s)s^2 + k_1x_1(s) + [x_1(s) - x_2(s)]k_{c12} = 0 \\ m_2x_2(s)s^2 + k_2x_2(s) + [x_2(s) - x_1(s)]k_{c12} = 0 \end{cases} \quad (4.5)$$

Which can be written by posing $s = j\omega$:

$$\begin{cases} m_1x_1(j\omega_1)(-\omega_1^2) + k_1x_1(j\omega_1) + [x_1(j\omega_1) - x_2(j\omega_2)]k_{c12} = 0 \\ m_2x_2(j\omega_2)(-\omega_2^2) + k_2x_2(j\omega_2) + [x_2(j\omega_2) - x_1(j\omega_1)]k_{c12} = 0 \end{cases} \quad (4.6)$$

¹Because the coupling is an electrostatic coupling, the resulting force will be negative leading to a negative "stiffness".

And which can finally be written in a matrix form with $-\omega^2 = \lambda$:

$$\underbrace{\begin{bmatrix} f_1 \\ f_2 \end{bmatrix}}_F = \underbrace{\begin{bmatrix} \lambda_1 & 0 \\ 0 & \lambda_2 \end{bmatrix}}_\lambda \underbrace{\begin{bmatrix} m_1 & 0 \\ 0 & m_2 \end{bmatrix}}_M \underbrace{\begin{bmatrix} x_1 \\ x_2 \end{bmatrix}}_\mu + \underbrace{\begin{bmatrix} k_1 + k_{c12} & -k_{c12} \\ -k_{c12} & k_2 + k_{c12} \end{bmatrix}}_K \underbrace{\begin{bmatrix} x_1 \\ x_2 \end{bmatrix}}_\mu$$

$$= \begin{bmatrix} 0 \\ 0 \end{bmatrix}$$
(4.7)

Or in its compact form :

$$M\lambda\mu + K\mu = 0$$

$$\Rightarrow M\lambda + K = 0,$$
(4.8)

Matrix system 4.7 therefore become :

$$F = \lambda \begin{bmatrix} m_1 & 0 \\ 0 & m_2 \end{bmatrix} + \begin{bmatrix} k_1 + k_{c12} & -k_{c12} \\ -k_{c12} & k_2 + k_{c12} \end{bmatrix}$$

$$= \begin{bmatrix} m_1\lambda_1 + k_1 + k_{c12} & -k_{c12} \\ -k_{c12} & m_2\lambda_2 + k_2 + k_{c12} \end{bmatrix}$$

$$= 0$$
(4.9)

With the shape of equation 4.9 the eigenvalues can easily be calculated (e.g. by computing λ in order to have the matrix determinant equal to 0 or with the matlab function *eig*²). Once the values of λ are known, the values of the frequencies can be directly known : $f = \pm \frac{\sqrt{-\lambda}}{2\pi}$

In-phase and Out-of-phase mode for the two degrees of freedom case

The advantage of starting with a two degrees of freedom model is the ability to intuitively predict the behavior of the system. And a first piece of information that can be extracted without calculation is about the resonant modes. One can feel that there are two interesting frequencies in which the two masses will oscillate at the same frequency. One will be the in-phase mode, where they move in the same direction ($\frac{\dot{x}_1}{\dot{x}_2} > 0$), and the other one will be the out-of-phase mode, where they move in opposite directions ($\frac{\dot{x}_1}{\dot{x}_2} < 0$). Figure 4.3 illustrates those two modes. Between and outside those two frequencies, a compound state should be met. A more rigorous result will be obtained by using MATLAB simulation and is available in section 5.1.1.

Two degrees of freedom with imposed frequency

In the previous paragraph, the natural resonant frequency was computed. It is now interesting to know what the amplitude of the displacement of masses at an imposed

²The MATLAB documentation of *eig*[16] give : $[\mu, \lambda] = \text{eig}(-K, M)$, so that $-K\mu = M\mu\lambda$.

frequency would be. Based on equation 4.4 in its compact form, we can conclude that :

$$\begin{aligned}
 F &= M\ddot{X} + KX \\
 \Rightarrow F &= -\omega^2 M X + KX \\
 \Rightarrow X &= (-\omega^2 M + K)^{-1} F
 \end{aligned}
 \tag{4.10}$$

This can also be used in MATLAB or any other computation software to get the frequency response curve of the system by sweeping the imposed frequency.

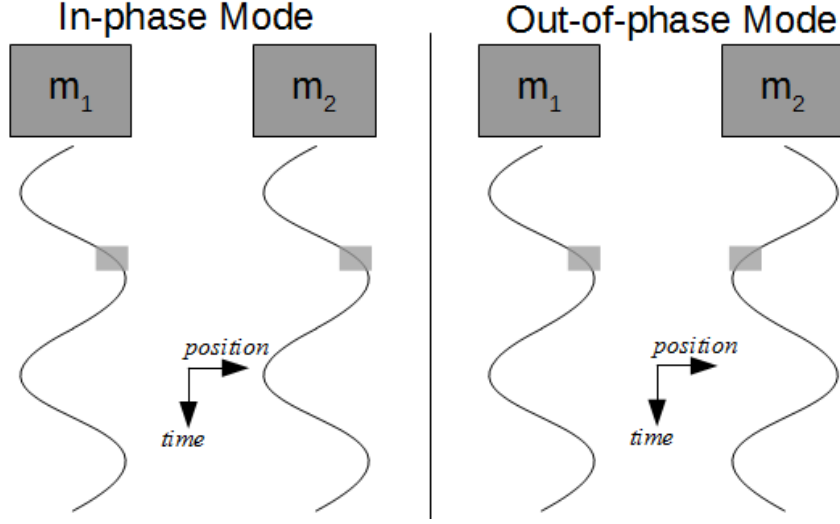


Figure 4.3: The two resonant frequencies exhibited by the system lead to two modes : the first one is the in-phase mode where the two masses oscillate at the same frequency in the same direction (left on the picture). The second one is the out-of-phase mode where the two masses oscillate at the same frequency but in opposite directions (right on the picture).

Two degrees of freedom with damping

Because the coupling between the mass and the medium is realized with non-ideal beams, a damping effect could occur. In order to take this effect into account, damping coefficient have to be added to the equation (b_1 and b_2 are not any more neglected). However it is still assumed that the MEMS is operating in vacuum and so b_{c12} remains neglected.

The new system of equations becomes :

$$\begin{cases}
 f_1(t) = m_1\ddot{x}_1(t) + b_1\dot{x}_1 + k_1x_1(t) + [x_1(t) - x_2(t)]k_{c12} = 0 \\
 f_2(t) = m_2\ddot{x}_2(t) + b_2\dot{x}_2 + k_2x_2(t) + [x_2(t) - x_1(t)]k_{c12} = 0
 \end{cases}
 \tag{4.11}$$

With the same development as before, system 4.11 reaches the following matrix form :

$$\begin{aligned}
\underbrace{\begin{bmatrix} f_1 \\ f_2 \end{bmatrix}}_F &= \underbrace{\begin{bmatrix} \lambda_1 & 0 \\ 0 & \lambda_2 \end{bmatrix}}_\lambda \underbrace{\begin{bmatrix} m_1 & 0 \\ 0 & m_2 \end{bmatrix}}_M \underbrace{\begin{bmatrix} x_1 \\ x_2 \end{bmatrix}}_\mu + j\omega \underbrace{\begin{bmatrix} b_1 & 0 \\ 0 & b_2 \end{bmatrix}}_B \underbrace{\begin{bmatrix} x_1 \\ x_2 \end{bmatrix}}_\mu \\
&+ \underbrace{\begin{bmatrix} k_1 + k_{c12} & -k_{c12} \\ -k_{c12} & k_2 + k_{c12} \end{bmatrix}}_K \underbrace{\begin{bmatrix} x_1 \\ x_2 \end{bmatrix}}_\mu \\
&= \begin{bmatrix} 0 \\ 0 \end{bmatrix}
\end{aligned} \tag{4.12}$$

Or in its compact form

$$\begin{aligned}
M\lambda\mu + j\omega B\mu + K\mu &= 0 \\
\Rightarrow M\lambda + j\omega B + K &= 0
\end{aligned} \tag{4.13}$$

The matrix system therefore becomes :

$$\begin{aligned}
F &= \lambda \begin{bmatrix} m_1 & 0 \\ 0 & m_2 \end{bmatrix} + j\omega \begin{bmatrix} b_1 & 0 \\ 0 & b_2 \end{bmatrix} + \begin{bmatrix} k_1 + k_{c12} & -k_{c12} \\ -k_{c12} & k_2 + k_{c12} \end{bmatrix} = \begin{bmatrix} 0 \\ 0 \end{bmatrix} \\
&= \begin{bmatrix} m_1\lambda_1 + j\omega b_1 + k_1 + k_{c12} & -k_{c12} \\ -k_{c12} & m_2\lambda_2 + j\omega b_2 + k_2 + k_{c12} \end{bmatrix}
\end{aligned} \tag{4.14}$$

Still in the same way as for the two degrees of freedom system without dumping, it can be shown that the amplitude of the displacement of the masses for a forced frequency excitation is :

$$X = (-\omega^2 M + j\omega B + K)^{-1} F \tag{4.15}$$

Three degrees of freedom

After the study of the two degrees of freedom system, it is easier to move to the three degrees of freedom model. The mechanical equivalent model is visible on figure 4.1. Assuming there is no external force and no damping ($b_1 = b_2 = b_3 = b_{12} = b_{23} = 0$) but an electrostatic coupling (k_{c12} and $k_{c23} < 0$), the equations that rule the system can be written as :

$$\begin{cases} f_1(t) = m_1\ddot{x}_1(t) + k_1x_1(t) + [x_1(t) - x_2(t)]k_{c12} = 0 \\ f_2(t) = m_2\ddot{x}_2(t) + k_2x_2(t) + [x_2(t) - x_1(t)]k_{c12} + [x_3(t) - x_2(t)]k_{c23} = 0 \\ f_3(t) = m_3\ddot{x}_3(t) + k_3x_3(t) + [x_3(t) - x_2(t)]k_{c23} = 0 \end{cases} \tag{4.16}$$

By doing the same operation as for the two degrees of freedom, i.e. using the Laplace transform, posing $s = j\omega$ and $\lambda = -\omega^2$, we can get the following matrix system :

$$\begin{aligned}
\underbrace{\begin{bmatrix} f_1 \\ f_2 \\ f_3 \end{bmatrix}}_F &= \underbrace{\begin{bmatrix} \lambda_1 & 0 & 0 \\ 0 & \lambda_2 & 0 \\ 0 & 0 & \lambda_3 \end{bmatrix}}_\lambda \underbrace{\begin{bmatrix} m_1 & 0 & 0 \\ 0 & m_2 & 0 \\ 0 & 0 & m_3 \end{bmatrix}}_M \underbrace{\begin{bmatrix} x_1 \\ x_2 \\ x_3 \end{bmatrix}}_\mu \\
&+ \underbrace{\begin{bmatrix} k_1 + k_{c12} & -k_{c12} & 0 \\ -k_{c12} & k_2 + k_{c12} + k_{c23} & -k_{c23} \\ 0 & -k_{c23} & k_3 + k_{c23} \end{bmatrix}}_K \underbrace{\begin{bmatrix} x_1 \\ x_2 \\ x_3 \end{bmatrix}}_\mu \\
&= \begin{bmatrix} 0 \\ 0 \\ 0 \end{bmatrix}
\end{aligned} \tag{4.17}$$

Which can also be written in its compact form :

$$\begin{aligned}
M\lambda\mu + K\mu &= 0 \\
\Rightarrow M\lambda + K &= 0,
\end{aligned} \tag{4.18}$$

Equations 4.18 are the same as 4.8. The method used to solve this system will therefore be the same as for the two degrees of freedom model.

Three degrees of freedom with imposed frequency

The amplitude of the displacement of masses at an imposed frequency is immediately obtained from equation 4.15. This equation is reminded hereunder :

$$X = (-\omega^2 M + K)^{-1} F \tag{4.19}$$

Three degrees of freedom with damping

This paragraph will be short since it is the generalization of the two degrees of freedom example. When the damping is added to system 4.16, it becomes :

$$\begin{cases} f_1(t) = m_1 \ddot{x}_1(t) + b_1 \dot{x}_1 + k_1 x_1(t) + [x_1(t) - x_2(t)]k_{c12} = 0 \\ f_2(t) = m_2 \ddot{x}_2(t) + b_2 \dot{x}_2 + k_2 x_2(t) + [x_2(t) - x_1(t)]k_{c12} + [x_2(t) - x_3(t)]k_{c23} = 0 \\ f_3(t) = m_3 \ddot{x}_3(t) + b_3 \dot{x}_2 + k_3 x_3(t) + [x_3(t) - x_2(t)]k_{c12} = 0 \end{cases} \tag{4.20}$$

Which has the matrix form :

$$\begin{aligned}
\underbrace{\begin{bmatrix} f_1 \\ f_2 \\ f_3 \end{bmatrix}}_F &= \underbrace{\begin{bmatrix} \lambda_1 & 0 & 0 \\ 0 & \lambda_2 & 0 \\ 0 & 0 & \lambda_3 \end{bmatrix}}_\lambda \underbrace{\begin{bmatrix} m_1 & 0 & 0 \\ 0 & m_2 & 0 \\ 0 & 0 & m_3 \end{bmatrix}}_M \underbrace{\begin{bmatrix} x_1 \\ x_2 \\ x_3 \end{bmatrix}}_\mu \\
&+ j\omega \underbrace{\begin{bmatrix} b_1 & 0 & 0 \\ 0 & b_2 & 0 \\ 0 & 0 & b_3 \end{bmatrix}}_B \underbrace{\begin{bmatrix} x_1 \\ x_2 \\ x_3 \end{bmatrix}}_\mu \\
&+ \underbrace{\begin{bmatrix} k_1 + k_{c12} & -k_{c12} & 0 \\ -k_{c12} & k_2 + k_{c12} + k_{c23} & -k_{c23} \\ 0 & -k_{c23} & k_3 + k_{c23} \end{bmatrix}}_K \underbrace{\begin{bmatrix} x_1 \\ x_2 \\ x_3 \end{bmatrix}}_\mu \\
&= \begin{bmatrix} 0 \\ 0 \\ 0 \end{bmatrix}
\end{aligned} \tag{4.21}$$

Or in its compact form

$$\begin{aligned}
M\lambda\mu + j\omega B\mu + K\mu &= 0 \\
\Rightarrow M\lambda + j\omega B + K &= 0
\end{aligned} \tag{4.22}$$

Here again, equations 4.22 are the same as 4.13. The method used to solve this system will therefore be the same as for the two degrees of freedom model with damping.

Finally, based on equation 4.15, the amplitude of the displacement of masses with damping at an imposed frequency is immediately obtained. The solution equation is :

$$X = (-\omega^2 M + j\omega B + K)^{-1} F \tag{4.23}$$

4.2 Electrical modelization

Once the two mechanical modelizations were made, it was interesting to convert this system into an electrical circuit. Because the values used in the test setup were different from the ones used by Chun Zhao, a new development had to be made. This section will start with an introduction to electrical conversion of mechanical systems and will be followed by the main steps which lead to the final model. Once the model is obtained in the electrical form, some information like quality factor (Q factor), resonant peak, output signal shape will be easily available and measurable.

4.2.1 Lump elements

To understand the equivalence between a mechanical system and an electrical one, it is important to start with easy examples. Let us take a simple RC circuit as in

figure 4.4.

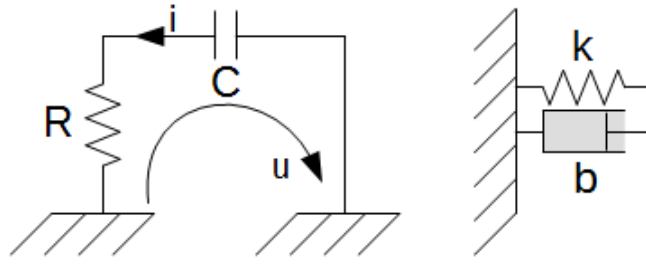


Figure 4.4: It can be shown that a circuit composed of a resistor in series with a capacitor behaves like a spring and a damping pot put in parallel.

By applying the second Kirchhoff's law, the following equation could be written :

$$u = Ri + \frac{1}{C} \int_t i dt = 0 \quad (4.24)$$

The current is the variation of the quantity of charges : $i = \frac{dq}{dt}$ which gives when replaced in the previous equation :

$$\begin{aligned} U &= R\dot{q} + \frac{1}{C}q = 0 \\ \Rightarrow \dot{q} &= -\frac{1}{RC}q \end{aligned} \quad (4.25)$$

The equivalent mechanical system is shown on figure 4.4 which is a spring and a damping pot in parallel. The behavior equation of this system is :

$$\begin{aligned} F &= F_{spring} + F_{damping} = 0 \\ \Rightarrow F &= kx + b\dot{x} = 0 \\ \Rightarrow kx &= -b\dot{x} \\ \Rightarrow \dot{x} &= -\frac{k}{b}x \end{aligned} \quad (4.26)$$

If we add a power supply to the RC circuit or an external force to the mechanical system (as shown on figure 4.5) equations 4.25 and 4.26 become :

$$\begin{aligned} U &= R\dot{q} + \frac{1}{C}q - V = 0 \\ \Rightarrow \dot{q} &= -\frac{1}{RC}q + \frac{V}{R} \end{aligned} \quad (4.27)$$

and

$$\begin{aligned} F &= F_{spring} + F_{damping} - f = 0 \\ \Rightarrow kx - f &= -b\dot{x} \\ \Rightarrow \dot{x} &= -\frac{k}{b}x + \frac{f}{b} \end{aligned} \quad (4.28)$$

The same approach could be made with a LC circuit represented in figure 4.6. As we did in the previous example, we write the second Kirchhoff's law :

$$\begin{aligned} u &= \frac{1}{C} \int_t i dt + L \frac{di}{dt} = 0 \\ \Rightarrow -\frac{1}{C}q &= L\dot{q} \\ \Rightarrow \ddot{q} &= -\frac{1}{LC}q \end{aligned} \quad (4.29)$$

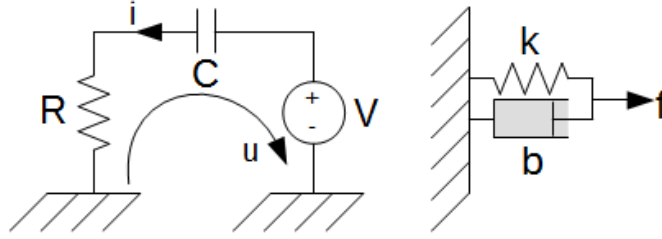


Figure 4.5: It can be shown that a circuit composed of a resistor in series with a capacitor and a source behaves like a spring and a damping pot put in parallel on which a force is applied.

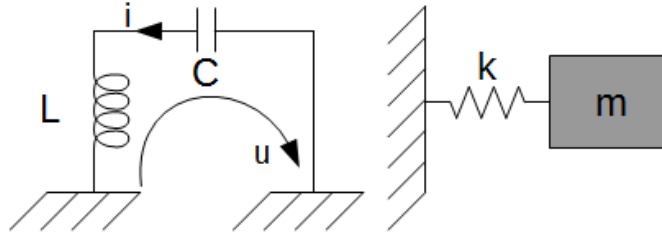


Figure 4.6: It can be shown that a circuit composed of an inductor in series with a capacitor behaves like a mass linked by a spring to the medium.

and

$$\begin{aligned}
 & F_{mass} + F_{spring} = 0 \\
 \Rightarrow & m\ddot{x} + kx = 0 \\
 \Rightarrow & \ddot{x} = -\frac{k}{m}x
 \end{aligned} \tag{4.30}$$

Based on those examples we could give four relations used to convert mechanical systems into electrical circuits :

$$\left\{ \begin{array}{ll}
 Force & \rightarrow Voltage \\
 Spring constant & \rightarrow 1/Capacitance \\
 Damping coefficient & \rightarrow Resistance \\
 Mass & \rightarrow Inductance
 \end{array} \right. \tag{4.31}$$

Now, by observing the MEMS, the first visible piece of information is that it is composed of three similar parts, all composed of a mass, a spring and a damping pot like in figure 4.1. This could be modeled by a RLC circuit in an analog way as the examples explained before. However, there remains one case that is still not explained, the case when masses are coupled. Let us study a system composed of two sub-systems not coupled, each composed of a mass and a spring as shown in figure 4.7.

The first system is a simple LC circuit just as the second one which are both represented in figure 4.7. When we link the two masses by a spring (as on figure 4.8, we get the following equations :

$$\left\{ \begin{array}{l}
 F_1 = m_1\ddot{x}_1 + k_1x_1 + (x_1 - x_2)k_c = 0 \\
 F_2 = m_2\ddot{x}_2 + k_2x_2 + (x_2 - x_1)k_c = 0
 \end{array} \right. \tag{4.32}$$

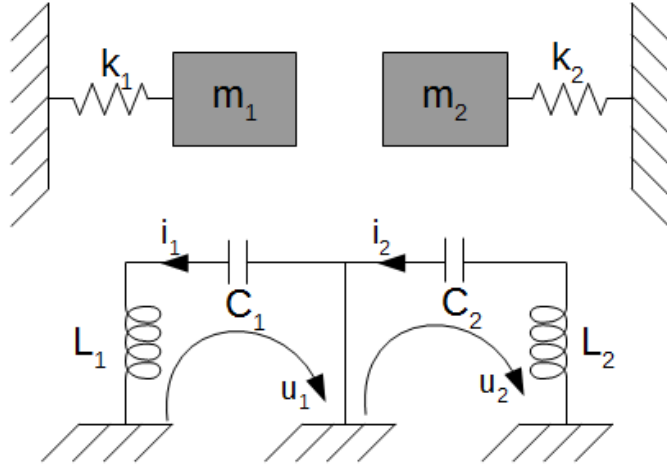


Figure 4.7: Two systems composed of a mass and a spring not coupled behave like two independents RL systems.

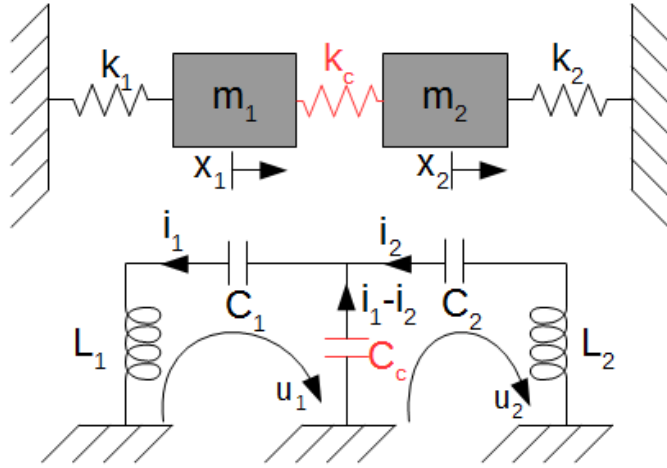


Figure 4.8: When two sub-systems, each of which is composed of a mass and a spring, are coupled by a spring, the resulting system behaves like two RL circuits connected by a same point to the ground through a capacitor.

Which can be converted into the electrical form by using the previous relations in :

$$\begin{cases} U_1 = L_1 \ddot{q}_1 + \frac{1}{c_1} q_1 + (q_1 - q_2) \frac{1}{c_c} = 0 \\ U_2 = L_2 \ddot{q}_2 + \frac{1}{c_2} q_2 + (q_2 - q_1) \frac{1}{c_c} = 0 \end{cases} \quad (4.33)$$

Which can be rearranged as :

$$\begin{cases} U_1 = L_1 \frac{di_1}{dt} + \frac{1}{c_1} \int_t i_1 dt + \frac{1}{c_c} \int_t (i_1 - i_2) dt = 0 \\ U_2 = L_2 \frac{di_2}{dt} + \frac{1}{c_2} \int_t i_2 dt + \frac{1}{c_c} \int_t (i_2 - i_1) dt = 0 \end{cases} \quad (4.34)$$

Which is the equation that rules the electrical circuit represented in figure 4.8.

Based on those few examples, the equivalent electrical circuit of the MEMS is easily obtained and displayed in figure 4.9.

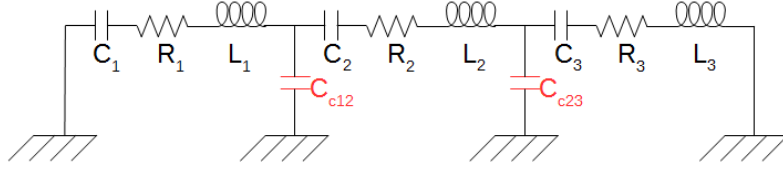


Figure 4.9: Electrical circuit that behave in the same way as the MEMS. The three horizontal R , L and C components model the three masses linked to the medium by beams. The two vertical capacitors (in red) model the two springs that coupled the three sub-systems.

By using the equation given by [12], and reminded here :

$$\begin{cases} R_{eq} = \frac{\gamma}{\eta^2} = \frac{\sqrt{KM}}{Q\eta^2} \\ C_{eq} = \frac{\eta^2}{K} , \\ L_{eq} = \frac{M}{\eta^2} \\ \eta = V_{dc}\epsilon \frac{A_{el}l}{d^2} \end{cases} \quad (4.35)$$

$$\text{with } \begin{cases} V_{dc} = 48V, \text{ the continuous voltage applied between the masses} \\ \epsilon = 8.85 \times 10^{-12} F.m^{-1}, \text{ the permittivity of the medium} \\ A_{el} = 50\mu m \times 300\mu m, \text{ the surface of electrodes} \\ d = 6\mu m, \text{ the distance between the two electrodes} \end{cases} \quad (4.36)$$

We can get the following value for the equivalent circuit :

$$\begin{cases} L_1 = L_2 = L_3 \approx 2.2131 \times 10^5 H \\ C_1 = C_3 \approx 5.4423 \times 10^{-16} F \\ C_2 \approx 1.5714 \times 10^{-16} F \\ C_{12} = C_{23} \approx -4.5447 \times 10^{-14} F \\ R_1 = R_3 \approx 2.0165 \times 10^5 \Omega \\ R_2 \approx 3.7527 \times 10^5 \Omega \end{cases} \quad (4.37)$$

4.2.2 Common value

The main drawback of the equivalent circuit is that it uses uncommon or non-physical values for the components. Using such huge inductances for coils or such tiny (and sometime negative) capacitances for capacitors makes it impossible to build the circuit for real. In order to solve the problem of the coil, there are two possible ways to do it. The first is to use an active equivalent circuit (gyrator like). However in the equivalent circuit of the gyrator, the coil is not connected in series but to the ground. It is thus very difficult to modelize the huge coil by its equivalent circuit properly. A second way would be to scale all the values of the circuit. This is the chosen solution. The two main properties that are important to keep, are the resonant frequency and the Q factor. If the inductance is divided by N, the

capacitance must be multiplied by a factor N to keep the same resonant frequency. Moreover, in order to keep the same Q factor, it is necessary to divide the resistance by N too. Because the coil is the component with the most difficult value to obtain precisely³ and because the three coils in the circuit need their inductance values as close as possible, the scaling ratio was computed based on a real coil available in shops. After tuning all those parameters, the new values obtained were :

$$\left\{ \begin{array}{l} L_1 = L_2 = L_3 \approx 360mH \\ C_1 = C_3 \approx 334.57pF \\ C_2 \approx 96.606pF \\ C_{12} = C_{23} \approx -279.39nF \\ R_1 = R_3 \approx 328m\Omega \\ R_2 \approx 610.4m\Omega \end{array} \right. \quad (4.38)$$

Those new values are much more realistic except for two things :

- Obtaining a total resistance of $328m\Omega$ for a coil of $360mH$ in series with a capacitor is very difficult⁴
- The negative capacitance is still a problem since it is not physical.

In order to solve the first problem it was decided to use a coil wound around a toroidal core made of nanocrystalline material. Indeed, using a ferrite core and wire copper to make the coil, would have required a wire with a diameter of approximately $2.5mm$ in order not to exceed this tiny resistance⁵. Even if it is feasible, that would have been heavy, large and difficult to make. By using the nanocrystalline material (which has a relative magnetic permeability approximately 10 times higher[7] than common ferrite material), a better result could be achieved. A commercial transformer of two windings of $90mH$ with a resistance of $110m\Omega$ was available. By putting the two windings in series, the coil obtained has an equivalent inductance of $360mH$ and a resistance of $220m\Omega$ which perfectly fulfill the needs of the circuit. Another solution would have been to create a floating negative resistance using a negative impedance converter. However, this solution was not chosen because it is more complex and could introduce other negative effects due to operational amplifiers⁶.

In order to solve the second problem, the solution would have been to use a gyrator circuit that would have modelled the behavior of a negative capacitance. However, even if the gyrator circuit is quite simple in theory, it was very hard, after many attempts, to make it work as wanted. Finally, it was decided to use a positive capacitor. This means that the modeled coupling is made mechanically instead of electrostatically and the consequences of this change are explained hereunder :

³Resistors and capacitors can be combined in series and parallel easily while it is harder to do with coil which have larger size

⁴Typical resistance for coil of $360mH$ is between few Ohms and hundreds of Ohms

⁵This value strongly depends on the type of ferrite used, its shape, the presence or not of a gap, etc.

⁶Some amplifiers, depending on their model and their brand will introduce distortion on the signal, parasitic signal, ...

Permutation of the two resonant peaks By using a mechanical spring (i.e. a positive spring constant), the force is applied in the opposite direction. The two modes (in-phase and out-of-phase) will then be swapped in terms of frequency. This modification is not very critical as long as we keep this information in mind while making measurements and conclusions.

Frequency shift Reversing the coupling force induces a small (less than 1% in this case) shift of the resonant frequency curve. However, the order of magnitude for commercial capacitor tolerance is typically 10% to 20%⁷ which introduces a higher frequency shift than the one caused by the positive capacitor.

In addition to the component tolerance, another problem is that the value computed above was a theoretical value. It is impossible to buy such a value in a shop. Even by combining in series and parallels many components to approach the estimated value, the resulting capacitance or resistance will never be exactly the same as the one computed. So, even with the negative capacitor, the system would not have behaved exactly as the MEMS and by using the positive capacitor, the circuit could be fully made of passive components which is an advantage. Based on those arguments, the decision was made to use a positive capacitance.

A last point to keep in mind is that the scaling of impedance in the circuit has introduced a scaling effect on the current which is also increased by N compared to the original one. This drawback is also an advantage in term of resolution of the measurement.

4.3 Approximated model with high quality factor

Since we are sure that a RLC circuit could not achieve a quality factor as high as 100,000⁸, it is important to find another model to experiment while usable MEMS and experimentation tools are not available. So far, only a (electro)mechanical system has shown such a high Q factor and the research will be oriented in that direction. As it was already exposed, the equivalent circuit of the MEMS is composed of three similar blocs, each made of a resistance, an inductor and a capacitor. This bloc is very similar to the equivalent circuit of a crystal quartz oscillator which only has an additional capacitor in parallel as shown in figure 4.10. The new equivalent circuit proposed is shown in figure 4.11 and is composed of three quartz resonators and two capacitors.

Since the equivalent model of the obtained circuit is not exactly the same as the equivalent circuit of the MEMS, the result will not be the same. However, the important part of this equivalent circuit is a small window of frequency in which the three-quartz circuit must behave close to the MEMS. There are many advantages of using crystal oscillators instead of RLC circuits. They are explained hereunder :

⁷It is possible to find 5% or even 1% but at a very high price. Moreover, capacitor are sensitive to temperature variation

⁸Such a high Q is not reachable because electrical components are not perfect and will introduce much loss

- The tolerance (imperfection in manufacturing) of crystal is much lower : while typical commercial coil tolerance is from 30% to 50%, the chosen quartz oscillators have a tolerance on the frequency of +/-10 ppm.
- The price of crystal is very low : the chosen crystal quartz costs about 50 times less than one (on three) RLC circuit built for the equivalent circuit.
- Better Q factor : quality factor of crystal quartz is typically 90'000 while RLC can hardly achieve 100 when discrete components are used.

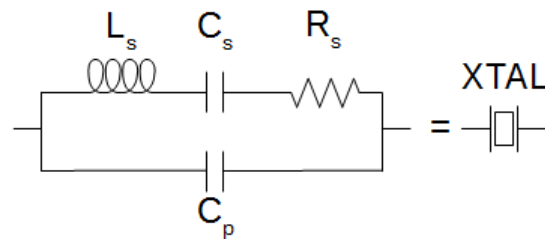


Figure 4.10: Electrical equivalent circuit of a quartz oscillator. The crystal resonator behaves like a RLC circuit in parallel with a capacitor.

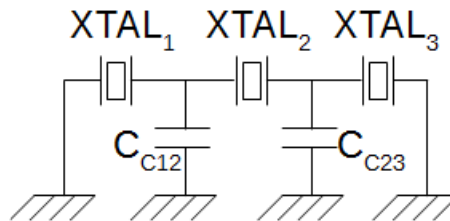


Figure 4.11: Circuit design to model the MEMS. Quartz oscillators are used to replace RLC series component but introduce an unwanted parallel capacitor. Chosen crystal resonators have a natural resonant frequency of 32.768kHz

The chosen quartz oscillators have a natural resonant frequency of 32.768kHz because they are common components and only have twice the resonant frequency of the MEMS⁹. The capacitors used between the quartz and the ground are chosen with a capacitance of 20pF which gives the highest similarity with the frequency response curve of the MEMS.

Due to its different equivalent circuit, the circuit made quartz oscillators will not behave as MEMS to perturbation. Thus, it will not be possible to use it to prove any sensitivity measurement in perturbation. However, it will be an important tool to test measurement circuit without risking to damage real costly and fragile MEMS.

⁹other typical values are of the order of MHz

Chapter 5

Modelization results

Before going further, it is necessary to study and compare the results got by the modelization process. This chapter will be organized in the same way as the previous one. It will start with the MATLAB two degrees of freedom model, followed by the MATLAB three degrees of freedom model. Then the electrical model and the quartz model will be studied in LTspice and finally, the built equivalent electrical circuit using RLC components and the one using quartz will be used to make real measurements. The results studied here emphasize the response of the MEMS to different frequencies. For both tests, the same convention will be followed :

- The first proof mass is excited (e.g. the left one) at certain frequencies
- A first measurement with symmetric system (i.e. without changing mass) is made
- Mass is added on the opposite proof mass (i.e. the 2nd in the 2 DOF¹ model, and the 3rd in 3 DOF model) (e.g. the right one)
- Amplitude of all masses in the system is displayed.

5.1 Mechanical Modelization

5.1.1 Two degrees of freedom without damping

The values that characterize the MEMS and which are used in MATLAB were given by Chun Zhao in his thesis[34]. They are displayed hereunder in figure 5.1.

Based on those values, a first simulation was made without any mass modification. Results are shown in figure 5.2. As it was anticipated, there are two interesting modes where both masses oscillate at the same frequency : the in-phase and the out-of-phase modes. In this simulation, the damping was put to zero and the Q factor is inversely proportional to the damping. This leads to a theoretical infinite Q factor and thus to theoretical infinite height and narrowness of peaks with too

¹DOF stand for degrees of freedom

high an amplitude for the movement of the masses. Using an undamped system allows us to concentrate on the resonant frequencies.

Two degrees of freedom	
Properties	Values
$k_1 = k_2$	57.62N/m
k_{c12}	-0.69N/m
$m_1 = m_2$	6.94 μ g

Figure 5.1: Values used in MATLAB for the two degrees of freedom model without damping

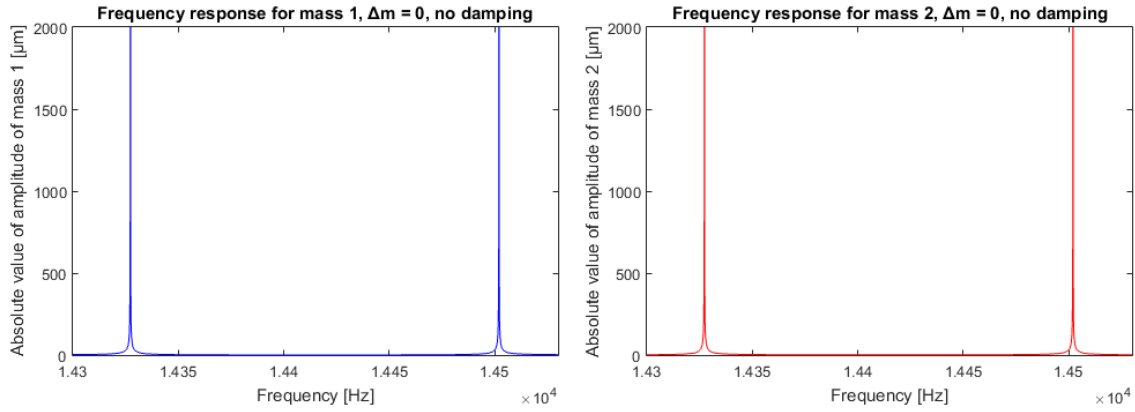


Figure 5.2: Amplitude of movement of mass 1 (blue, left) and mass 2 (red, right) in function of the frequency without mass perturbation for the two degrees of freedom system. Peaks are at the same frequencies for mass 1 and mass 2 (in-phase and out-of-phase mode). Because damping was put to 0, peaks theoretically reach infinity.

By using the same model (no damping) but increasing the mass of proof mass 2 by 2%, we obtained the curves shown on figure 5.3. The first change that is noticed is the variation of the resonant frequency. Both peaks have been shifted but not by the same amount. The peak with the lowest frequency (out-of-phase) has been more shifted than the peak with the highest frequency (in-phase). This first observation leads to a first type of technique to measure the variation in mass of the system, which uses frequency variation. Since the Q is still infinite, no conclusion can be made about amplitude.

5.1.2 Two degrees of freedom with damping

By introducing some damping effect into the model, the Q factor will not be infinite anymore. The values used for the simulation are shown in figure 5.4 hereunder and the results of the simulation are shown in figure 5.5.

As shown in the graph, the damping does not affect the resonant frequency of the system but has an impact on the amplitude of the signal and the peaks shape (which is linked to the Q factor). In this case, the value of the amplitudes (which is of the order of some microns) become more realistic than in the previous case.

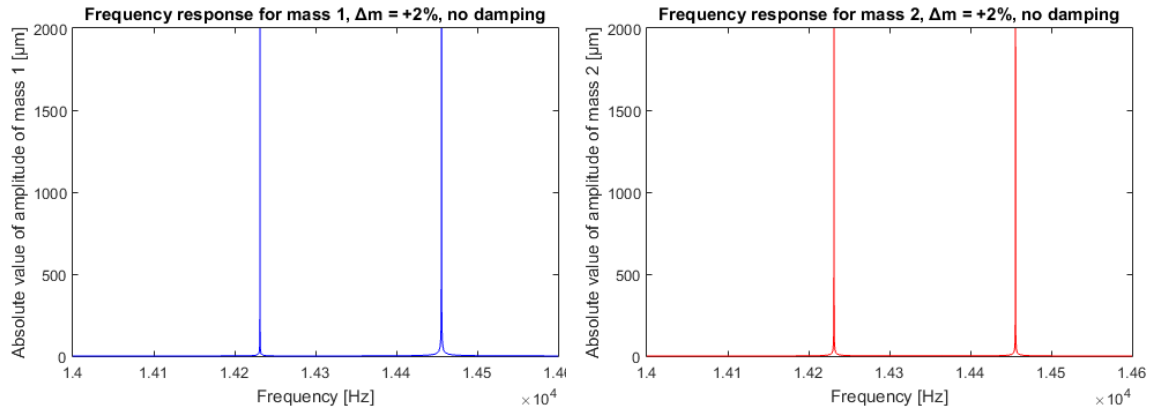


Figure 5.3: Amplitude of movement of mass 1 (blue, left) and mass 2 (red, right) in function of the frequency after adding a perturbation of 2% of the initial mass on proof mass 2 for the two degrees of freedom system. Peaks are at the same frequencies for mass 1 and mass 2 (in-phase and out-of-phase mode) but have been shifted for the model without perturbation. Moreover, both peak have not moved equivalently. Because damping were put to 0, peaks theoretically tend to infinity.

Two degrees of freedom	
Properties	Values
$k_1 = k_2$	57.62N/m
k_{c12}	-0.69N/m
$m_1 = m_2$	6.94 μ g
$b_1 = b_2$	10 ⁻⁶ kg/s

Figure 5.4: Values used in MATLAB for the two degrees of freedom model with damping

If a mass perturbation is then introduced in the damped model, a frequency shift is visible like for the undamped model but amplitude variation can also be measured. The curves of the two proof masses are shown in figure 5.6. As it can be seen on the graph, the peak of mass 1 with the lowest frequency (out-of-phase) has strongly decreased while the peak of mass 1 with the highest frequency (in-phase) has increased. For mass 2, both peaks have been reduced but the peak with the lowest frequency (out-of-phase) is a little bit higher than the second one (in-phase). This second observation introduces another type of technique to measure mass variation which uses amplitude variation.

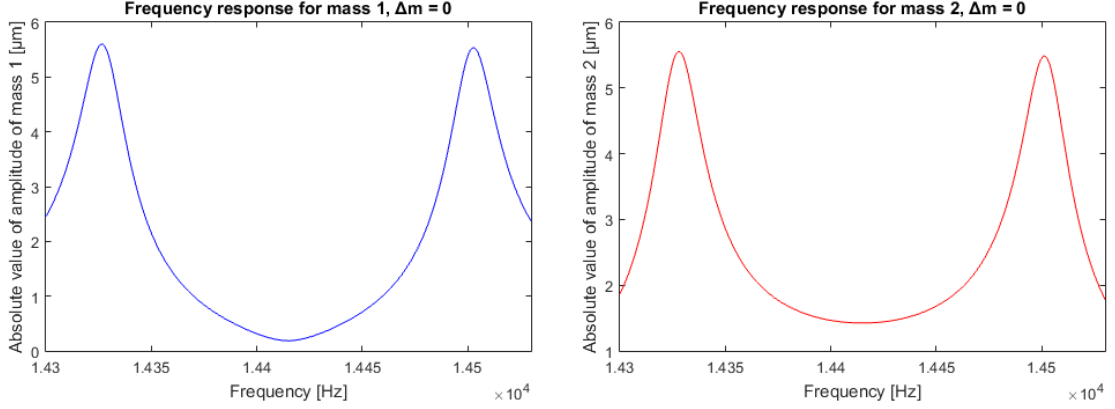


Figure 5.5: Amplitude of movement of mass 1 (blue, left) and mass 2 (red, right) in function of the frequency without mass perturbation for the two degrees of freedom system. Peaks are at the same frequencies for mass 1 and mass 2 (in-phase and out-of-phase mode). Since damping is taken into account peaks have a finite height and finite narrowness. Unlike for the undamped system, the amplitude of the movement of masses is realistic with an order of a few microns.

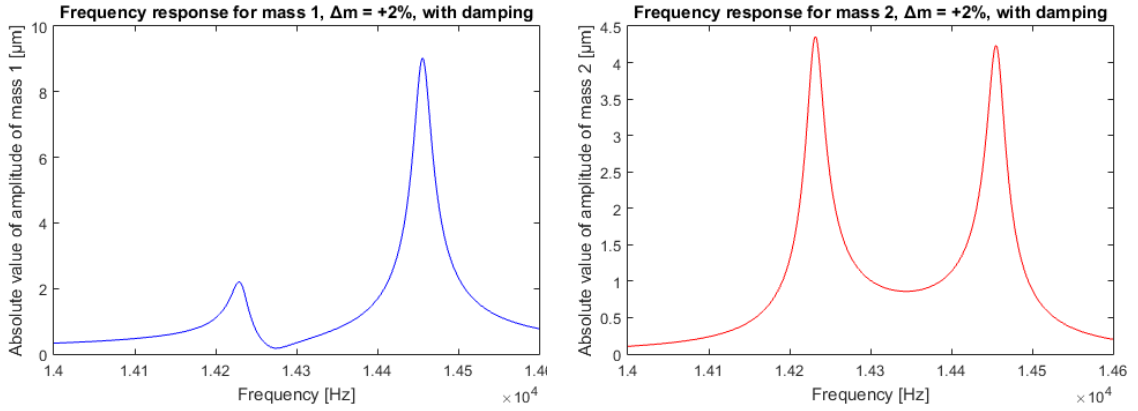


Figure 5.6: Amplitude of movement of mass 1 (blue, left) and mass 2 (red, right) in function of the frequency after adding a perturbation of 2% of the initial mass on proof mass 2 for the two degrees of freedom system. Peaks are at the same frequencies for mass 1 and mass 2 (in-phase and out-of-phase mode) but have been shifted compared to the model without perturbation. Moreover, both peaks have not moved equivalently. The peak of mass 1 with the lowest frequency has strongly decreased in amplitude while peak of mass 1 with highest frequency has been increased. About mass 2, both peaks have decreased but the peak with the lowest frequency is higher than the other peak.

5.1.3 Three degrees of freedom without damping

After having studied the two degrees of freedom model, the three degrees of freedom model was simulated and compared with the previous one. The analysis will start with an undamped and unperturbed system ($\Delta m = 0$). The values used for this model are shown in figure 5.7 and the results of the simulations are shown in figure 5.8.

Three degrees of freedom	
Properties	Values
$k_1 = k_3$	57.62N/m
k_2	199.55N/m
$k_{c12} = k_{c23}$	-0.69N/m
$m_1 = m_2 = m_3$	6.94 μ g

Figure 5.7: Values used in MATLAB for the three degrees of freedom model without damping.

One more time, since the damping is neglected, the Q tends to infinity. This model will thus be only useable to analyze resonant frequency values. The centering is deliberately made on a relatively equivalent frequency window, ignoring any other outer effects. Those outer effects will be detailed in section 5.1.4 : the first main change compared to the two degrees of freedom except the presence of three masses is the behavior of the second mass which only has one visible peak. This is logical, the red peak corresponds to the in-phase mode where the three masses oscillate in the same direction. For the "missing" peak, the system is in the out-of-phase mode where mass 1 and mass 3 are oscillating in opposite directions leading to a not moving mass 2. Just as for the two degrees of freedom model, amplitude peaks of the three masses are aligned at the same frequencies.

If a mass perturbation of +0.05% is imposed to mass 3, the system will not be symmetrical anymore and new results will be obtained. They are shown in figure 5.9. Here again, the frequencies of the two modes are shifted as for the two degrees of freedom model. Peaks with the lowest frequency move a lot while peaks with the highest frequency change little. Another very important variation when a mass is added is the emergence of a new peak for the second proof mass. This effect can easily be explained since this peak corresponds to the out-of-phase mode : mass 1 and mass 3 oscillate in opposite directions. If, before mass perturbation, the movements of the two masses were equal and compensated each other; this is not the case any more since mass 3 is heavier than mass 1. The middle mass then starts to oscillate too in the same direction (in-phase) as the third mass.

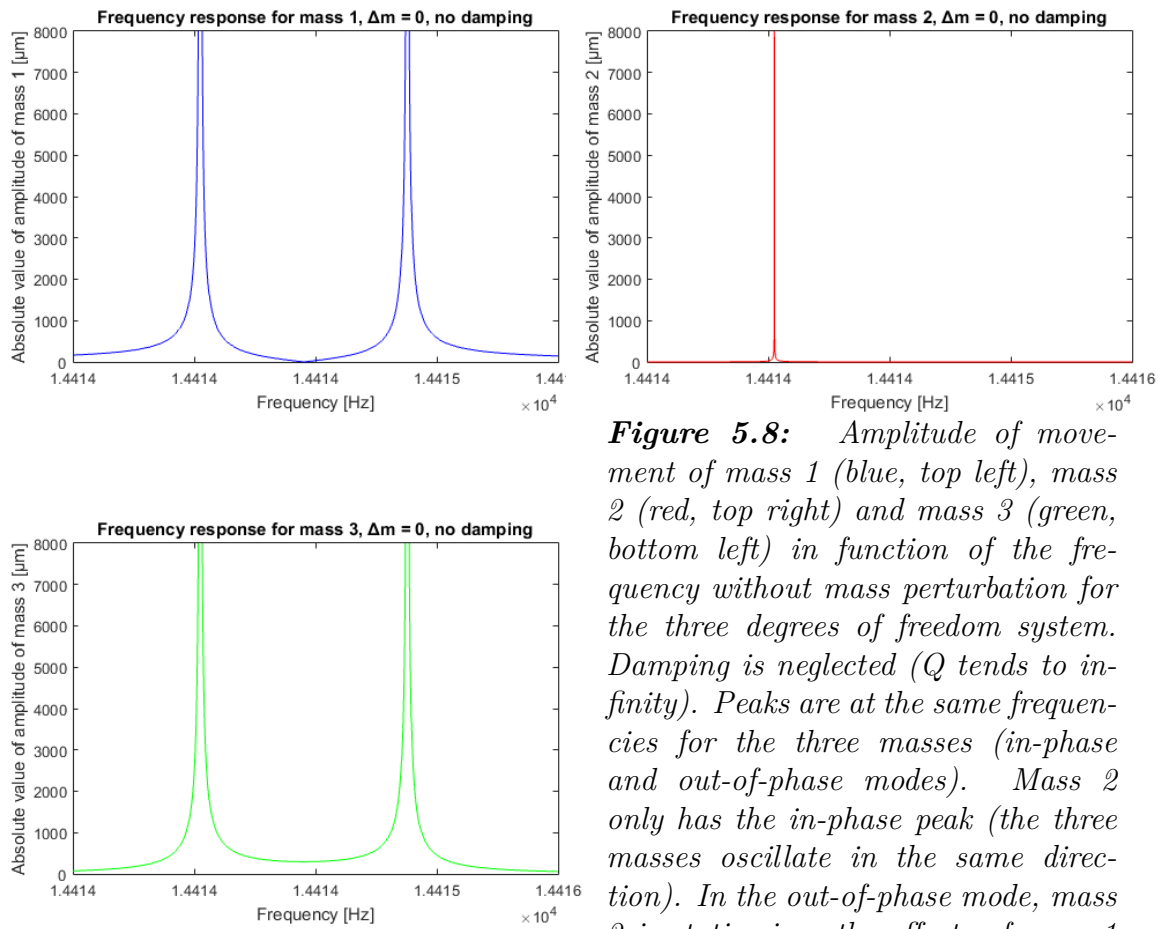


Figure 5.8: Amplitude of movement of mass 1 (blue, top left), mass 2 (red, top right) and mass 3 (green, bottom left) in function of the frequency without mass perturbation for the three degrees of freedom system. Damping is neglected (Q tends to infinity). Peaks are at the same frequencies for the three masses (in-phase and out-of-phase modes). Mass 2 only has the in-phase peak (the three masses oscillate in the same direction). In the out-of-phase mode, mass 2 is static since the effects of mass 1 and mass 3 cancel each other out.

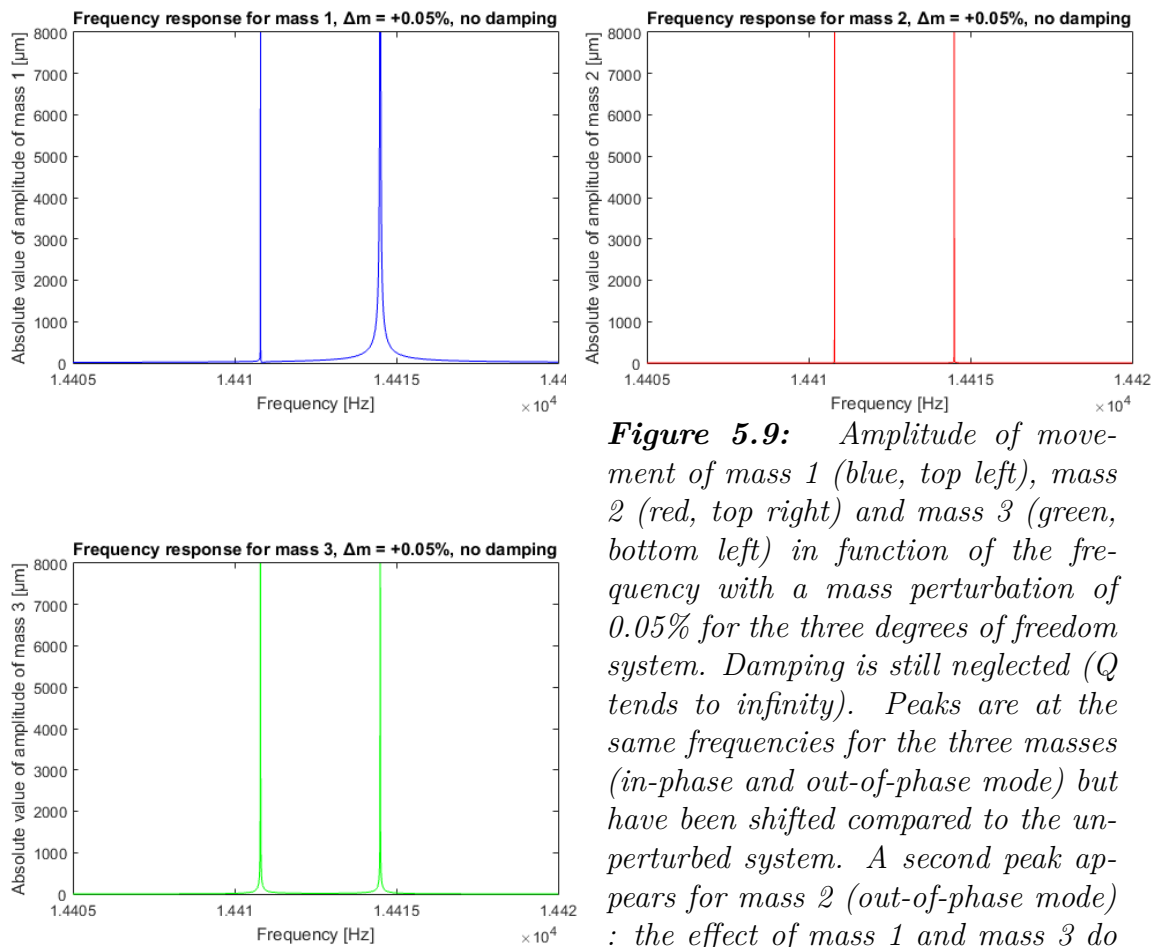


Figure 5.9: Amplitude of movement of mass 1 (blue, top left), mass 2 (red, top right) and mass 3 (green, bottom left) in function of the frequency with a mass perturbation of 0.05% for the three degrees of freedom system. Damping is still neglected (Q tends to infinity). Peaks are at the same frequencies for the three masses (in-phase and out-of-phase mode) but have been shifted compared to the unperturbed system. A second peak appears for mass 2 (out-of-phase mode) : the effect of mass 1 and mass 3 do not cancel each other out anymore due to asymmetry in the system.

5.1.4 Three degrees of freedom with damping

In order to finish with the mathematical model of the MEMS, a damping was added to the three degrees of freedom model and simulations were made using the values shown in figure 5.10. This gives curves displayed in figure 5.11.

Three degrees of freedom	
Properties	Values
$k_1 = k_3$	57.62N/m
k_2	199.55N/m
$k_{c12} = k_{c23}$	-0.69N/m
$m_1 = m_2 = m_3$	6.94 μ g
$b_1 = b_2 = b_3$	10 ⁻⁸ kg/s

Figure 5.10: Values used in MATLAB for the three degrees of freedom model with damping

Since we have already studied the two degrees of freedom system with damping and the three degrees of freedom system without damping, those curves are not surprising. One more time there is a "missing" peak for the second mass which can be explained as before. We can notice that the amplitude of the movement of mass 2 is much smaller than for the other masses. This is because stronger beams are used to attach this mass to the medium. The resulting stiffness is 3.5 times larger than that for other masses. Another important remark to make is that the damping used to compute those curves is smaller than the one used for the two degrees of freedom (100 times smaller)².

The last missing curves are the ones obtained by imposing a mass variation to the three degrees of freedom damped system. Here again the mass perturbation was chosen to be +0.05% of the initial mass. An important note is that this mass variation is much smaller than for the two degrees of freedom case. This is due to the higher sensitivity³ of the three degrees of freedom model which would be too much perturbed by an additional mass of 2% (one peak would have decreased so much that it would not have been visible anymore). The results obtained by this simulation are shown in figure 5.12. Mass 1 and mass 2 have the same behavior as for the two degrees of freedom system. Both peaks are shifted, the one at the lowest frequency moves more than the other one and decreases while the second one increases. Peaks of mass 3 have both decreased but the first peak remains a little bit higher. Finally, the asymmetry of the system has made the second mass move in the out-of-phase mode. The in-phase peak of mass 2 has also decreased.

As it was exposed, the chosen damping was much smaller in the three degrees of freedom case than in the two degrees of freedom one. This is because the in-phase and out-of-phase peaks are much closer to each other in the three degrees of freedom

²This choice will be explained later

³sensitivity of model will be studied in section 6

model. If the MEMS is operating with too high a damping (for example 10^{-6} kg/s) the Q factor will decrease leading to larger peaks which will merge into a single peak. Figure 5.13 shows the same curves as figure 5.11 (i.e. three degrees of freedom damped model without mass perturbation) but with a higher damping.

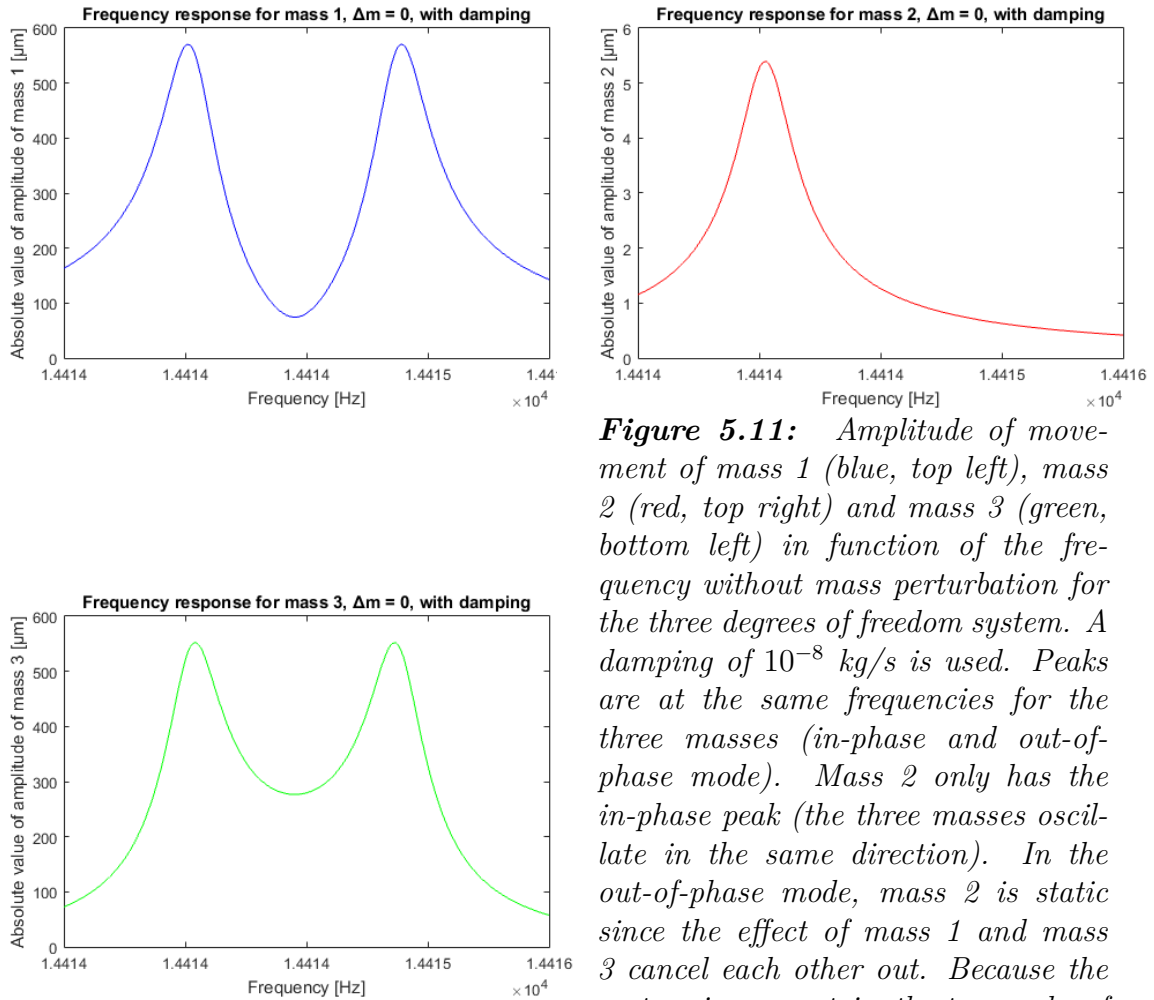


Figure 5.11: Amplitude of movement of mass 1 (blue, top left), mass 2 (red, top right) and mass 3 (green, bottom left) in function of the frequency without mass perturbation for the three degrees of freedom system. A damping of 10^{-8} kg/s is used. Peaks are at the same frequencies for the three masses (in-phase and out-of-phase mode). Mass 2 only has the in-phase peak (the three masses oscillate in the same direction). In the out-of-phase mode, mass 2 is static since the effect of mass 1 and mass 3 cancel each other out. Because the system is symmetric, the two peaks of both masses have the same amplitude. Mass 2 has lower amplitude due to its stronger beams.

As it was briefly introduced, the three degrees of freedom also introduce a third peak. However this peak is located at a much higher frequency and its amplitude is very small compared to the two peaks studied until now. The frequency window was expanded to display the third peak which is shown in figure 5.14. The curves were obtained using the same parameters as for the curves we got in figure 5.11 (i.e. three degrees of freedom damped model without mass perturbation). As it can be seen, the amplitude is about 9000 times lower.

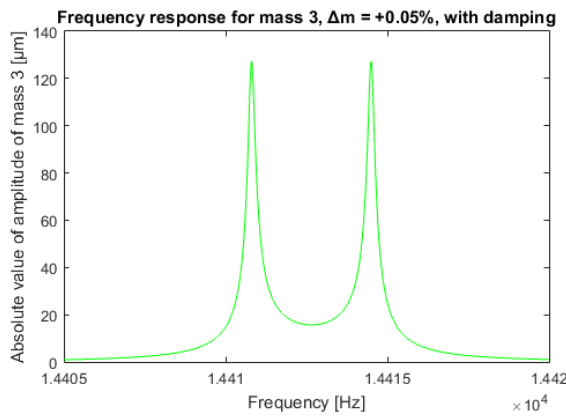
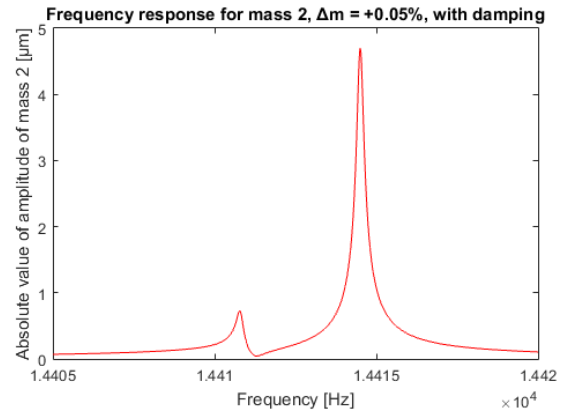
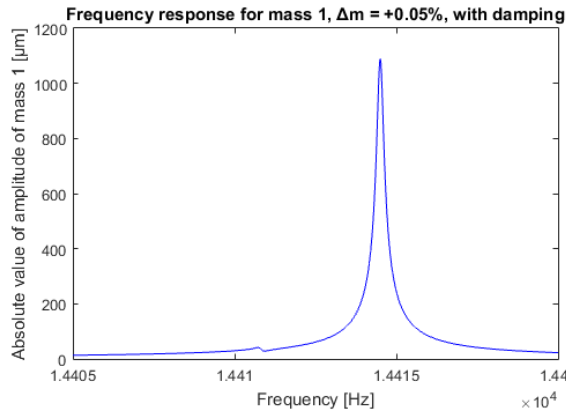


Figure 5.12: Amplitude of movement of mass 1 (blue, top left), mass 2 (red, top right) and mass 3 (green, bottom left) in function of the frequency with a mass perturbation of 0.05% and a damping of 10^{-8} kg/s for the three degrees of freedom system. Peaks are at the same frequencies for the three masses (in-phase and out-of-phase mode) but have been shifted compared to the unperturbed system. Mass 2 has a second peak since the effect of mass 1 and mass 2 do not cancel each other out anymore due to asymmetry in the system. The out-of-phase peaks have increased for mass 1 and mass 2 while in-phase peaks have decreased. The opposite behavior happened for mass 3.

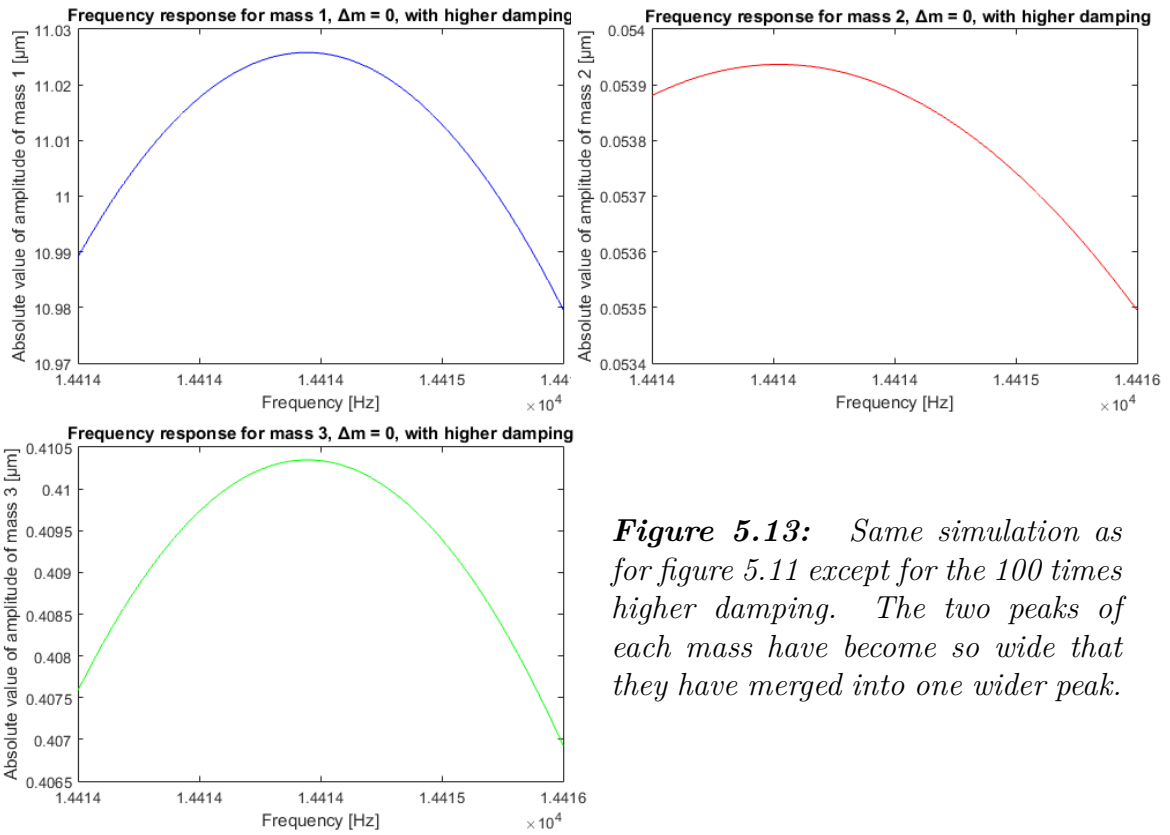


Figure 5.13: Same simulation as for figure 5.11 except for the 100 times higher damping. The two peaks of each mass have become so wide that they have merged into one wider peak.

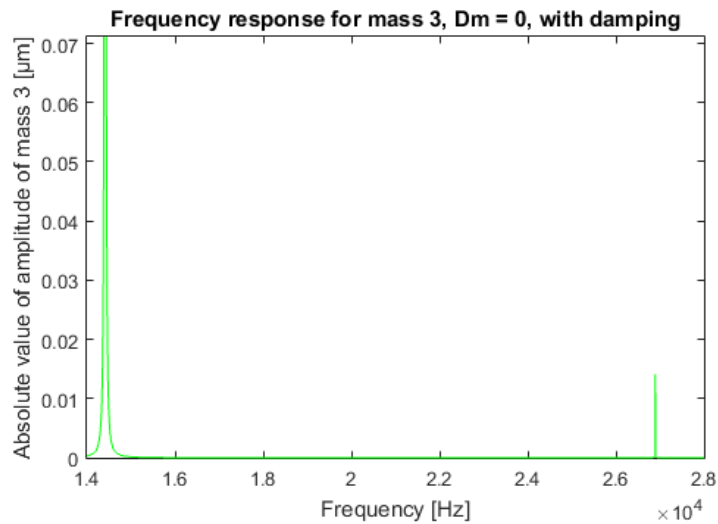


Figure 5.14: The third peak of mass 3 is at twice the frequency of the two other peaks and is 9000 times smaller. It is thus not interesting for the measurement process.

To conclude with mechanical simulations, it is important to notice that only the case of positive mass variation was exposed in this report. This is because the goal of the project is to measure an additional mass on a proof mass. The effect of decreasing the mass of one proof mass was also studied. Figure 5.15 shows a superposition of the three possible cases just for information.

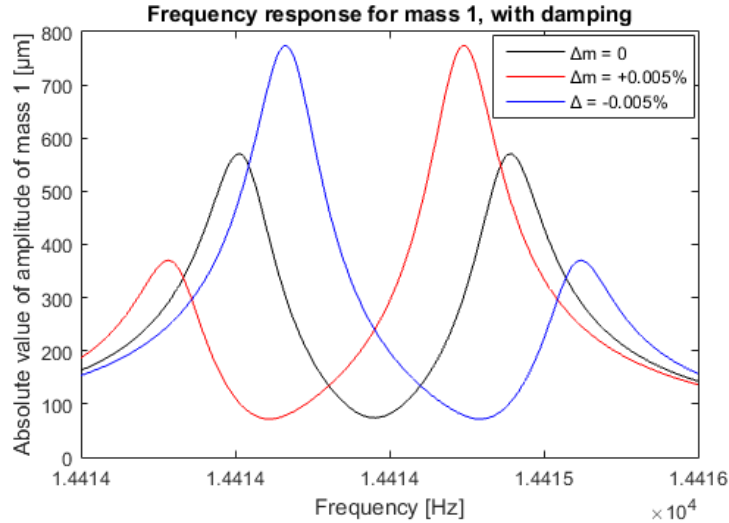


Figure 5.15: Comparison of the effect on mass 1 of positive and negative mass variation of mass 3 in the system. The black curve is obtained for a symmetric system. The red curve is obtained by adding some mass on proof mass 3. The blue curve is obtained by removing some mass from proof mass 3. One can see that the effect of removing some mass is opposite to the effect when adding some mass. A more detailed study will be made in section 6.

5.2 Electrical Modelization

Having studied the results of the mathematical model, the electrical model was used to create new results and compare them with the previous model. Since we are interested in the three degrees of freedom system with damping, only this case will be exposed in this section.

5.2.1 Three degrees of freedom with damping using LTspice

The results shown in figure 5.17 were obtained using LTspice. The values used for the RLC equivalent circuit are shown in figure 5.16. As can be seen in the table, the system used is symmetric (i.e. without mass perturbation).

Three degrees of freedom	
Components	Values
$C_1 = C_3$	2.543×10^{-16} F
C_2	8.477×10^{-17} F
$C_{c12} = C_{c23}$	-1.90725×10^{-14} F
$L_1 = L_2 = L_3$	2.2131×10^5 H
$R_1 = R_3$	0.44×10^6 Ω
R_2	44×10^6 Ω

Figure 5.16: Values used in LTspice for the three degrees of freedom system modeled by a RLC equivalent circuit. Damping is added to have a Q factor of 100,000

As can be seen in the results which represent the voltage across the three capacitors (i.e. the amplitude of movement of the masses⁴), the shape for the electrical equivalent circuit is similar to the shape obtained by the mathematical model : mass 1 and mass 3 have two peaks (in-phase and out-of-phase) and mass 2 only has one peak due to the symmetry (as explained in section 5.1.4), peaks of different masses are at the same frequencies, peak of mass 2 is much smaller than peaks of mass 1 and mass 3 because of the higher stiffness used for the middle mass.

In order to check if the electrical system behaves like the MEMS when perturbation is applied, coil L3 (which corresponds to mass 3) was modified and its inductance was increased by 0.05%. This modification leads to the results shown in figure 5.18.

As it can be seen, the electrical circuit output changes in the same way as the MEMS. Peaks have been shifted in the same way as the mathematical model. The amplitude of both peaks has also changed like the mechanical model. A special attention should be paid to the vertical axis which is now in dB unlike for the mathematical model which had linear axis.

⁴mechanical position is linked to the electrical charge and $Q = CV \Rightarrow V \propto Q$

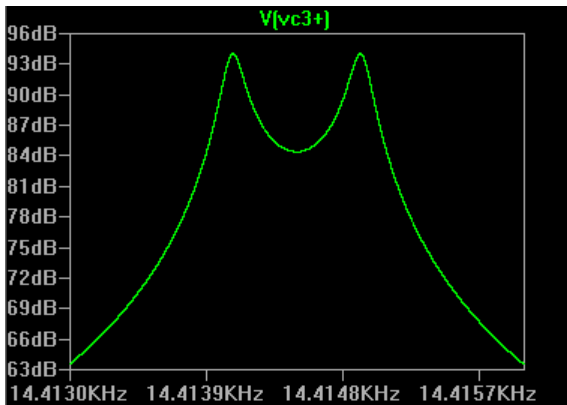
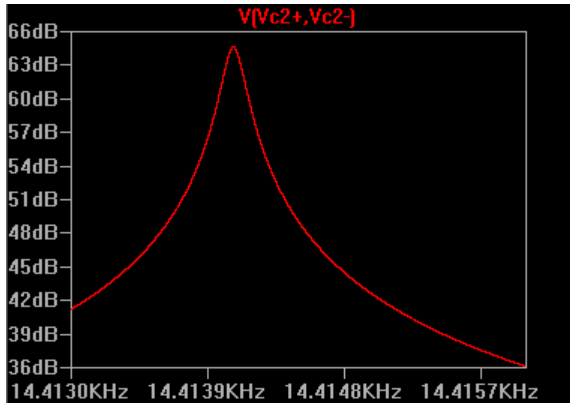
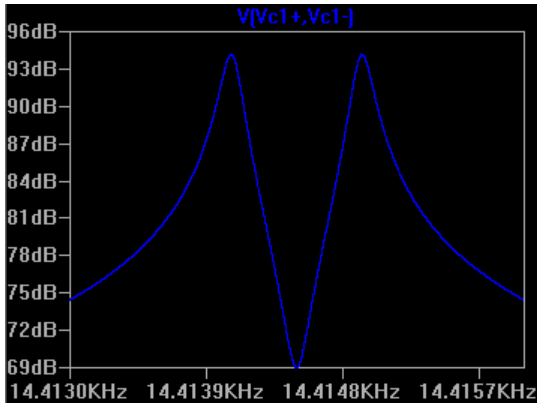


Figure 5.17: Voltage across capacitor 1 (blue, top left), capacitor 2 (red, top right) and capacitor 3 (green, bottom left) in function of the frequency without mass perturbation and with a damping (in order to obtain a Q factor of 100,000) for the three degrees of freedom system modeled by electrical circuit. The equivalent circuit behaves very closely to the mathematical model when used in symmetric configuration : two peaks for mass 1 and mass 3, one peak for mass 2 due to symmetry, peaks from different masses are at the same frequencies, peak of mass 2 is much smaller than peaks of mass 1 and 3.

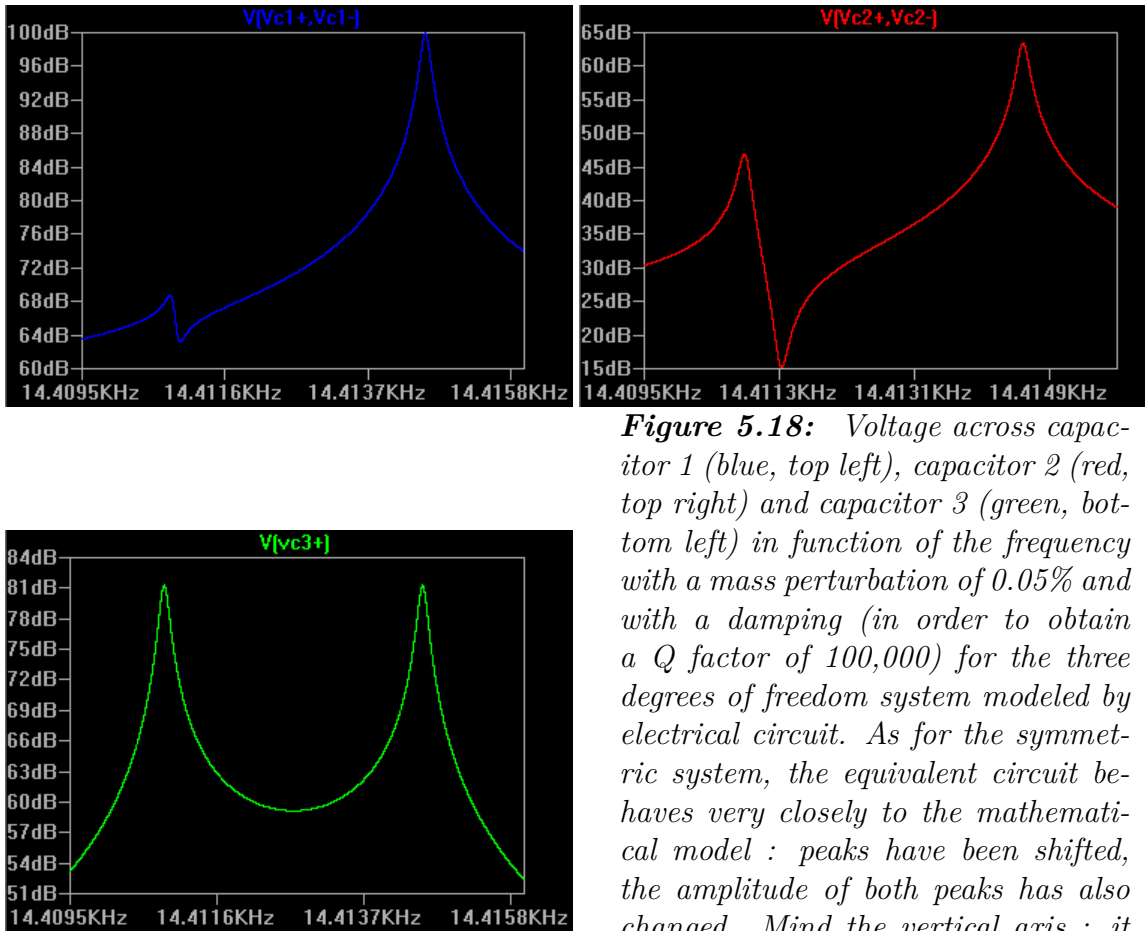


Figure 5.18: Voltage across capacitor 1 (blue, top left), capacitor 2 (red, top right) and capacitor 3 (green, bottom left) in function of the frequency with a mass perturbation of 0.05% and with a damping (in order to obtain a Q factor of 100,000) for the three degrees of freedom system modeled by electrical circuit. As for the symmetric system, the equivalent circuit behaves very closely to the mathematical model : peaks have been shifted, the amplitude of both peaks has also changed. Mind the vertical axis : it is in dB whereas in the mathematical model it was a linear axis.

5.2.2 Effect of adaptation process

Now the electrical model is validated, it is important to check whether the scaling process has not altered the output of the circuit. The scaled circuit was simulated with LTspice using the values displayed in figure 5.19. Here again, the model was used in its symmetric configuration.

Three degrees of freedom	
Components	Values
$C_1 = C_3$	3.3457×10^{-10} F
C_2	9.6606×10^{-11} F
$C_{c12} = C_{c23}$	-2.7939×10^{-8} F
$L_1 = L_2 = L_3$	0.36 H
$R_1 = R_3$	0.328 Ω
R_2	0.6104 Ω

Figure 5.19: Value used in LTspice for the three degrees of freedom system modeled by a RLC equivalent circuit after the scaling process was made.

The results obtained from the simulation of the electrical equivalent scaled circuit are shown in figure 5.20. As can be seen, this does not affect the correct behavior of the model. The only variation between the two models was a frequency shift estimated to be of 0.08Hz which was only due to the approximation of values during the computation process.

As a penultimate subject for the theoretical electrical model, it is important to check if the theoretical Q factor is effectively about 100'000 after the scaling. One formula to compute a Q factor is :

$$Q = \frac{f_c}{W_{3dB}} \quad (5.1)$$

where f_c is the resonant frequency and W_{3dB} the bandwidth for which the amplitude is decreased by 3dB. Figure 5.21 shows the value used to compute the theoretical Q of the first peak of mass 1.

By using equation 5.1 with the following values :

$$\begin{cases} f_c = 14.414172kHz \\ f_{1-3dB} = 14.413994kHz \\ f_{2-3dB} = 14.414139kHz \\ \Rightarrow W_{3dB} = 0.145Hz \end{cases} \quad (5.2)$$

we get $Q = \frac{f_c}{W_{3dB}} = 99408 \approx 100,000$

In order to conclude with this theoretical electrical model, a last verification has to be made about the effect of using positive capacitance instead of a negative one. The circuit used was the first one (no scaling) except for the capacitor which had a positive capacitance. In order to be able to see both peaks for mass 2, a small perturbation will be added (0.05%) on mass 3. The resulting curves are shown in figure 5.22.

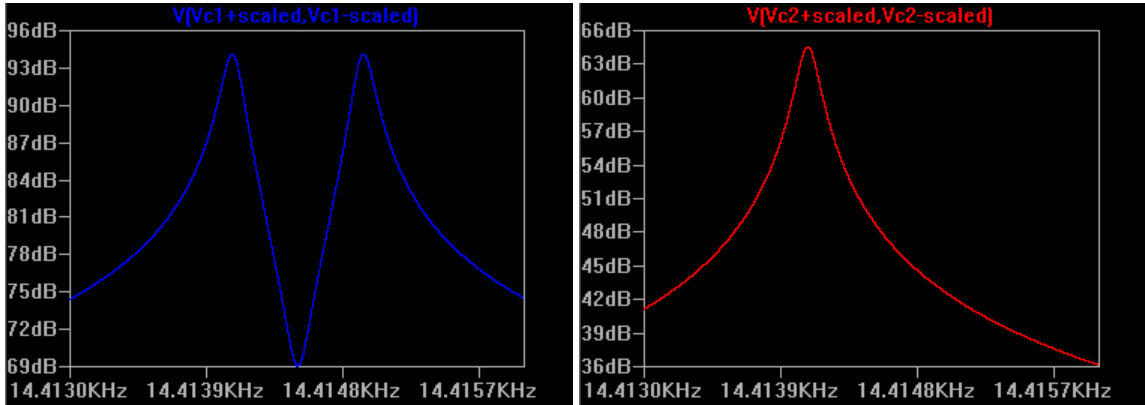


Figure 5.20: Voltage across capacitor 1 (blue, top left), capacitor 2 (red, top right) and capacitor 3 (green, bottom left) in function of the frequency without mass perturbation and with a damping (in order to obtain a Q factor of 100,000) for the three degrees of freedom system modeled by electrical circuit after using the scaling process. The resulting curves are the same as before the process. The only difference is a frequency shift (0.08Hz) due to approximation errors.

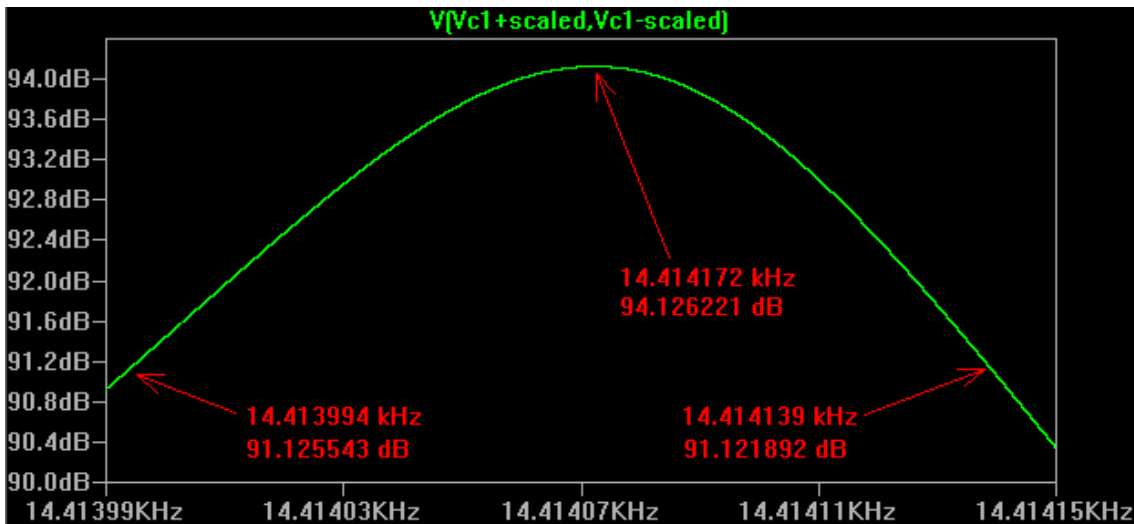
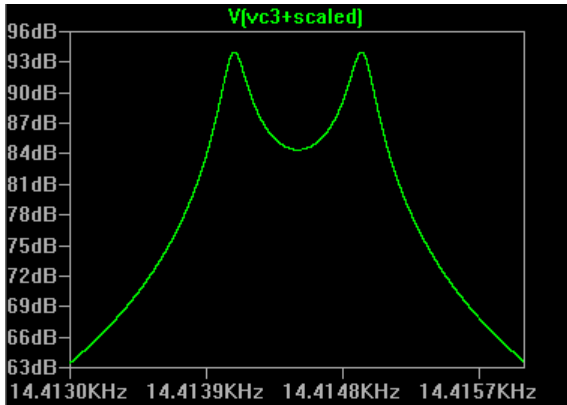


Figure 5.21: This figure represents the way to obtain values used in the computation of the Q factor for the first peak of mass 1.

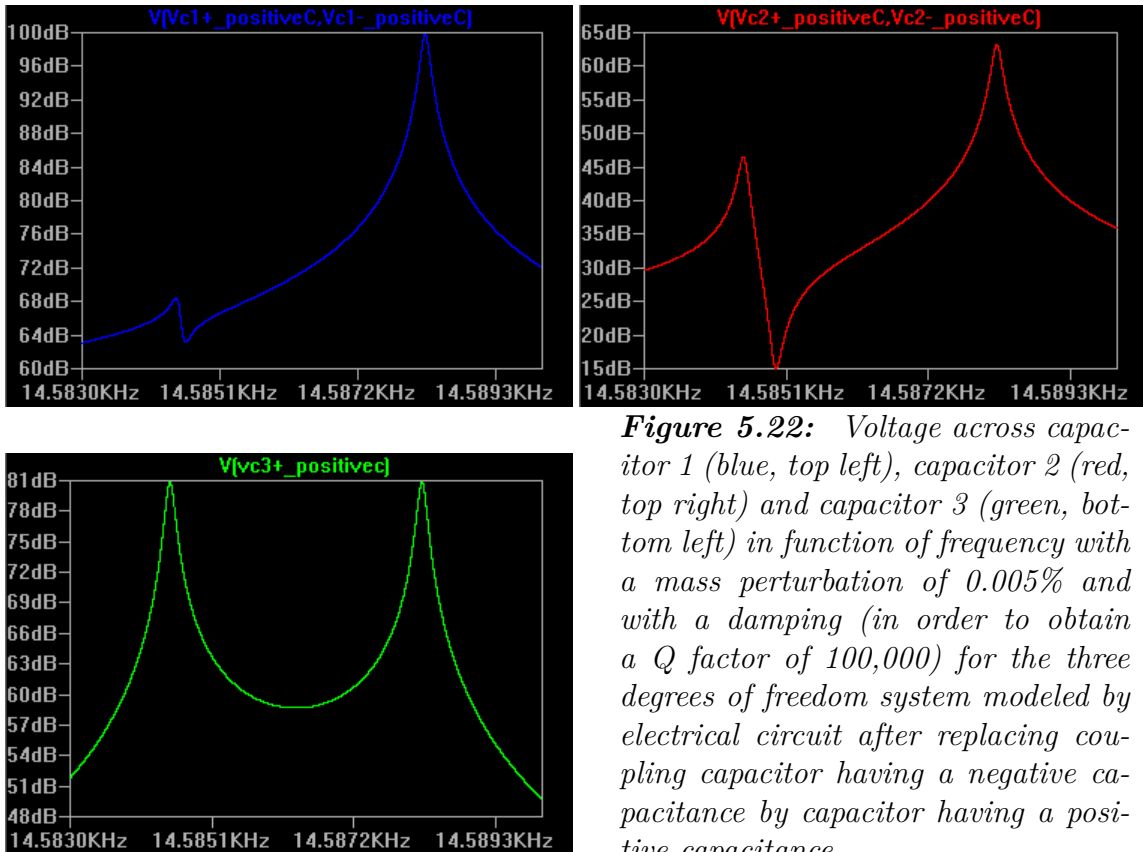


Figure 5.22: Voltage across capacitor 1 (blue, top left), capacitor 2 (red, top right) and capacitor 3 (green, bottom left) in function of frequency with a mass perturbation of 0.005% and with a damping (in order to obtain a Q factor of 100,000) for the three degrees of freedom system modeled by electrical circuit after replacing coupling capacitor having a negative capacitance by capacitor having a positive capacitance.

One can notice that, except for a frequency shift of less than 200Hz there are no significant effects on the measurement process. The only effect is an inversion of the in-phase and out-of-phase modes. However this is not visible on this graph and would not be visible on MATLAB graphs which use absolute amplitude.

5.2.3 Experimental measurement

The RLC circuit was built in order to see how close it behaves compared to the MEMS. A picture of the circuit is shown in figure 5.23.

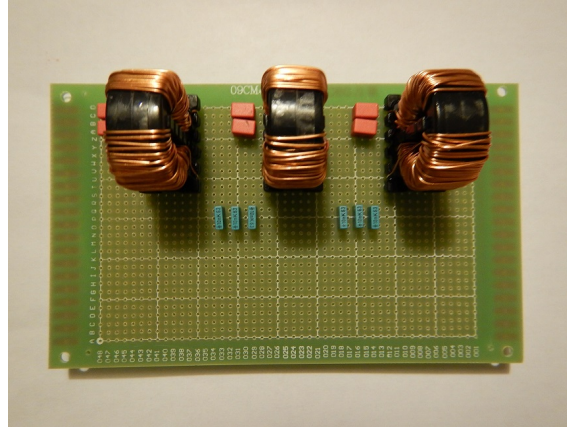


Figure 5.23: Picture of the built RLC equivalent circuit used to make the experimental measurements.

The generator used to make the measurement having an equivalent output resistance of 50Ω , would have completely ruined the Q factor of the circuit. A simple solution to overcome this problem is to use a down transformer. Since a voltage of 1V was required to excite the circuit and since the voltage output of the generator can reach 10V, the ratio of the transformer was chosen to be 10:1. The output impedance of the source is thus divided par 100 and is $500m\Omega$. Moreover, the input of the measurement tool (connected to the circuit via probes) strongly perturbed the circuit. Figure 5.24 shows the variation with and without a measurement probe connected to the circuit across capacitor 1.

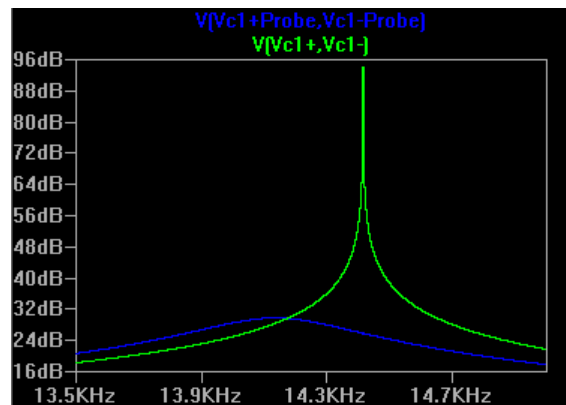


Figure 5.24: Comparison between voltage across first capacitor with probe (blue) and without probe (green). This figure emphasizes that measurement processes strongly affect the behavior of the circuit.

In order to overcome this problem, three solutions can be taken into account :

Using very high impedance input measurement circuit By using a measurement circuit that has a very high impedance input, the measurement process would not be disturbed, or less anyway. Mr. Kleijer[14] has proposed a circuit with that characteristic. However, the decision was made not to investigate this solution due to the time and money it would have requested.

Using a very small resistance in series to measure the current With this solutions, the Q factor would barely be affected and the effect of probe would be negligible.

Measuring the voltage across the coupling capacitor It was noticed that the evolution of the voltage across coupling capacitor 1 is similar to that across capacitor 1. Moreover, due to the higher capacitance of the coupling capacitor, the effect of the probe will be very low. The main advantage of this technique is that the circuit does not need any new component.

Based on the last measurement technique, the curves shown in figure 5.25 were obtained.

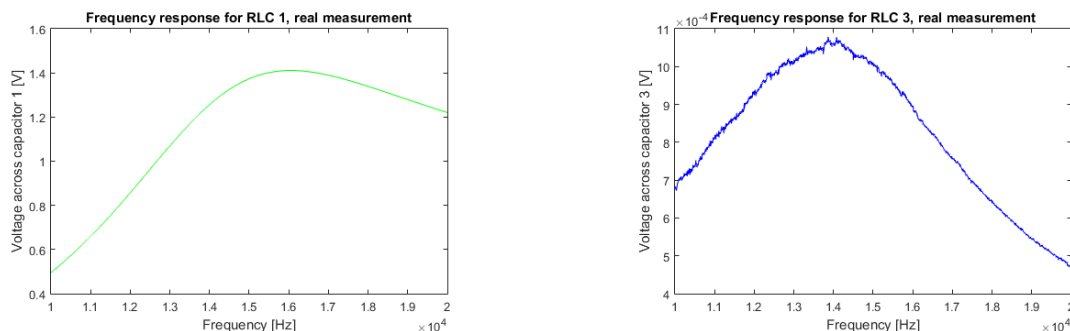


Figure 5.25: Amplitude of the voltage across coupling capacitor 1 (green, left) and coupling capacitor 2 (blue, right) measured on the real equivalent circuit composed of RLC components. Due to the still too high resistance of the components, both peak are merged

As can be seen, the Q factor is very low.

5.3 Approximated model with high quality factor

In order to understand the variation induced by the use of crystal quartz instead of RLC components, a first simulation of an equivalent quartz crystal circuit is made and is shown on figure 5.26.

The next step was to simulate the approximate equivalent circuit made of three quartz oscillators. Because it is not possible to make a real measurement of the voltage across the capacitor in the equivalent circuit (which is not a physical component), it was decided to make the measurement at the solder point of two quartz

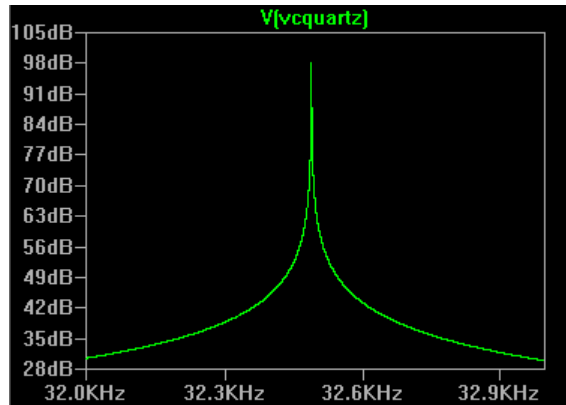


Figure 5.26: Frequency response of a quartz based on a typical equivalent circuit.

(across the coupling capacitor). The curves measured at those points have high similarity with the MEMS curves for mass 1 and mass 3 when the frequency window is limited. They are represented on figure 5.27. Figure 5.28 shows that outside the interesting frequency window, the quartz circuit behaves in a different manner than the MEMS.

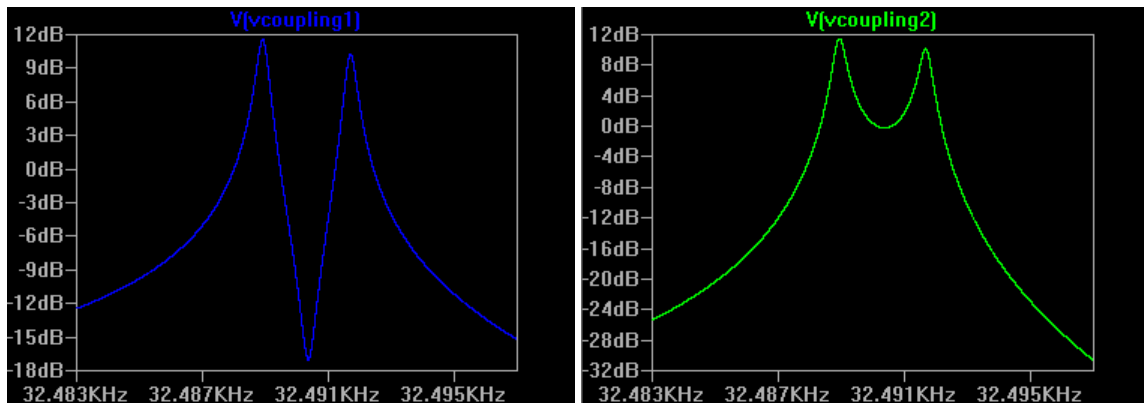


Figure 5.27: Voltage across coupling capacitor 1 (blue, left) which is similar to mass 1 response and coupling capacitor 2 (green, right) which is similar to mass 3. The response simulated is in function of the excitation frequency. Only the interesting frequency window was displayed.

In order to check the real behavior of the equivalent circuit made of quartz oscillator, the circuit was excited with a sweep of frequency and the output was measured by a lock-in amplifier⁵ The two experimental curves are displayed in figure 5.29.

As can be seen, the system is not totally symmetric since the two peaks have a different amplitude. This is mainly due to tolerance on crystal quartz and coupling capacitor but also to probe of the lock-in amplifier used to make measurements. They have a non negligible capacitance (13pF) compared to the coupling capacitor (20pF), they also have a 1M Ω input resistance. A picture of the real circuit is displayed in figure 5.30.

⁵The frequency sweep was made by the lock-in amplifier which gives its reference signal as an output.

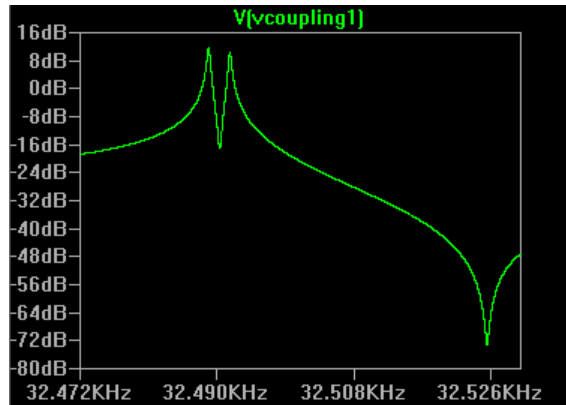


Figure 5.28: Voltage across coupling capacitor 1 for a larger frequency window. An anti resonant peak is found for higher frequency. The curves does not fit well the MEMS curves outside the initial frequency window.

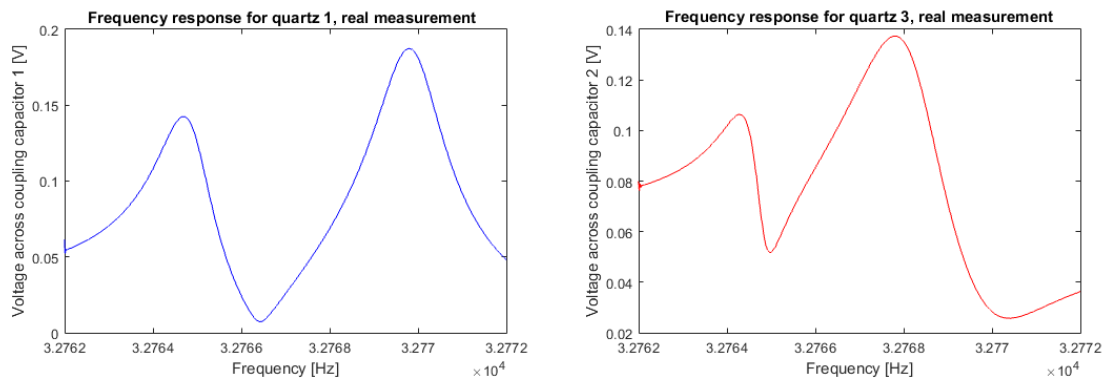


Figure 5.29: Voltage across coupling capacitor 1 (blue, left) and coupling capacitor 2 (red, right) measured on the real equivalent circuit composed of three quartz oscillators. Due to the tolerance of the components and the non infinite input impedance of the probe, the circuit is not symmetric and non negligible differences between peaks are visible.

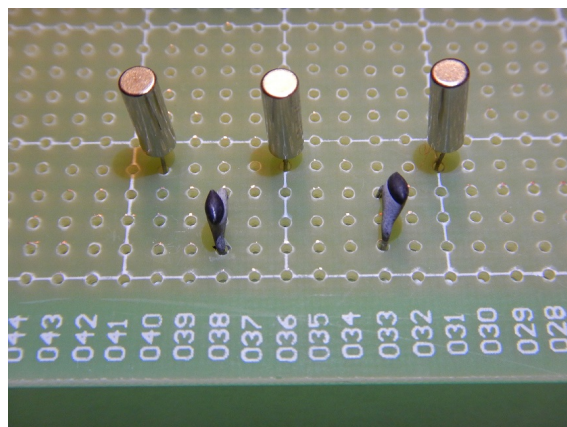


Figure 5.30: Photography of the circuit used to characterize the frequency response of the MEMS equivalent circuit using quartz oscillators.

In order to conclude with the first intermediate results, it is interesting to compare all those simulations and modelization results with a real measurement made on the MEMS. Since all the tools were not ready (or available) to generate mass perturbation, only the curves of the stiffness perturbed MEMS are available. They are shown in figure 5.31. As the MEMS was not designed to measure the position of the middle mass, it will only be possible to compare curves of mass 1 and mass 3. To realize those measurement, the MEMS was put into a vacuum chamber with a pressure of $10^{-6}mbar$.

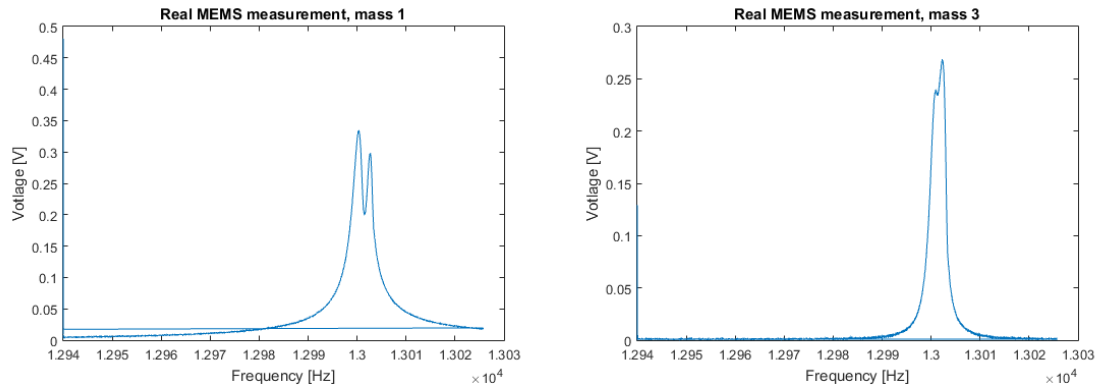


Figure 5.31: Amplitude of the position of mass 1 and mass 3 measured with the real MEMS. Those curves are very similar to the ones obtained with simulation and modelization.

Chapter 6

Measurement strategy for mass variation

Initially, the MEMS was designed with the goal to measure the stiffness variation of one of its beams. As exposed before, it was asked to modify the measurement process in order to be able to measure a modification in mass of one proof mass. Based on the first intermediate results obtained in section 5, three main strategies were selected to be investigated. They are detailed in the following sections. They all have the same working principle : the change in mass of one proof mass will change some characteristics, each of which will be measured by one of the three techniques.

6.1 Resonant frequency shift

This first technique has already been explored in scientific literature for many measurands (length[25], force[25], tilt[25], stiffness[25], etc.) and usually shows interesting results. It is thus logical to start by experiencing this strategy for mass variation. The principle is the following : the variation of one proof mass will change the resonant frequency of the whole system. By tracking this resonant frequency, it is possible to determine the new mass. By using the MATLAB model built in the modelization chapter, the relation between mass variation and frequency variation can easily be obtained. The electrical model is also a good solution to simulate theoretical results. However, if we want to collect practical measurements, it is necessary to test them on a real device (MEMS or equivalent circuit). In order to do so, there are two solutions. The first one is to manually find the resonant frequency, after every change of mass , with laboratory equipments. However this technique is very slow and can introduce much measurement imprecision. The second technique is to use a feedback loop that will automatically track the resonant frequency. This second solution will lead to a real sensor solution.

6.1.1 Frequency tracking circuit

Chun Zhao has already developed a circuit that has the ability to lock on the resonant frequency of the MEMS[34]. The schematics of its feedback loop is shown in

appendix in figure B.1. However the circuit is quite complex and it takes quite a long time to stabilize its output ($\approx 0.5s$). In this project, it was decided to simply use a Pierce oscillator[26, 1] to make the resonator oscillate. Its main advantage is its simplicity. The schematics of the circuit is shown in figure 6.1.

The output of this circuit is a signal with a frequency based on the oscillator properties. Measuring a frequency is quite an easy process. Good frequency meters can easily be found. It is also possible to build one with a counter based on a high speed clock.

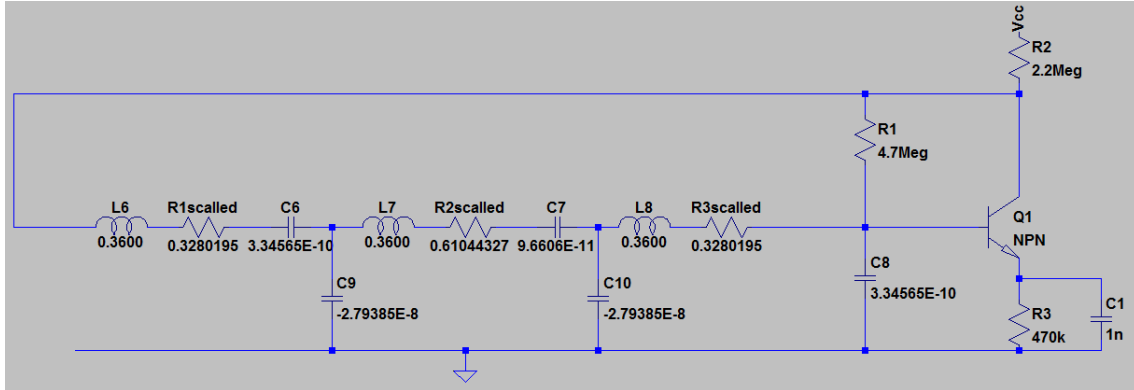


Figure 6.1: Schematics of the resonator in its closed loop circuit.

6.2 Relative amplitude variation at resonant frequency

The second technique consists in measuring the variation of the amplitude of the oscillation of the masses in the MEMS. The main problem with the MEMS is the tiny voltage and current used (with an amplitude of the order of microvolts and microamps). Moreover, the output signal is a sine wave with noise. However, there is a powerful tool used to measure the amplitude of a specific frequency component of a signal which is the LockIn Amplifier. As it was explained in section 3.4, this tool multiplies the unknown signal with a reference signal at the wanted frequency and filters it to get the DC component which is the amplitude of the input signal.

6.2.1 Amplitude detection circuit

An example of circuit that uses synchronous detection is proposed to measure the amplitude of the MEMS output. It is composed of a multiplier and a low pass filter. The reference signal used is the output of the feedback and the input signal is the output of the MEMS. The schematics of a synchronous detector is shown in figure 6.2. When it is added to the MEMS with its feedback, the complete circuit becomes such as in figure 6.3.

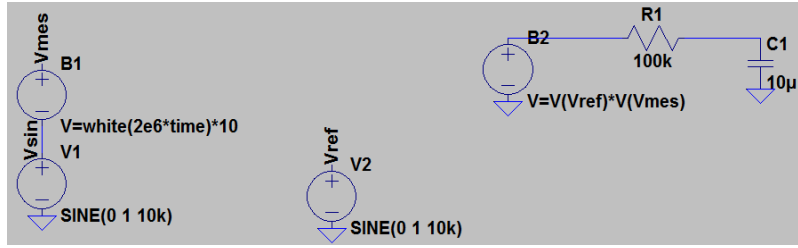


Figure 6.2: Schematics of a simple synchronous detector.

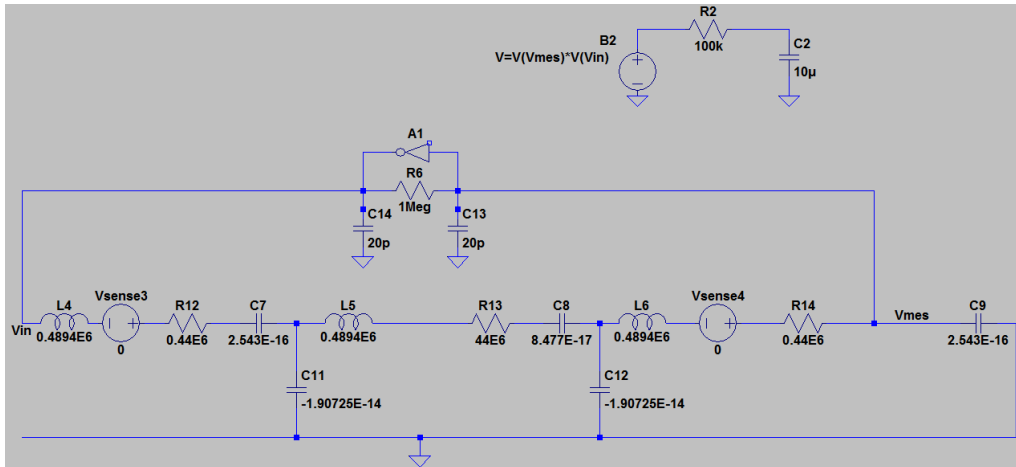


Figure 6.3: Schematics of the resonator in its closed loop circuit with the synchronous detector used to measure the amplitude of the signal.

6.3 Amplitude ratio variation at resonant frequency

This third technique is very similar to the previous one. The first step is to measure the amplitude of the oscillation of the masses in the MEMS as in the previous section and to compute the ratio between the two opposite masses. Since it is very difficult to build a circuit that "computes" a ratio between two voltages in an analog way, the decision to sample the input signals and numerically compute their ratio was made. A proposed circuit is shown in figure 6.4 and used two synchronous detectors with a microcontroller.

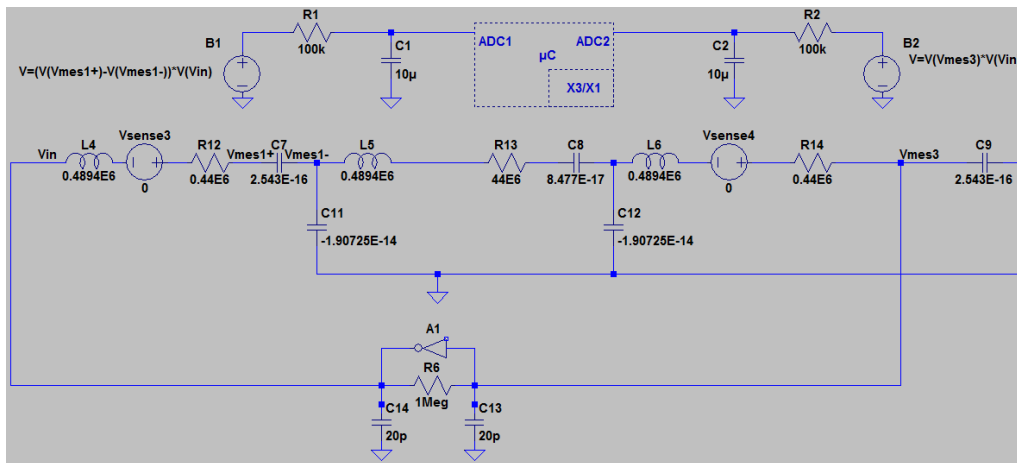


Figure 6.4: Schematics of the resonator in its closed loop circuit with two synchronous detectors and the microcontroller used to measure the ratio of amplitude of the signal.

Chapter 7

Results about measurement strategy

Now different solutions has been suggested, it is important to compare their sensitivity, strengths and weaknesses. Here again, two and three degrees of freedom will be studied to compare the interest of using three degrees of freedom. Finally, the theoretical perturbation of a virus (supposed to be 10^{-20} kg) and of a bacteria (supposed to be 10^{-16} kg) will be computed. Results and discussions will be exposed in the same order as in the previous chapter. All MATLAB codes used hereunder are available in appendix..

7.1 Resonant frequency shift

The measurement analysis started with the relation between the frequency and the mass for the two degrees of freedom system. The sensitivity curves are shown in figure 7.3. Unlike for the case with stiffness perturbation, the frequency sensibility is not linear anymore. However, the in-phase mode (reps. out-of-phase mode) frequency is still nearly constant for positive (resp. negative) mass variation as it was the case for the stiffness perturbed model.

If the same graph is computed for the three degrees of freedom, we get the curves shown in figure 7.4. It can be noticed that the result is very similar to the two degrees of freedom, except for two differences : a third peak has come in and around zero, the three degrees of freedom system has a sharper variation (as can be seen in the zoomed figure).

The effect on the frequency of an added virus and bacteria is shown in figure 7.11.

Added mass	2 DOF	3 DOF
bacteria	$\approx 10^{-4}$ Hz	$\approx 10^{-4}$ Hz
Virus	$\approx 10^{-8}$ Hz	$\approx 10^{-8}$ Hz

Figure 7.1: Effect on the resonant frequency if a virus or a bacteria is added on a proof mass.

The self-oscillating circuit proposed in section 6.1.1 which was built (as shown in figure 7.5) has been tested in two modes :

1. Equivalent circuit with three quartz without perturbation
2. Equivalent circuit with three quartz with perturbation of coil 3 by 0.00023%

The result of the measurement is shown in figure 7.2. As said before, this result cannot be used to check the sensitivity result but can be used to check that the circuit is effectively an auto-adaptive circuit.

Testing Mode	Measurements on "mass" 1	
	frequency	amplitude
Without perturbation	32767.76Hz	158mV
Perturbation of 0.00023%	32767.71 Hz	170mV

Figure 7.2: Value measured when using self-oscillating circuit. Experimentation has been done 15 times by alternating the two modes each time.

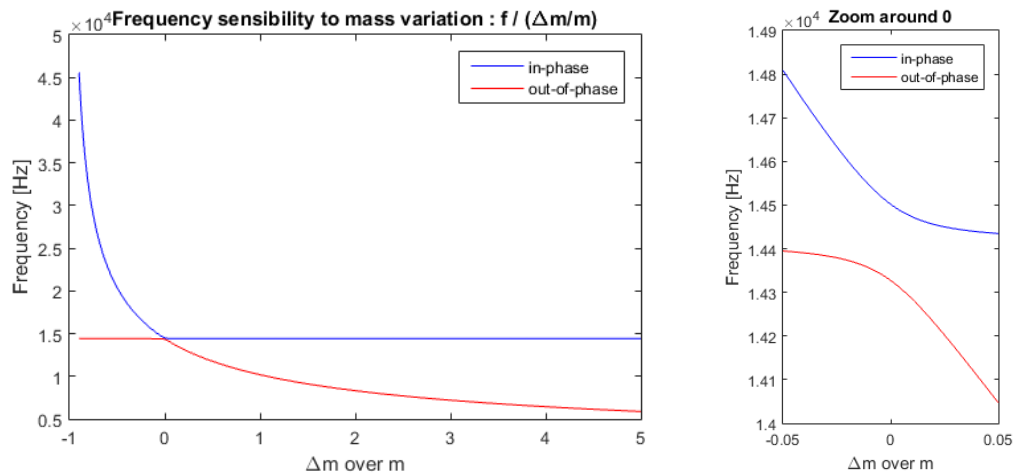


Figure 7.3: sensitivity of the frequency due to mass variation of proof mass 2 in the two degrees of freedom model.

7.2 Relative amplitude variation at resonant frequency

Now the frequency sensibility has been computed, the amplitude variation must be investigated. Figure 7.6 shows the relative variation of the amplitude at the resonant frequency in function of mass variation for the two degrees of freedom.

Those curves have to be compared with the three degrees of freedom whose curves are shown in figure 7.7.

As can be seen on the graph, those curves have a higher sensitivity than frequency shifting curves. However, the range of mass variations in which this technique can

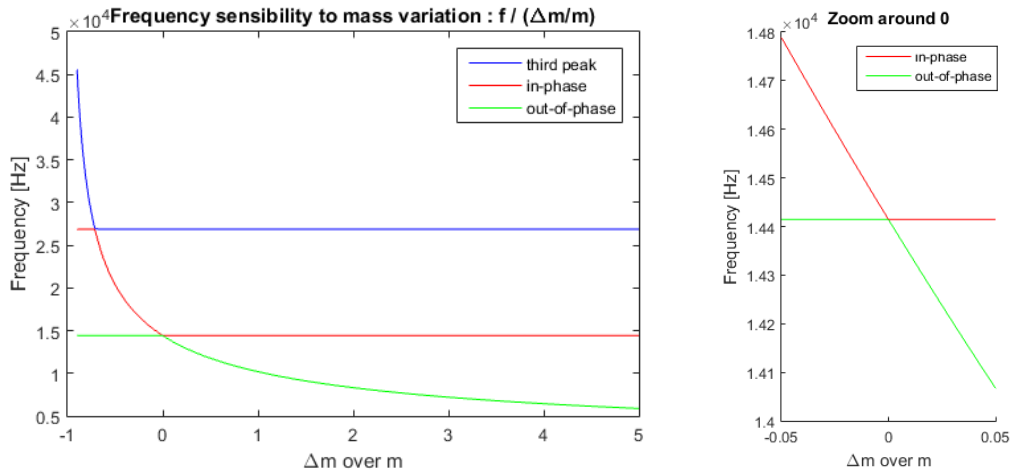


Figure 7.4: Sensitivity of the frequency due to mass variation of proof mass 3 in the three degrees of freedom model.

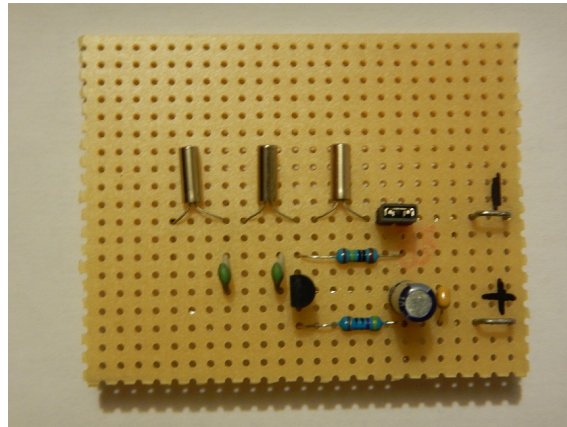


Figure 7.5: Self oscillating MEMS equivalent circuit using quartz oscillators.

be used is smaller than for the frequency. If this technique was used to measure the mass of a virus or a bacteria, the perturbation that would be measured on the amplitude is shown in figure 7.8.

7.3 Amplitude ratio variation at resonant frequency

The third technique investigated in the previous chapter was about amplitude ratio. The sensibility of the two degrees of freedom system is shown in figure 7.9. The value measured is the amplitude ratio between mass 2 and mass 1.

The two degrees of freedom is then compared with the three degrees of freedom for which the ratio is computed as the amplitude of mass 3 over mass 1 and for which curves are shown in figure 7.10.

Here again the three degrees of freedom system has a better sensitivity to mass variation compared to the two degrees of freedom model. In the same way, its sensitivity is higher than the previous technique (section 7.2).

We compute one more time the variation of the amplitude ratio due to virus or

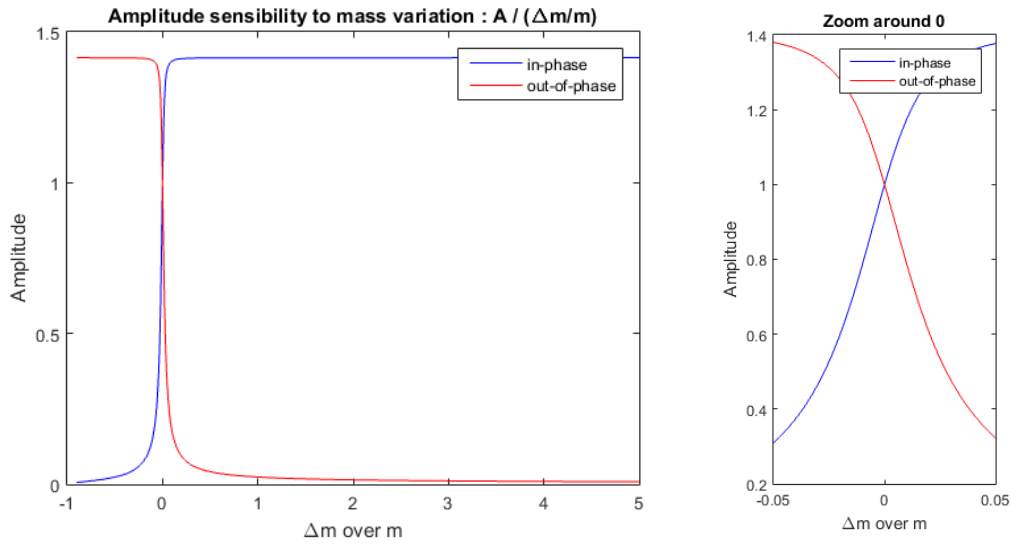


Figure 7.6: Sensitivity of the amplitude at the resonant frequency due to mass variation of proof mass 2 in the two degrees of freedom model.

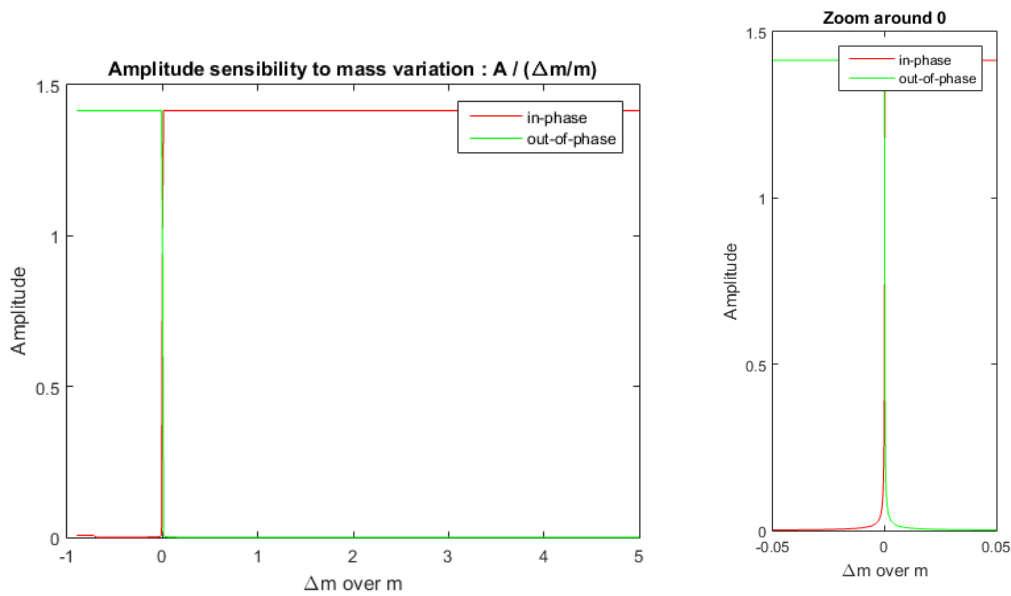


Figure 7.7: Sensitivity of the amplitude at the resonant frequency due to mass variation of proof mass 2 in the two degrees of freedom model.

Added mass	2 DOF	3 DOF
bacteria	$\approx 10^{-4} \%$	$\approx 10^{-2} \%$
Virus	$\approx 10^{-8} \%$	$\approx 10^{-6} \%$

Figure 7.8: Variation of the amplitude if a virus or a bacteria is added on proof mass.

bacteria perturbation.

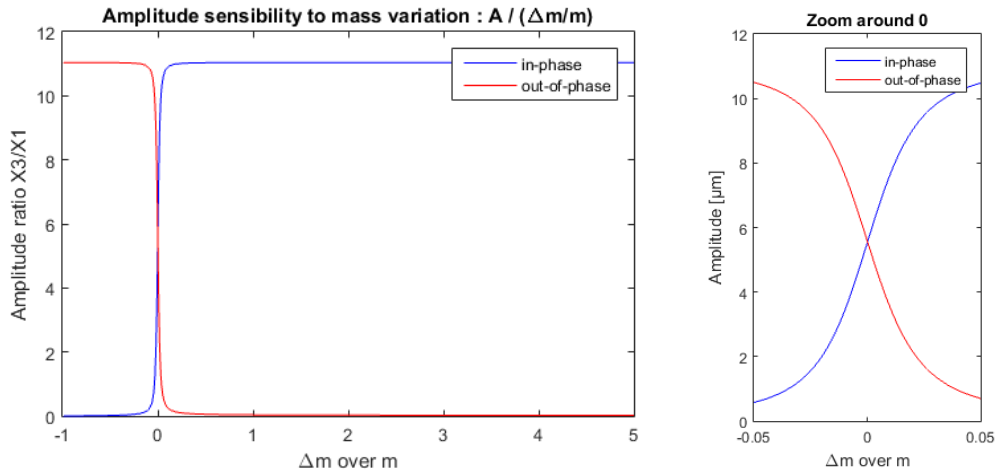


Figure 7.9: sensitivity of the amplitude ratio due to mass variation of proof mass 2 in the two degrees of freedom model.

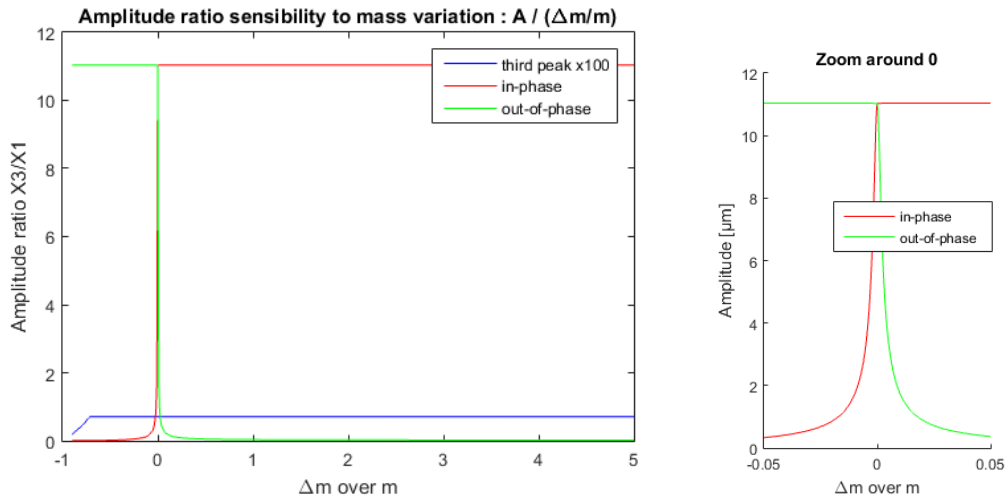


Figure 7.10: sensitivity of the amplitude ratio due to mass variation of proof mass 3 in the three degrees of freedom model.

Added mass	2 DOF	3 DOF
bacteria	$\approx 10^{-5}$	$\approx 10^{-5}$
Virus	$\approx 10^{-9}$	$\approx 10^{-9}$

Figure 7.11: Effect on the amplitude ratio if a virus or a bacteria is added on proof mass.

7.4 Low sensitivity for small measurements

For all techniques, the three degrees of freedom system has shown a better sensitivity than the two degrees of freedom system. However, we can notice that when the measurement of a tiny mass like a bacteria or a virus is made, the sensitivity is relatively identical and small. This is due to a knee that is always present on the curves whether it is for mass 1, 2 or 3, with in-phase mode or out-of-phase mode.

This curvy shape makes the sensitivity around zero perturbation low.

Chapter 8

Conclusion

This project was started with an existing MEMS designed to measure stiffness variation. Several models have been built and compared, each having its own strengths and weaknesses. The comparison of the models has shown that the behavior of the MEMS is well characterized and relatively well known. When the results of the real RLC were analyzed, it was clear that MEMS are used because of their very high quality factor, small size, low power consumption, etc. compared to electrical components (resistances, capacitors, coils, ...).

It was also shown that complex resonators could be built using several single resonators electrically coupled. This is very interesting since building complex MEMS costs a lot and often leads to many defective components. However, the ability to cut the fabrication process of complex resonator systems strongly depends on the type of resonators.

This project has also provided some measurement techniques used to convert additional mass into electrical measurands (frequency shift, amplitude variation, amplitude ratio variation). Frequency is the least sensitive but can be used with a larger mass perturbation range. Those measurement techniques have also proven that three degrees of freedom systems are effectively more sensitive to mass variation than two degrees of freedom systems.

The question about measuring a virus or a bacteria mass is, however, still open. The variation of mass induced by their tiny mass can be amplified by the MEMS, but the values to measure remain very low. The feasibility will depend on the measurement techniques used, the type of resonator used, and the signal to noise ratio of this resonator (which was not investigated in this master thesis).

Finally, an important step realized during this project is the design of a real closed loop. Until now, this MEMS was used with external laboratories equipments and only simulated circuits were created.. With the proposed closed loop that was built, only a DC power supply is needed. This closed loop turned the MEMS into a sensor, which was not the case before.

Chapter 9

Further Improvements

This project which was made in research orientation is only a part of many other projects. Weakly coupled resonators are still evolving. Based on this work, some further improvements can be considered :

Coupling damping Since the damping between coupled masses was supposed to be very small, the created models have always neglected it. However, in order to reach higher reliability, damping should be added.

N degrees of freedom The two degrees of freedom system has shown a better sensitivity than the one degree of freedom system, and the three degrees of freedom has shown a better sensitivity than two degrees of freedom system. How would a 4, 5 or N degrees of freedom system behaves? Some instability will probably limit the number of degrees of freedom, but this is an interesting way to explore.

New shape Increasing the degrees of freedom has improved the sensibility, however, many designs can be investigated. This modification is already explored by team members.

Measurement technique This report only introduces three types of measurands variations due to mass change. However, other measurands can be analyzed (the phase plot of the masses contains very sharp edges which could lead to a high sensitivity, the MEMS could be used as a trigger sensor by measuring the amplitude at a constant frequency (the initial resonant frequency for instance)).

Measurement circuit The proposed circuit should be characterized. A lot of information should be obtained about them like the bandwidth, the lower and higher variation they can measure, the perturbation introduced by connecting the measurement circuit to the MEMS, ...

Initial perturbation It was seen that even if the three degrees of freedom model has a better sensitivity, there is a knee around no perturbation which strongly limits the measurement of small variations. It should be interesting to determine the best initial perturbation to add on the MEMS before adding the interesting mass to move in a very sensitive zone on the curves.

Bibliography

- [1] Oscillators.
<http://www.kb6nu.com/category/classesting/extra-class-question-of-the-day/page/5/>.
- [2] Tarun Agarwal. Steps to fabrication of mems.
<https://www.elprocus.com/understanding-fabrication-mems/>.
- [3] Rashid Bashi. *BioMEMS and Biomedical Nanotehcnoogy*. 2007.
- [4] Pierre-Alain Binz. Mass spectrometry in proteomics.
http://www.ch.embnet.org/CoursEMBnet/PROT04/Slides/mass_spectrometry.pdf, 2004.
- [5] Jianbing Xie Honglong Chang Suan Hui Pu Michael Kraft Chun Zhao, Graham S. Wood. A three degree-of-freedom weakly coupled resonator sensor with enhanced stiffness sensitivity. *IEEE*, 2015.
- [6] Rashid Bashir Demir Akin, Amit Gupta. Detection of bacterial cells and antibodies using surface micromachined thin silicon cantilever resonators. *Purdue e-Pubs*, 2004.
- [7] Mouser Electronics. Wurth electronics we-cmbnc : Common mode nanocrystalline power line chokes.
<http://www.mouser.be/new/Wurth-Electronics/wurth-we-cmbnc-power-chokes/>.
- [8] Christoph Gerber Hans Peter Lang, Martin Hegner. Cantilever array sensors. *materialstoday*, pages 30–36, 2005.
- [9] HistoryWorld. History of measurement.
<http://www.historyworld.net/wrldhis/PlainTextHistories.asp?historyid=ac07>.
Accessed: 2016-05-16.
- [10] Hsin-Hung Lin Shiue-Wen Tsai Alice L. Yu Richie L. C. Chen Huan-Chang Lin, Jung-Lee Lin and Chung-Hsuan Chen. High-speed mass measurement of nanoparticle and virus. *ACS Publications*, pages 4965–4969, 2012.
- [11] Gratiela Isai. Surface micromachining.
<http://81.161.252.57/ipci/courses/technology/inde374.htm>.
- [12] Ville kaajakari. (electrical) equivalent circuits for microresonators.

- [13] Daniel Irimia Jennifer Sturgis James Lee-J. Paul Robinson Mehmet Toner Kidong Park, Jaesung Jang and Rashid Bashir. Living cantilever arrays' for characterization of mass of single live cells in fluids. *Lab on a Chip*, 2008.
- [14] Dick Kleijer. Fet versterker voor het meten aan lc kringen.
<http://crystal-radio.eu/index.html>.
- [15] Pr. M. Kraft. Micro-and nanosystemtechnology, surface micromachiningand othemicrofabricationtechniques.
- [16] mathworks. eig.
<http://nl.mathworks.com/help/matlab/ref/eig.html>.
- [17] H. Chang Z. Chao G. Wood-M. Kraft M.H. Montaseri, J. Xie. Atmospheric pressure mode localization coupled resonators force sensor. *IEEE*, 2015.
- [18] Liesbet Lagae Nima Arjmandi, Willem Van Roy. Measuring mass of nanoparticles and viruses in liquids with nanometer-scale proes. *ACS Publications*, pages 4637–4641, 2014.
- [19] Wolfgang Osten. *Optical Inspection of Microsystems*. 2016.
- [20] Phys.org. Msu technology spin-out company to market portable biohazard detection.
<http://phys.org/news/2012-01-msu-technology-spin-out-company-portable.html>. Accessed: 2016-05-30.
- [21] N. R. Silvester R. E. Burge. The measurement of mass, thickness, and density in the electron microscope. *The Journal of Biophysical and Biochemical Cytology*, 8(1):1–11, 1960.
- [22] William Reusch. Mass spectrometry.
<http://www2.chemistry.msu.edu/faculty/reusch/virttxtjml/spectrpy/massspec/masspec1.htm>. Accessed: 2016-06-04.
- [23] Dr. Thara Srinivasan. Surface micromachinig iii.
- [24] Pr. P. Vanderbemden. Application of electrical measurement systems : Noise reduction using a lock-in amplifier.
- [25] Pr. P. Vanderbemden. Sensors, microsensors and instrumentation.
- [26] Eric Vittoz. *Low-Power Crystal and MEMS Oscillators*. 2010.
- [27] Wikipedia. Carat (mass).
<https://en.wikipedia.org/wiki/Carat> *Accessed:2016–05–16*.
- [28] Wikipedia. Electron microscope.
https://en.wikipedia.org/wiki/Electron_microscope. *Accessed : 2016 – 05 – 16*.

- [29] Wikipedia. History of ancient numeral systems.
https://en.wikipedia.org/wiki/History_of_ancient_numeral_systems. Accessed : 2016 – 05 – 16.
- [30] Wikipedia. History of measurement.
https://en.wikipedia.org/wiki/History_of_measurement. Accessed : 2016 – 05 – 16.
- [31] Wikipedia. Orders of magnitude (mass).
https://en.wikipedia.org/wiki/Orders_of_magnitude Accessed:2016–05–16.
- [32] Wikipedia. Prehistoric technology.
https://en.wikipedia.org/wiki/Prehistoric_technology. Accessed : 2016 – 05 – 16.
- [33] Wikipedia. Tally marks.
https://en.wikipedia.org/wiki/Tally_marks. Accessed : 2016 – 05 – 16.
- [34] Chun Zhao. *A MEMS Sensor For Stiffness Change Sensing Applications Based on Three Weakly Coupled Resonators*. PhD thesis, UNIVERSITY OF SOUTHAMPTON, 2015.

Appendices

Appendix A

MATLAB codes

A.1 TwoDofNoDamp.m

This code was used to mathematically modelize the behavior of the two degrees of freedom system without damping :

```
close all;
clear all;
clc;

% definition of spring constants
k = 57.62;
k1 = k;
k2 = k;
kc = -0.69;
K = [k1+kc, -kc; -kc, k1+kc];

% definition of forces
f1 = 0;
f2 = 0;
F = [f1; f2];
m = 6.94e-9;

%% forced movement with constant mass
%let asume a force of 1
force = [1; 0]; % only the first mass is excited
m2 = m + 0.02*m;
m1 = m;
M = [m1 0; 0 m2];

% definition of frequency range
[X, LAMBDA] = eig(-K, M);
f1 = sqrt(-LAMBDA(1,1))/2/pi;
f2 = sqrt(-LAMBDA(2,2))/2/pi;
```

```

if f2 > f1
    f = (5/6)*f1 : 0.1 : (7/6)*f2;
else
    f = (5/6)*f2 : 0.1 : (7/6)*f1;
end

%  $F = -wM X + K X$ 
%  $\Rightarrow X = F / (-wM + K)$ 

omega = 2*pi*f;
for i = 1:length(omega)
    X(:, i) = inv(K - M*(omega(i)^2)) *force;
end;

figure;
plot(f, abs(X(1,:)), 'b');
xlabel('Frequency [Hz]');
ylabel('Absolute value of amplitude of mass 1 [ m ]');
title('Frequency response for mass 1, Dm=+10%, no damping');

figure;
plot(f, abs(X(2,:)), 'r');
xlabel('Frequency [Hz]');
ylabel('Absolute value of amplitude of mass 2 [ m ]');
title('Frequency response for mass 2, Dm=+10%, no damping');

```

A.2 TwoDofWithDamp.m

This code was used to mathematically modelize the behavior of the two degrees of freedom system with damping :

```

close all;
clear all;
clc;

% definition of spring constants
k = 57.62;
k1 = k;
k2 = k;
kc = -0.69;
K = [k1+kc, -kc; -kc, k1+kc];

% definition of forces
f1 = 0;
f2 = 0;
F = [f1; f2];

```

```

m = 6.94e-9;

%% forced movement with constant mass
%let asume a force of 1
force = [1; 0]; % only the first mass is excited
m2 = m + 0.02*m;
m1 = m;
M = [m1 0; 0 m2];

% definition of damping coefficient
c = 10^(-6);
c1 = c;
c2 = c;
C = [c1, 0; 0, c2];

% definition of frequency range
[X, LAMBDA] = eig(-K, M);
f1 = sqrt(-LAMBDA(1,1))/2/pi
f2 = sqrt(-LAMBDA(2,2))/2/pi

if f2 > f1
    f = (5/6)*f1 : 0.1 : (7/6)*f2;
else
    f = (5/6)*f2 : 0.1 : (7/6)*f1;
end

%  $F = -wM X + j w C X + K X$ 
%  $\Rightarrow F = -wM X + (j w C + K) X$ 
%  $\Rightarrow X = F / (-wM + jwC + K)$ 

omega = 2*pi*f;
for i = 1:length(omega)
    X(:, i) = inv(K + 1i*omega(i)*C - M*(omega(i)^2)) * force;
end;

figure;
plot(f, abs(X(1,:)), 'b');
xlabel('Frequency [Hz]');
ylabel('Absolute value of amplitude of mass 1 [ m ]');
title('Frequency response for mass 1, m=+2%, with damping');
figure;
plot(f, abs(X(2,:)), 'r');
xlabel('Frequency [Hz]');
ylabel('Absolute value of amplitude of mass 2 [ m ]');
title('Frequency response for mass 2, m=+2%, with damping');

```

A.3 ThreeDofNoDamp.m

This code was used to mathematically modelize the behavior of the three degrees of freedom system without damping :

```
close all;
clear all;
clc;

% definition of spring constants
k = 57.62;
k1 = k;
k2 = 199.55;
k3 = k;
k12 = -0.69;
k23 = -0.69;
K = [k1+k12, -k12, 0; -k12, k2+k12+k23, -k23; 0, -k23, k3+k23];
% definition of forces
f1 = 0;
f2 = 0;
f3 = 0;
F = [f1; f2; f3];
m = 6.94e-9;

%% forced movement with constant mass
%let asume a force of 1
force = [1; 0; 0]; % only the first mass is excited
m3 = m + 0.0005*m;
m2 = m;
m1 = m;
M = [m1 0 0; 0 m2 0; 0 0 m3];

% definition of frequency range
[X, LAMBDA] = eig(-K, M);
f1 = sqrt(-LAMBDA(1,1))/2/pi;
f2 = sqrt(-LAMBDA(2,2))/2/pi;
f3 = sqrt(-LAMBDA(3,3))/2/pi;

%f = 14413.5 : 0.001 : 14415.5; % no perturbation
f = 14405 : 0.0001 : 14420; % with perturbation

% F = -wM X + K X
% => X = F / (-wM + K)

omega = 2*pi*f;
for i = 1:length(omega)
    X(:, i) = inv(K - M*(omega(i)^2)) * force;
```

```

end;

figure;
plot(f, abs(X(1,:)), 'b');
xlabel('Frequency [Hz]');
ylabel('Absolute value of amplitude of mass 1 [ m ]');
title('Frequency response for mass 1, \Delta m = +0.05%, no damping');

figure;
plot(f, abs(X(2,:)), 'r');
xlabel('Frequency [Hz]');
ylabel('Absolute value of amplitude of mass 2 [ m ]');
title('Frequency response for mass 2, \Delta m = +0.05%, no damping');

figure;
plot(f, abs(X(3,:)), 'g');
xlabel('Frequency [Hz]');
ylabel('Absolute value of amplitude of mass 3 [ m ]');
title('Frequency response for mass 3, \Delta m = +0.05%, no damping');

```

A.4 ThreeDofWithDamp.m

This code was used to mathematically modelize the behavior of the three degrees of freedom system with damping. This model is the closest to the MEMS :

```

close all;
clear all;
clc;

% definition of spring constants
k = 57.62;
k1 = k;
k2 = 199.55;
k3 = k;
k12 = -0.69;
k23 = -0.69;
K = [k1+k12, -k12, 0; -k12, k2+k12+k23, -k23; 0, -k23, k3+k23];
% definition of forces
f1 = 0;
f2 = 0;
f3 = 0;
F = [f1; f2; f3];
m = 6.94e-9;

%% forced movement with constant mass
%let asume a force of 1

```

```

force = [1; 0; 0]; % only the first mass is excited
m3 = m + 0.0005*m;
m2 = m;
m1 = m;
M = [m1 0 0; 0 m2 0; 0 0 m3];

% definition of damping coefficient
c = 10^(-8);
c1 = c;
c2 = c;
c3 = c;

C = [c1, 0, 0; 0, c2, 0; 0, 0, c3];

% definition of frequency range
[X, LAMBDA] = eig(-K, M);
f1 = sqrt(-LAMBDA(1,1))/2/pi;
f2 = sqrt(-LAMBDA(2,2))/2/pi;
f3 = sqrt(-LAMBDA(3,3))/2/pi;

%f = 14413.5 : 0.001 : 14415.5; % no perturbation
f = 14405 : 0.0001 : 14420; % with perturbation
%f = 14000 : 0.1 : 28000; % three peaks
%f = 14413.5 : 0.001 : 14415.5; % +, 0, -

% F = -wM X + j w C X + K X
% => F = -wM X + (j w C + K) X
% => X = F / (-wM + jwC + K)

omega = 2*pi*f;
for i = 1:length(omega)
    X(:, i) = inv(K + 1i*omega(i)*C - M*(omega(i)^2)) * force;
end;
figure;
plot(f, abs(X(1,:)), 'b');
xlabel('Frequency [Hz]');
ylabel('Absolute value of amplitude of mass 1 [ m ]');
title('Frequency response for mass 1, Dm=+0.05%, with damping');

figure;
plot(f, abs(X(2,:)), 'r');
xlabel('Frequency [Hz]');
ylabel('Absolute value of amplitude of mass 2 [ m ]');
title('Frequency response for mass 2, Dm=+0.05%, with damping');

figure;

```

```

plot(f, abs(X(3,:)), 'g');
xlabel('Frequency [Hz]');
ylabel('Absolute value of amplitude of mass3 [ m ]');
title('Frequency response for mass3, Dm=+0.05%, with damping');

```

A.5 Meca2Elec.m

This code was used to compute the values of the scaled and not scaled electrical circuits based on the values of the MEMS :

```

close all;
clear all;
clc;

M1 = 6.94e-9; %[kg] 6.94 g
M2 = M1;
M3 = M1;
K1 = 57.62; % [N/m]
K2 = 199.55;
K3 = K1;
Q = 1e5;
Kc12 = -0.69;
Kc23 = -0.69;

epsilon0 = 8.85418782e-12; % [F / m]
epsilonR = 1;
epsilon = epsilon0 * epsilonR;

Vdc = 48; %[V]
A_el = 50e-6 * 300e-6; %[m^2] 50 m x 300 m
d = 6e-6; %[m] 6 m

n = Vdc * epsilon*A_el/(d^2);
n2 = n^2;

%ratio = 6.1475e+05
%ratio = 4.9180e+07/80;
ratio = 1;
L1 = 1E20*M1/n2 / ratio;
L2 = 1E20*M2/n2 / ratio;
L3 = 1E20*M3/n2 / ratio;
R1 = 1E20*sqrt(K1*M1)/(Q*n2) / ratio;
R2 = 1E20*sqrt(K2*M2)/(Q*n2) / ratio;
R3 = 1E20*sqrt(K3*M3)/(Q*n2) / ratio;
C1 = 1E20*n2/K1 * ratio;
C2 = 1E20*n2/K2 * ratio;

```

```

C3 = 1E20*n2/K3 * ratio;
Cc12 = 1E20*n2/Kc12 * ratio;
Cc23 = 1E20*n2/Kc23 * ratio;

```

A.6 amplitudeRatioShift__2Dof.m

This code was used to compute the sensitivity of the amplitude ratio of the two degrees of freedom model.

```

close all;
clear all;
clc;

```

```

% definition of spring constants

```

```

k = 57.62;
k1 = k;
k2 = k;
kc = -0.69;
K = [k1+kc, -kc; -kc, k1+kc];

```

```

% definition of forces

```

```

f1 = 0;
f2 = 0;
F = [f1; f2];

```

```

%% free movement, with changing mass

```

```

m = 6.94e-9;
m1 = m;
m2 = m;
delta_m = -0.9*m : 0.01*m : 5*m;
%delta_m = -0.05*m : 0.0001*m : 0.05*m; %zoom
%delta_m = 0 : m*10^-11: m*10^-11; %virus
%delta_m = 0 : m*10^-7: m*10^-7; %bacteria
force = [1; 0]; % only the first mass is excited

```

```

% definition of damping coefficient

```

```

c = 10^(-6);
c1 = c;
c2 = c;
C = [c1, 0; 0, c2];

```

```

for i = 1:length(delta_m)
    m2 = m + delta_m(i);
    M = [m1 0; 0 m2];

```

```

    %eig used to compute X, LAMBDA so that M*X*LAMBDA = -K*X

```

```

%V,      D      A, B
[X, LAMBDA] = eig(-K, M);
f1 = sqrt(-LAMBDA(1,1))/2/pi;
f2 = sqrt(-LAMBDA(2,2))/2/pi;

omega1 = 2*pi*f1;
omega2 = 2*pi*f2;
X1 = (inv(K + 1i*omega1*C - M*(omega1^2)) *force);
X2 = (inv(K + 1i*omega2*C - M*(omega2^2)) *force);

x1_1(i) = (X1(1));
x1_2(i) = (X1(2));
x2_1(i) = (X2(1));
x2_2(i) = (X2(2));
end

M = [m 0; 0 m];
[X, LAMBDA] = eig(-K, M);
f1 = sqrt(-LAMBDA(1,1))/2/pi;
f2 = sqrt(-LAMBDA(2,2))/2/pi;

omega1 = 2*pi*f1;
omega2 = 2*pi*f2;

X1_0 = (inv(K + 1i*omega1*C - M*(omega1^2)) *force);
X2_0 = (inv(K + 1i*omega2*C - M*(omega2^2)) *force);
%% x1_1_0 = (X1_0(1));
%% x1_2_0 = (X1_0(2));
%% x2_1_0 = (X2_0(1));
%% x2_2_0 = (X2_0(2));

% abs(x1_1(1)) - abs(x1_1(2))
% abs(x2_1(1)) - abs(x2_1(2))

figure;
plot(delta_m/m, abs(x1_1), 'b');
hold on;
plot(delta_m/m, abs(x2_1), 'r');
hold off;
title(strcat('Amplitude_ratio_sensitivity_to_mass_variation: A/(\Delta
xlabel(strcat('\Delta ', 'm_over_m'));
ylabel('Amplitude [ m ]');
legend('in-phase', 'out-of-phase')

```

```

% figure;
% plot(delta_m/m, abs(x1_1)/abs(x1_1_0), 'b');
% hold on;
% plot(delta_m/m, abs(x2_1)/abs(x2_1_0), 'r');
% figure;
% plot(delta_m/m, abs(x1_2)/abs(x1_2_0), 'b');
% hold on;
% plot(delta_m/m, abs(x2_2)/abs(x2_2_0), 'r');
% hold off;
% title('Sensibility using eigen value');
% xlabel('\Delta_m over m');
% ylabel('amplitude ratio (x_i / x_i_0)');
% legend('out phase', 'in phase');

```

A.7 amplitudeRatioShift_3Dof.m

This code was used to compute the sensitivity of the amplitude ratio of the three degrees of freedom model.

```

close all;
clear all;
clc;

% definition of spring constants
k = 57.62;
k1 = k;
k2 = 199.55;
k3 = k;
k12 = -0.69;
k23 = -0.69;
K = [k1+k12, -k12, 0; -k12, k2+k12+k23, -k23; 0, -k23, k3+k23];
% definition of forces
f1 = 0;
f2 = 0;
f3 = 0;
F = [f1; f2; f3];

%% free movement, with changing mass
m = 6.94e-9;
m1 = m;
m2 = m;
m3 = m;
delta_m = -0.9*m : 0.01*m : 5*m;
%delta_m = -0.05*m : 0.0001*m : 0.05*m; %zoom
%delta_m = 0 : m*10^-11 : m*10^-11; %virus
%delta_m = 0 : m*10^-7 : m*10^-7; %bacteria

```

```

force = [1; 0; 0]; % only the first mass is excited

% definition of damping coefficient
c = 10(-6);
c1 = c;
c2 = c;
c3 = c;
C = [c1, 0, 0; 0, c2, 0; 0, 0, c3];

for i = 1:length(delta_m)
    m3 = m + delta_m(i);
    M = [m1 0 0; 0 m2 0; 0 0 m3];

    % eig used to compute X, LAMBDA so that M*X*LAMBDA = -K*X
    %V,      D      A, B
    [X, LAMBDA] = eig(-K, M);
    f1 = sqrt(-LAMBDA(1,1))/2/pi;
    f2 = sqrt(-LAMBDA(2,2))/2/pi;
    f3 = sqrt(-LAMBDA(3,3))/2/pi;

    omega1 = 2*pi*f1;
    omega2 = 2*pi*f2;
    omega3 = 2*pi*f3;
    X1 = (inv(K + 1i*omega1*C - M*(omega12)) * force);
    X2 = (inv(K + 1i*omega2*C - M*(omega22)) * force);
    X3 = (inv(K + 1i*omega3*C - M*(omega32)) * force);

    x1_1(i) = (X1(1));
    % x1_2(i) = (X1(2));
    x2_1(i) = (X2(1));
    % x2_2(i) = (X2(2));
    x3_1(i) = (X3(1));
end

M = [m 0 0; 0 m 0; 0 0 m]
[X, LAMBDA] = eig(-K, M);

f1 = sqrt(-LAMBDA(1,1))/2/pi;
f2 = sqrt(-LAMBDA(2,2))/2/pi;
f3 = sqrt(-LAMBDA(3,3))/2/pi;

omega1 = 2*pi*f1;
omega2 = 2*pi*f2;
omega3 = 2*pi*f3;

```

```

X1_0 = (inv(K + 1i*omega1*C - M*(omega1^2)) * force);
X2_0 = (inv(K + 1i*omega2*C - M*(omega2^2)) * force);
X3_0 = (inv(K + 1i*omega3*C - M*(omega3^2)) * force);

```

```

abs(x1_1(1)) - abs(x1_1(2))
abs(x2_1(1)) - abs(x2_1(2))
abs(x3_1(1)) - abs(x3_1(2))
figure;
hold on;
plot(delta_m/m, abs(x2_1), 'r');
plot(delta_m/m, abs(x3_1), 'g');
hold off;
title(strcat('Amplitude ratio sensitivity to mass variation: A/(\Delta
xlabel(strcat('\Delta', 'm over m'));
ylabel('Amplitude [ m ]');
legend('third peak x100', 'in-phase', 'out-of-phase');

```

A.8 amplitudeShift_2Dof.m

This code was used to compute the sensitivity of the amplitude of the two degrees of freedom model.

```

close all;
clear all;
clc;

```

```

% definition of spring constants

```

```

k = 57.62;
k1 = k;
k2 = k;
kc = -0.69;
K = [k1+kc, -kc; -kc, k1+kc];

```

```

% definition of forces

```

```

f1 = 0;
f2 = 0;
F = [f1; f2];

```

```

% free movement, with changing mass

```

```

m = 6.94e-9;
m1 = m;
m2 = m;
delta_m = -0.9*m : 0.01*m : 5*m;
%delta_m = -0.05*m : 0.0001*m : 0.05*m; %zoom

```

```

%delta_m = 0 :m*10^-11: m*10^-11; %virus
%delta_m = 0 :m*10^-7: m*10^-7; %bacteria
force = [1; 0]; % only the first mass is excited

% definition of damping coefficient
c = 10^(-6);
c1 = c;
c2 = c;
C = [c1, 0; 0, c2];

for i = 1:length(delta_m)
    m2 = m + delta_m(i);
    M = [m1 0; 0 m2]; %

    %eig used to compute X, LAMBDA so that M*X*LAMBDA = -K*X
    %V, D A, B
    [X, LAMBDA] = eig(-K, M);
    x1_1(i) = X(1,1);
    x1_2(i) = X(1,2);
    x2_1(i) = X(2,1);
    x2_2(i) = X(2,2);
end

M = [m 0; 0 m];
[X0, LAMBDA0] = eig(-K, M);
x1_1_0 = X0(1,1);
x1_2_0 = X0(1,2);

% abs(x1_1(1)/x1_1_0) - abs(x1_1(2)/x1_1_0)
% abs(x1_2(1)/x1_2_0) - abs(x1_2(2)/x1_2_0)

figure;
plot(delta_m/m, abs(x1_1/x1_1_0), 'b');
hold on;
plot(delta_m/m, abs(x1_2/x1_2_0), 'r');
hold off;
title(strcat('Amplitude_sensitivity_to_mass_variation: A/(\Delta', 'm/m
xlabel(strcat('\Delta', 'm_over_m'));
ylabel('Amplitude');
legend('in-phase', 'out-of-phase')

% figure;
% plot(delta_m/m, abs(x1_1)/abs(x1_1_0), 'b');
% hold on;
% plot(delta_m/m, abs(x2_1)/abs(x2_1_0), 'r');

```

```

% figure;
% plot(delta_m/m, abs(x1_2)/abs(x1_2_0), 'b');
% hold on;
% plot(delta_m/m, abs(x2_2)/abs(x2_2_0), 'r');
% hold off;
% %title('Sensibility using eigen value');
% xlabel('\Delta_m over m');
% ylabel('amplitude ratio (x_i / x_i_0)');
% legend('out phase', 'in phase');

```

A.9 amplitudeShift_3Dof.m

This code was used to compute the sensitivity of the amplitude of the three degrees of freedom model.

```

close all;
clear all;
clc;

% definition of spring constants
k = 57.62;
k1 = k;
k2 = 199.55;
k3 = k;
k12 = -0.69;
k23 = -0.69;
K = [k1+k12, -k12, 0; -k12, k2+k12+k23, -k23; 0, -k23, k3+k23];
% definition of forces
f1 = 0;
f2 = 0;
f3 = 0;
F = [f1; f2; f3];

%% free movement, with changing mass
m = 6.94e-9;
m1 = m;
m2 = m;
m3 = m;
delta_m = -0.9*m : 0.01*m : 5*m;
%delta_m = -0.05*m : 0.0001*m : 0.05*m; %zoom
%delta_m = 0 : m*10^-11: m*10^-11; %virus
%delta_m = 0 : m*10^-7: m*10^-7; %bacteria
force = [1; 0; 0]; % only the first mass is excited

% definition of damping coefficient
c = 10^(-6);

```

```

c1 = c;
c2 = c;
c3 = c;
C = [c1, 0, 0; 0, c2, 0; 0, 0, c3];

for i = 1:length(delta_m)
    m3 = m + delta_m(i);
    M = [m1 0 0; 0 m2 0; 0 0 m3]; %

    % eig used to compute X, LAMBDA so that M*X*LAMBDA = -K*X
    %V,      D      A, B
    [X, LAMBDA] = eig(-K, M);
    x1_1(i) = X(1,1);
    x1_2(i) = X(1,2);
    x1_3(i) = X(1,3);
    %      x2_1(i) = X(2,1);
    %      x2_2(i) = X(2,2);
    %      x2_3(i) = X(2,3);
    %      x3_1(i) = X(2,1);
    %      x3_2(i) = X(2,2);
    %      x3_3(i) = X(2,3);
end
m3 = m + delta_m(i);
M = [m 0 0; 0 m 0; 0 0 m];

[X0, LAMBDA0] = eig(-K, M);
x1_1_0 = X0(1,1);
x1_2_0 = X0(1,2);
x1_3_0 = X0(1,3);

% abs(x1_1(1)/x1_1_0) - abs(x1_1(2)/x1_1_0)
% abs(x1_2(1)/x1_2_0) - abs(x1_2(2)/x1_2_0)
% abs(x1_3(1)/x1_3_0) - abs(x1_3(2)/x1_3_0)

figure;
%plot(delta_m/m, abs(x1_1), 'b-o');
plot(delta_m/m, abs(x1_2/x1_2_0), 'r');
hold on;
plot(delta_m/m, abs(x1_3/x1_3_0), 'g');
hold off;
title(strcat('Amplitude sensitivity to mass variation: A/(\Delta', 'm/m
xlabel(strcat('\Delta', 'm over m'));
ylabel('Amplitude');
legend('in-phase', 'out-of-phase');

% figure;

```

```

% plot(delta_m/m, abs(x1_1)/abs(x1_1_0), 'b');
% hold on;
% plot(delta_m/m, abs(x2_1)/abs(x2_1_0), 'r');
% figure;
% plot(delta_m/m, abs(x1_2)/abs(x1_2_0), 'b');
% hold on;
% plot(delta_m/m, abs(x2_2)/abs(x2_2_0), 'r');
% hold off;
% title('Sensibility using eigen value');
% xlabel('\Delta_m over m');
% ylabel('amplitude ratio (x_i / x_i_0)');
% legend('out phase', 'in phase');

```

A.10 freqShift_2Dof.m

This code was used to compute the sensitivity of the frequency of the two degrees of freedom model.

```

close all;
clear all;
clc;

% definition of spring constants
k = 57.62;
k1 = k;
k2 = k;
kc = -0.69;
K = [k1+kc, -kc; -kc, k1+kc];

% definition of forces
f1 = 0;
f2 = 0;
F = [f1; f2];

%% free movement, with changing mass
m = 6.94e-9;
m1 = m;
m2 = m;

delta_m = -0.9*m : 0.01*m : 5*m;
%delta_m = -0.05*m : 0.0001*m : 0.05*m; %zoom
%delta_m = 0 : m*10^-11 : m*10^-11; %virus
%delta_m = 0 : m*10^-7 : m*10^-7; %bacteria

for i = 1:length(delta_m)

```

```

m1 = m + delta_m(i);
M = [m1 0; 0 m2];

% eig used to compute X, LAMBDA so that M*X*LAMBDA = -K*X
% V, D A, B
[X, LAMBDA] = eig(-K, M);
% AV = BVD
% -K*X = M*X*LAMBDA
omega_square_1(i) = -LAMBDA(1,1);
omega_square_2(i) = -LAMBDA(2,2);

```

end

```

% M = [m 0; 0 m];
% [X, LAMBDA] = eig(-K, M);
% omega_square_0_1 = -LAMBDA(1,1);
% omega_square_0_2 = -LAMBDA(2,2);
%
% figure;
% plot(delta_m/m, sqrt(omega_square_1)/sqrt(omega_square_0_1), 'b');
% hold on;
% plot(delta_m/m, sqrt(omega_square_2)/sqrt(omega_square_0_2), 'r');
% title(strcat('Frequency sensibility to mass variation : (\Delta', 'f/f)'));
% xlabel(strcat('\Delta', 'm over m'));
% ylabel(strcat('\Delta', 'f over f'));
% legend('in-phase', 'out-of-phase')

```

```

%(sqrt(omega_square_1(1)) - sqrt(omega_square_1(2)))/2/pi;
%(sqrt(omega_square_2(1)) - sqrt(omega_square_2(2)))/2/pi;

```

figure;

```
plot(delta_m/m, sqrt(omega_square_1)/2/pi, 'b');
```

```
hold on;
```

```
plot(delta_m/m, sqrt(omega_square_2)/2/pi, 'r');
```

```
title(strcat('Frequency□sensibility□to□mass□variation□:□f□/□(\Delta', 'm/m
```

```
xlabel(strcat('\Delta', 'm□over□m'));

```

```
ylabel('Frequency□[Hz]');

```

```
legend('in-phase', 'out-of-phase')

```

A.11 freqShift_3Dof.m

This code was used to compute the sensitivity of the frequency of the three degrees of freedom model.

```
close all;
```

```
clear all;
```

```

clc;

% definition of spring constants
k = 57.62;
k1 = k;
k2 = 199.55;
k3 = k;
k12 = -0.69
k23 = -0.69;
K = [k1+k12, -k12, 0; -k12, k2+k12+k23, -k23; 0, -k23, k3+k23];
% definition of forces
f1 = 0;
f2 = 0;
f3 = 0;
F = [f1; f2; f3];

%% free movement, with changing mass
m = 6.94e-9;
m1 = m;
m2 = m;
m3 = m;

delta_m = -0.9*m : 0.01*m : 5*m;
%delta_m = -0.05*m : 0.0001*m : 0.05*m; %zoom
%delta_m = 0 : m*10^-11 : m*10^-1 1; %virus
%delta_m = 0 : m*10^-7 : m*10^-7; %bacteria

for i = 1:length(delta_m)
    m3 = m + delta_m(i);
    M = [m1 0 0; 0 m2 0; 0 0 m3];

    %eig used to compute X, LAMBDA so that M*X*LAMBDA = -K*X
    %V,      D          A, B
    [X, LAMBDA] = eig(-K, M);
    %AV = BVD
    %-K*X = M*X*LAMBDA
    omega_square_1(i) = -LAMBDA(1,1);
    omega_square_2(i) = -LAMBDA(2,2);
    omega_square_3(i) = -LAMBDA(3,3);

end

% M = [m 0 0; 0 m 0; 0 0 m];
% [X, LAMBDA] = eig(-K, M);
% omega_square_0_1 = -LAMBDA(1,1);
% omega_square_0_2 = -LAMBDA(2,2);

```

```

% omega_square_0_3 = -LAMBDA(3,3);
%
% figure;
% plot(delta_m/m, sqrt(omega_square_1)/sqrt(omega_square_0_1), 'b');
% hold on;
% plot(delta_m/m, sqrt(omega_square_2)/sqrt(omega_square_0_2), 'r');
% plot(delta_m/m, sqrt(omega_square_3)/sqrt(omega_square_0_3), 'g');
% title(strcat('Frequency sensibility to mass variation : (\Delta', 'f/f)');
% xlabel(strcat('\Delta', 'm over m'));
% ylabel(strcat('\Delta', 'f over f'));
% legend('third peak', 'in-phase', 'out-of-phase');

% (sqrt(omega_square_1(1)) - sqrt(omega_square_1(2)))/2/pi
% (sqrt(omega_square_2(1)) - sqrt(omega_square_2(2)))/2/pi
% (sqrt(omega_square_3(1)) - sqrt(omega_square_3(2)))/2/pi

figure;
% plot(delta_m/m, sqrt(omega_square_1)/2/pi, 'b');
hold on;
plot(delta_m/m, sqrt(omega_square_2)/2/pi, 'r');
plot(delta_m/m, sqrt(omega_square_3)/2/pi, 'g');
title(strcat('Frequency_sensibility_to_mass_variation : f/(\Delta', 'm/m)');
xlabel(strcat('\Delta', 'm over m'));
ylabel('Frequency [Hz]');
legend('third_peak', 'in-phase', 'out-of-phase');

```

Appendix B

Others

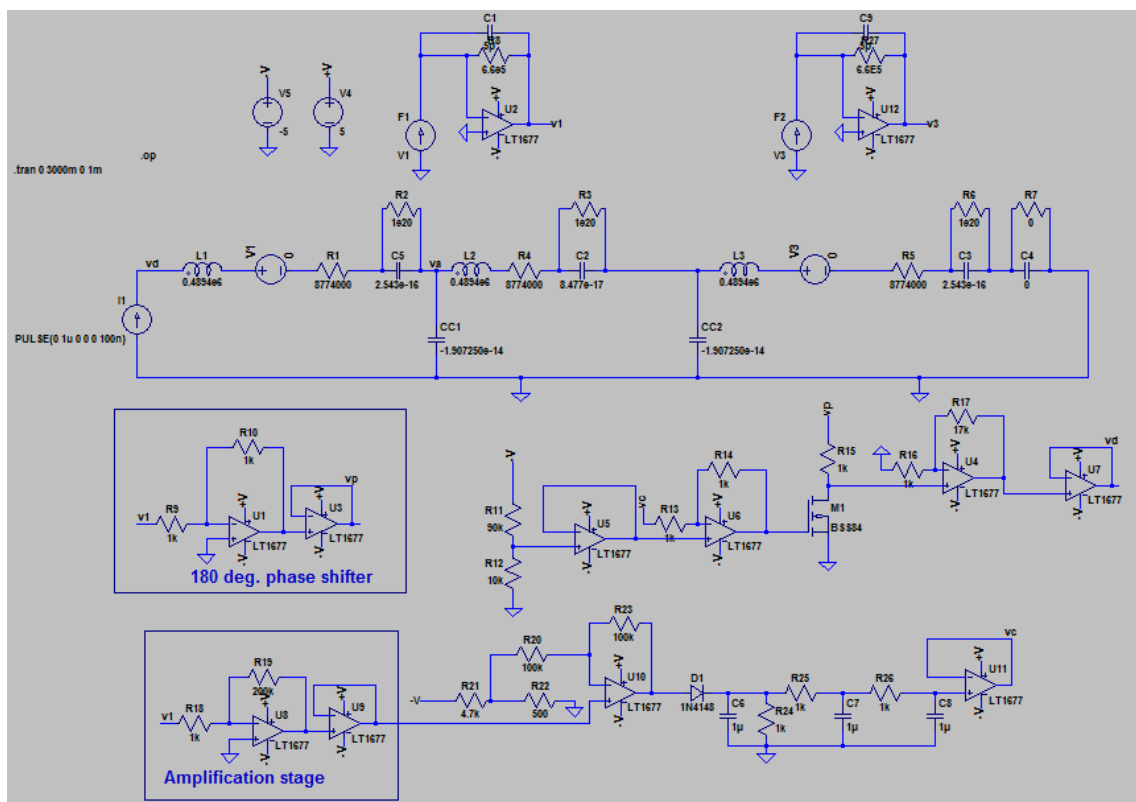


Figure B.1: Feedback loop proposed by Chun Zhao[34].